UNIVERSITAT POLITÈCNICA DE CATALUNYA
BARCELONATECH
Departament d'Enginyeria Telemàtica

Contributions to provide a QoS-aware self-configured framework for video-streaming services over ad hoc networks

by
Ahmad Mohamad Mezher

Ph.D. Advisor:
Dra. Mónica Aguilar Igartua

Thesis submitted in partial fulfillment of the requirements
for the degree of Doctor of Philosophy in Network Engineering
in the
Department of Network Engineering

Barcelona, March 2016

UNIVERSITAT POLITÈCNICA DE CATALUNYA
BARCELONATECH
Escola de Doctorat

Curs acadèmic:

Acta de qualificació de tesi doctoral

Nom i cognoms

Programa de doctorat

Unitat estructural responsable del programa

Resolució del Tribunal

Reunit el Tribunal designat a l'efecte, el doctorand / la doctoranda exposa el tema de la seva tesi doctoral titulada

_____

_____.

Acabada la lectura i després de donar resposta a les qüestions formulades pels membres titulars del tribunal, aquest atorga la qualificació:

☐ NO APTE ☐ APROVAT ☐ NOTABLE ☐ EXCEL·LENT

(Nom, cognoms i signatura) President/a	(Nom, cognoms i signatura) Secretari/ària	
(Nom, cognoms i signatura) Vocal	(Nom, cognoms i signatura) Vocal	(Nom, cognoms i signatura) Vocal

_____, _____ d'/de _____ de _____

El resultat de l'escrutini dels vots emesos pels membres titulars del tribunal, efectuat per l'Escola de Doctorat, a instància de la Comissió de Doctorat de la UPC, atorga la MENCIÓ CUM LAUDE:

☐ SÍ ☐ NO

(Nom, cognoms i signatura) President de la Comissió Permanent de l'Escola de Doctorat	(Nom, cognoms i signatura) Secretari de la Comissió Permanent de l'Escola de Doctorat

Barcelona, _____ d'/de _____ de _____

To my son Mohamad,
to my nephews Karim and Larissa,
to my parents.

"It is never too late to be what you might have been."

~ George Eliot

Agradecimientos

- Primeramente quiero agradecer a Dios por todo lo que me ha dado en esta vida.
- A Mónica Aguilar, directora de mi tesis. Diga lo q diga yo aquí nunca será suficiente todo lo q me hubiese gustado decir. Es un placer haber trabajado contigo. Sinceramente tu constante motivación fue la que me hizo creer que sí se puede. Gracias por darme la oportunidad de trabajar contigo.
- A mis padres, por apoyarme siempre en todo lo que he hecho a lo largo de mi vida y especialmente estos últimos 15 años que llevo viviendo lejos.
- A mis hermanos, que siempre están apoyándome de manera incondicional.
- A mi esposa, que es el tesoro que he encontrado para el resto de mi vida. Siempre me dices q puedo con todo cuando a veces ni yo me lo creía, gracias habibi.
- A mis amigos, los que están aqui y los que están en el Líbano.
- A todos los proyectistas que trabajaron conmigo durante estos años y especialmente a Juan Jurado que aparte de proyectista se ha convertido en un amigo.
- A los profesores Jordi Forné, Esteve Pallarès, Luis de la cruz y los demás compañeros de los proyectos de investigación. A Carolina Tripp por su ayuda.
- Finalmente, a FI-AGAUR por darme la beca que me permitió desarollar esta tesis doctoral.

Abstract

Ad hoc networks have attracted much attention from the research community over the last years and important technical advances have risen as a consequence. These networks are foreseen as an important kind of next generation access networks, where multimedia services will be demanded by end users from their wireless devices everywhere. In this thesis, we specially focus our research work on mobile ad hoc networks (MANETs) and on vehicular ad hoc networks (VANETs), two kind of ad hoc networks over which interesting multimedia services can be provided.

The special characteristics of MANETs/VANETs, such as mobility, dynamic network topology (specially in VANETs), energy constraints (in case of MANETs), infrastructureless and variable link capacity, make the QoS (Quality of Service) provision over these networks an important challenge for the research community. Due to that, there is a need to develop new routing protocols specially designed for MANETs and VANETs able to provide multimedia services.

The main objective of this thesis is to contribute in the development of the communication framework for MANETs and VANETs to improve decisions to select paths or next hops in the moment of forwarding video-reporting messages. In this way, it would be possible to have a quick answer to manage daily problems in the city and help the emergency units (*e.g.*, police, ambulances, health care units) in case of incidents (*e.g.*, traffic accidents). Furthermore, in case of VANETs, a real scenario must be created and thus we have analysed the presence of obstacles in real maps. Also, in case of an obstacle found between the current forwarding node and the candidate next forwarding node, the packet is stored in a buffer, for a maximum time, until a forwarding neighbour node is found; otherwise, the packet is dropped.

To improve the communication framework for MANETs, we propose a new routing protocol based on a game-theoretical scheme for N users specially designed to transmit video-reporting messages. Our proposal makes the network more efficient and provides a higher degree of satisfaction of the users by receiving much more packets with a lower average end-to-end delay, lower jitter and higher PSNR (Peak Signal-to-Noise Ratio).

In addition, we propose a geographical routing protocol for VANETs that considers multiple metrics named 3MRP (Multimedia Multimetric Map-Aware Routing Protocol) [1]. 3MRP is a geographical protocol based on hop-by-hop forwarding. The metrics considered in 3MRP are the distance, the density of vehicles in transmission range, the available bandwidth, the future trajectory of the neighbouring nodes and the MAC layer losses. Those metrics are weighted to obtain a multimetric score. Thus, a node selects another node among its neighbours as the best forwarding node to increase the percentage of successful packet delivery, minimizing the average packet delay and offering a certain level of quality and service. Furthermore, a new algorithm named DSW (Dynamic Self-configured Weights) computes for each metric its corresponding weight depending on the current network conditions. As a consequence, nodes are classified in a better way.

Finally, we propose a new routing protocol for VANETs named G-3MRP (Game Theoretical Multimedia Multimetric Map-aware Routing Protocol) [2] based on a game-theoretical scheme for N users to transmit video-reporting messages in an urban scenarios. G-3MRP is based on 3MRP and uses up to three neighbour nodes through which the three types of video frames I, P and B will be sent. The metrics used are the same as in 3MRP. G-3MRP achieves a higher degree of satisfaction of the users who receive much more packets with a higher average of PSNR, compared to 3MRP+DSW.

We have also analysed the issue of detecting obstacles in real maps for VANETs in urban scenarios. For this purpose, we have developed our REVsim [3] tool so that our proposed routing protocols can easily be building aware, thus avoiding nodes behind buildings to be chosen as next forwarding nodes. Also, our simulations are more realistic.

Resumen

Las redes *ad hoc* han llamado mucho la atención por parte de la comunidad científica en los últimos años, además de los importantes avances técnicos que han surgido. Estas redes se prevén como un tipo importante de redes de acceso de nueva generación, donde los servicios multimedia serán requeridos por los usuarios a través de sus dispositivos inalámbricos desde todas partes. En esta tesis, centramos nuestro trabajo de investigación especialmente en las redes móviles *ad hoc* (MANET, *Mobile Ad hoc Network*) y las redes vehiculares *ad hoc* (VANET, *Vehicular Ad hoc Network*).

Las características especiales de las MANETs y las VANETs, como la movilidad, la topología dinámica de la red (especialmente en VANETs), las restricciones de batería (en caso de MANETs), la ausencia de infrastructura y la capacidad variable del enlace inalámbrico hace que la provisión de la calidad de servicio en estas redes sea un reto importante para la comunidad científica. Debido a esto, existe la necesidad de desarrollar nuevos protocolos de encaminamiento especialmente diseñados para MANETs y VANETs capaces de proporcionar los servicios de multimedia requeridos.

El objetivo principal de esta tesis es proveer mejoras en la comunicación para las redes *ad hoc* MANET y VANET para mejorar las decisiones a la hora de seleccionar los próximos caminos o nodos, respectivamente, en el momento del envío de las tramas del vídeo y de esta manera sería posible tener una respuesta rápida para resolver los problema diarios en la ciudad y ayudar a las unidades de emergencia (por ejemplo, policía, ambulancias, unidades de salud) en caso de incidentes, como accidentes de tráfico. Para analizar adecuadamente nuestras propuestas sobre VANETs hemos diseñado un entorno de simulación realista que incorpora la presencia de edificios en mapas reales. En el caso de que haya un obstáculo entre el nodo actual y el candidato para ser el próximo salto el paquete se almacena en un *buffer*, durante un tiempo máximo, hasta encontrar un nuevo candidato; en caso contrario, se descarta el paquete.

Para mejorar las comunicaciones en las MANETs, proponemos un nuevo protocolo de encaminamiento basado en teoriá de juegos para N usuarios especialmente diseñado para enviar mensajes de vídeo.

Esto hace que la red sea más eficiente, y así se consigue un mayor grado de satisfacción de los usuarios al recibir muchos más paquetes con un menor promedio de retardo de extremo a extremo, variación de retardo (*jitter*) y mayor PSNR (Relación Señal a Ruido de Pico).

Además, se propone un protocolo de encaminamiento geográfico basado en el reenvío de salto-a-salto para VANETs llamado 3MRP (*Multimedia multimetric Map-Aware Routing Protocol*) [1] que incluye diversas métricas. Las métricas consideradas en 3MRP son la distancia al destino, la densidad de vehículos en el rango de transmisión, el ancho de banda disponible, la trayectoria futura de los nodos vecinos y la pérdida de paquetes en la capa MAC. Estas métricas se ponderan para obtener una puntuación multimétrica final. Así, un nodo puede seleccionar el mejor nodo de reenvío entre todos sus vecinos para aumentar la probabilidad de éxito de entrega de paquetes, minimizando el retardo

medio de los paquetes y ofreciendo un cierto nivel de calidad de servicio. Por otra parte, se ha diseñado un nuevo algoritmo capaz de dar a cada métrica su correspondiente peso en función de las condiciones actuales de la red. De esta forma, los nodos se pueden clasificar de una mejor manera.

Por último, se propone un nuevo protocolo de encaminamiento para VANETs llamado G-3MRP (*Game Theoretical Multimedia Multimetric Map-aware Routing Protocol*) [2] para enviar mensajes de vídeo basado en teoría de juegos para N usuarios en escenarios urbanos. G-3MRP se basa en el protocolo de encaminamiento 3MRP. G-3MRP utiliza hasta tres nodos a través de los cuales los tres tipos de cuadros de vídeo I, P y B serán enviados. Las métricas utilizadas son las mismas que en 3MRP. G-3MRP logra una mayor grado de satisfacción de los usuarios mediante la recepción de muchos más paquetes de vídeo y con un mayor nivel de PSNR, que la anterior propuesta 3MRP+DSW.

También hemos analizado el problema de detección de obstáculos en mapas reales para VANETs en escenarios urbanos. Para este propósito, hemos desarrollado nuestra herramienta REVsim [3] de tal forma que puede estar fácilmente integrada en nuestra propuesta de protocolo de encaminamiento para que las simulaciones sean más realistas.

Resum

Les xarxes sense fils *ad hoc* han captat molt l'atenció per part de la comunitat científica en els últims anys, a més dels importants avenços tècnics que han sorgit. Aquestes xarxes es preveuen com un tipus important de xarxes d'accés de nova generació, a on els serveis multimèdia seran requerits pels usuaris a través dels seus dispositius sense fils desde tot arreu. En aquesta tesi, centrem el nostre treball especialment en les xarxes mòbils ad hoc (MANET, *Mobile Ad hoc Network*) i en les xarxes vehiculars *ad hoc* (VANET, *Vehicular Ad hoc Network*).

Les característiques especials de les MANETs i les VANETs, com la mobilitat, la topologia dinàmica de la xarxa (especialment en VANETs), les restriccions de bateria (en cas de MANETs), l'absència d'infrastructura i la capacitat variable de l'enllaç sense fil fa que la provisió de la qualitat de servei en aquestes xarxes sigui un repte important per a la comunitat científica. A causa d'això, hi ha la necessitat de desenvolupar nous protocols d'encaminament especialment dissenyats per a MANETs i VANETs capaços de proporcionar els serveis de multimèdia requerits.

L'objectiu principal d'aquesta tesi és proveir millores en la comunicació per a les xarxes ad hoc MANET i VANET per millorar les decisions a l'hora de seleccionar els propers camins o nodes, respectivament, en el moment de l'enviament de les trames del vídeo. D'aquesta manera serà possible tenir una resposta ràpida per resoldre els problema diaris a la ciutat i ajudar a les unitats d'emergència (per exemple, policia, ambulàncies, unitats de salut) en cas d'incidents, com ara els accidents de trànsit. Per analitzar adequadament les nostres propostes sobre VANETs hem dissenyat un entorn de simulació realista que incorpora la presència d'edi cis en mapes reals i en el cas que hi hagi un obstacle entre el node actual i el candidat per a ser el pròxim salt el paquet s'emmagatzema en un *buffer*, per un temps màxim, fins a trobar un nou candidat; en cas contrari, es descarta el paquet.

Per millorar les comunicacions en les MANETs, proposem un nou protocol d'encaminament basat en teoria de jocs per a N usuaris especialment dissenyat per a enviar missatges de vídeo. Això fa que la xarxa sigui més eficient, i així s'aconsegueix un major grau de satisfacció dels usuaris en rebre molts més paquets amb un menor retard mig extrem a extrem, menor variació del retard (*jitter*) i major PSNR (Relació Senyal Soroll de Pic) .

A més, es proposa un protocol d'encaminament geogràfic basat en el reenviament *hop-by-hop* per a VANETs anomenat 3MRP (*Multimedia Multimetric Map-Aware Routing Protocol*) [1] que prèn en consideració múltiples mètriques. Les mètriques considerades en 3MRP són la distància a destinació, la densitat de vehicles en el rang de transmissió, l'ample de banda disponible, la trajectòria futura dels nodes veïns i la pèrdua de paquets a la capa MAC. Aquestes mètriques es ponderen per a obtenir una puntuació multimètrica. Així, un node pot seleccionar el millor node de reenviament entre tots els seus veïns per augmentar la probabilitat d' èxit de lliurament de paquets, minimitzant el retard mitjà dels paquets i oferint un cert nivell de qualitat de servei.

D'altra banda, s'ha dissenyat un nou algorisme capaç de donar a cada mètrica el seu corresponent pes en funció de les condicions actuals de la xarxa. Així, els nodes es poden classificar d'una millor manera.

Finalment, es proposa un nou protocol d'encaminament per a VANETs anomenat G-3MRP (*Game Theoretical Multimedia Multimetric Map-aware Routing Protocol*) [2] per a enviar missatges de vídeo basat en teoria de jocs per a N usuaris en escenaris urbans. G-3MRP es basa en el protocol d' ecaminament 3MRP. G-3MRP utilitza fins a tres nodes a través dels quals els tres tipus de quadres de vídeo I, P i B seran enviats. Les mètricas utilitzades són les mateixes que en 3MRP. G-3MRP aconsegueix una major grau de satisfacció on dels usuaris mitjançant la recepció de molts més paquets de vídeo i amb un major nivell de PSNR que amb 3MRP + DSW.

També hem analitzat el problema de la detecció d'obstacles en mapes reals per a VANETs en escenaris urbans. Per a aquest propòsit, hem desenvolupat la nostra eina REVsim [3] de tal manera que pot estar fácilment integrada en la nostra proposta de protocol d'encaminament per a que les simulacions siguin més realistes.

Contents

List of Figures

List of Tables

Glossary

3MRP	Multimedia Multimetric Map-Aware Routing Protocol
AC	Access Category
ACK	Acknowledgement
ACO	Ant Colony Optimization
ADAS	Advanced Driver assistance systems
AIFS	Arbitration Inter-Frame Space
AODV	Ad hoc On-Demand Distance Vector
AP	Access Point
AVC	Advanced Video Coding
BE	Best Effort
BSS	Basic Service Set
C4R	Citymob For Roadmaps
CBR	Constant Bit Rate
CC	Contributing SouRCe Identifier count
CCH	Control Channel
CI	Confidence Intervals
CPU	Central Processing Unit
CRP	Congestion-adaptive Routing Protocol
CSMA/CA	Carrier Sense Multiple Access with Collision Avoidance
CSRC	Contributing SouRCe Identifier
CW	Contention Window
DCF	Distributed Coordination Function
DIFS	Distributed Inter-Frame Space
DSR	Dynamic Source Routing
DSRC	Dedicated Short-Range Communications

DSW	Dynamic Self-configured Weights
ECC	Electronic Communications Committee
EDCA	Enhanced Distributed Channel Access
FEC	Forward Error Correction
FGRP	Forwarding Game Routing Protocol
FMLB	Fibonacci Multipath Load Balancing protocol
FPL	Fraction of Packet Losses
FQ-MP-OLSR	Fuzzy-based Quality of service Multipath Optimized Link State Routing protocol
GA	Genetic Algorithm
GDF	Geographic Data Files
GloMoSim	Global Mobile Information System Simulator
GoP	Group of Pictures
GPS	Global Positioning System
GPSR	Greedy Perimeter Stateless Routing
GPSR-MA	Greedy Perimeter Stateless Routing with Movement Awareness
HDTV	High Definition Television
HEVC	High Efficiency Video Coding
HM	Hello Messages
HVS	Human Visual System
I-GPSR	Improvement Greedy Perimeter Stateless Routing
IBSS	independent Basic Service Set
ICT	Information and Communications Technologies
ISO	International Organization for Standardization
ITS	Intelligent Transportation System
ITU	International Telecommunication Union
MAC	Medium Access Control
MANET	Mobile Ad hoc Network
MMDSR	Multipath Multimedia Dynamic Source Routing
MMMR	Multimetric Map-aware Routing protocol
MN	Mobile Node
MOPR	Movement Prediction-based Routing
MOS	Mean Opinion Score

MP-OLSR	Multipath Optimized Link State Routing protocol
MPEG	Moving Picture Experts Group
MSE	Mean Squared Error
NE	Nash equilibrium
NHM	New Hello Messages
NS-2	Network Simulator 2
OSI	Open Systems Interconnection
OSM	Open Street Maps
PDV	Packet Delay Variation
PM	Probe Message
PMR	Probe Message Reply
PSNR	Peak Signal-to-Noise Ratio
PT	Payload Type
QoE	Quality of Experience
QoS	Quality of Service
RFC	Request for Comments
RR	Receiver Report
RTP/RTCP	Real Time Protocol/Real Time Control Protocol
SCH	Service Channel
SIFS	Short Inter-Frame Space
SINR	Signal to Interference plus Noise Ratio
SR	Sender Report
SSIM	Structural Similarity Index
SSRC	Synchronization SouRCe Identifier
SUMO	Simulation of Urban MObility
TCP	Transmission Control Protocol
TR	Transmission Range
UDP	User Datagram Protocol
V2I	Vehicle-to-Infrastructure
V2V	Vehicle-to-Vehicle
VANET	Vehicular Ad hoc Network

VanetMobiSim	Vanet Mobility Simulator
VBR	Variable Bit Rate
VCEG	Video Coding Experts Group
VD	Vehicle Density
VIRTUS	VIdeo Reactive Tracking-based UnicaSt
VoIP	Voice over IP
VQM	Video Quality Measure
WLAN	Wireless Local Area Network

Chapter 1

Introduction

This Chapter is devoted to give a brief introduction to this PhD thesis. Besides, the general objectives of the thesis are defined.

1.1 Overview

During the last decade, video-streaming over the Internet has been established as a well-known service with many successful applications such as video conferencing, surveillance systems, news on demand, etc. The technical communications platform to provide these video-streaming services and other multimedia applications to the increasing number of mobile end users is a reality thanks to the recent developments in mobile computing devices and in wireless networking. Nevertheless, there are still many challenges to face in order to provide video-streaming services with sufficient quality to the end users. These challenges are caused by limited resources (*i.e.*, CPU power, bandwidth, storage capacity and battery), a dynamic environment (*i.e.*, availability of resources) and a higher error rate (*i.e.*, bit errors, route changes, connection loss). Furthermore, theses challenges are specially difficult in 802.11 networks in infrastructureless mode, where nodes may act as servers, clients and routers. These networks may cover large geographic areas and they operate without any existing infrastructure. In this thesis we will focus on mobile ad hoc networks (MANETs) and on vehicular ad hoc networks (VANETs).

A Mobile Ad hoc NETwok (MANET) is a group of self-organized wireless mobile nodes (MNs) able to communicate with each other without the need of any fixed network infrastructure nor centralized administrative support. Applications for MANETs include data communication during emergency response in remote areas, or where a disaster (*e.g.*, an earthquake) has fully or partially destroyed the existing infrastructure.

Other applications for MANETs may improve the quality of life of citizens in their daily behaviour. Given the high percentage of citizens that carry at least one smart communications device in their pockets or bags, that are capable of capturing and presenting video content, it is most likely that a significant percentage of the network traffic that in the future will be transmitted will be video. As an example, Cisco estimates that by 2019, 80% of the mobile data traffic will be video [4]. There are numerous applications for video-streaming over MANETs. In rescue operations for example, a firemen could wear a head-mounted camera and transmit live video from their location to the remote command control center, giving a better overview of the situation. Another example could be during sports events by sharing video streams received from cameras carried by sportsmen. Another example could be a situation when an accident happens and dynamic sensors (e.g., citizens with smart phones) could make a short video of the accident and send it through the MANET. This would help to have a quick answer by warning other emergency units and citizens and as a consequences it could even save lives. Many research problems must be tackled to make video-streaming applications in such environments a reality.

Regarding vehicular ad hoc networks (VANETs), they can be considered as a subset of Mobile Ad hoc Networks (MANETs) [5] where nodes are vehicles. VANETs have been studied extensively in the literature during the last decade. The development of VANETs was highly motivated by a large number of interesting applications for Intelligent Transportation Systems (ITS) [6] [7]. In these networks, nodes are vehicles which can communicate with other vehicles directly forming vehicle to vehicle (V2V) communications or communicate with fixed equipment next to the road, referred to as roads ide unit(RSU), forming vehicle to infrastructure (V2I) communications.

V2V and V2I communications can provide a wide range of information to drivers and authorities. Smart VANET vehicles have the ability to collect, process and disseminate information about themselves and their environment to RSUs or to other neighbour vehicles in their transmission range by integrating on-board devices such as network interface, different types of sensors and GPS receivers [8, 9].

VANET applications can be classified into:

- Safety applications: These applications use the wireless communication between vehicles (V2V) or between vehicles and infrastructure (V2I), in order to improve road safety and avoid accidents. The main goals are save people's lives and provide a clean city environment in order to upgrade citizens' daily life.

- Comfort/entertainment applications: These applications aim to enhance traffic efficiency and mobility in the city, improve drivers and passengers comfort levels (*e.g.*, making the journey more enjoyable). Furthermore, weather and traffic information can be provided to drivers or passengers so they can be alerted about bad whether or traffic jams. The nearest restaurant to the driver's location or a near hotel location and their prices can also be consulted. In addition, passengers can send or receive instant messages, play online games and access to the Internet.

In this thesis work we focus our research on the provision of video-streaming services over MANETs and VANETs in smart cities. For instance, upon the occurrence of an accident, a camera mounted on a vehicle could make a light and short video of the accident and send it through the VANET to alert the emergencies service (*e.g.*, 911 or 112). In this way, a good management of video-reporting messages after accidents would lead to an immediate call to health units and ambulances. The prevention of accidents is one of the most important goals in smart cities, and nowadays Information and Communication Technologies (ICTs) and citizens play an essential role to enhance this issue.

1.2 Objectives of the thesis

The main motivation of this thesis is to contribute in the development of ad hoc communication technologies for multimedia services such as video-streaming. We focus our work on both mobile and vehicular ad hoc networks in urban environments. The today reality of smart cities opens a new type of interesting services. Nonetheless, the design of routing protocols to transmit video-reporting messages over ad hoc networks presents challenging issues that it is necessary to tackle.

In this thesis we aim at designing a framework to report the occurrence of incidents in the roads of the city to fast alarm authorities, which is an important goal in smart cities. To achieve this objective, efficient routing protocols specially designed for ad hoc networks are needed.

To achieve this general objective in MANETs, we have developed a new routing protocol based on a game-theoretical scheme for N users to improve the performance of video-reporting messages over MANETs. As a starting point, the multimedia multipath dynamic source routing protocol (MMDSR) [10] was the base for this development. This way, instead of sending the most important information always through the best available path, users play a strategic routing game where these information will be sent through one of the two best paths according to a certain probability p^*.

Regarding VANETs, we have developed approaches to improve the routing operation specially designed for video reporting services in smart cities. As a starting point, the geographic protocol GPSR (Greedy Perimeter Stateless Routing) [11] was the base in all our proposals of routing protocols for VANETs. As the establishment of an end-to-end path is not suitable in VANET scenarios due to the high mobility of the nodes (*i.e*, vehicles), it is not advisable to use any topology-based routing protocol, such as DSR (Dynamic Source Routing protocol) [12]. Besides, we have improved the hop-by-hop forwarding decision by using decisive metrics to choose the best next forwarding node. Furthermore, we have included a map-aware capability through the development of a tool named REVsim [3] so that each vehicle is aware of the presence of buildings around. This way, vehicles behind obstacles can be prevented to be selected as next forwarding nodes. In addition, our simulations are more realistic by mimicking what would happened in real life since buildings may attenuate the signal and even

block a packet being forwarded to a neighbour vehicle behind a building. In addition, we have included a buffer to store packets as a mechanism to reduce packet losses in case that no neighbour was around or because an obstacle was detected between the current forwarding node and every candidate node to be the next hop. Finally, we have included a game theoretical forwarding scheme to the new proposal routing protocol for VANETs so that instead of sending the most important information always through the best available forwarding node, users can play a strategic routing game where these information will be sent through one of the two best available forwarding nodes according to a certain probability p^*

We have used the NS2 simulator to carry out the simulations of our proposals. Moreover, we have used real maps in our simulations so we can approximate our results to a real scenario that can be presented in a real life.

1.3 Organization of the thesis

This thesis is organized in seven Chapters. In Chapter 2 an overview of the main available video platforms is presented. Next, we detail which QoS parameters have been used to evaluate and design our proposals. Besides, we discuss the main available tools to analyse the video performance.

In Chapter 3, a new routing protocol based on a game-theoretical approach is proposed to transmit video-reporting messages in MANETs. The end-to-end path routing protocol used is an improvement of the multipath multimedia dynamic source (MMDSR) [10]. In addition, we have included our game-theoretical forwarding scheme to finally calculate the probability p of sending the most important video frames (*i.e.*, I+P frames) through the best available path. Finally, we present the comparison between the case of using our game-theoretical approach against the case of non using it for different number of sources.

Chapter 4 deals with the development of a tool able to detect buildings efficiently. Buildings in a real map could attenuate or even block the signal. Due to this fact, it is extremely important to take into account obstacles that can actually be found in any real map. To achieve that, a tool named *REVsim* [3] has been developed and a validation of our proposal has been made.

In Chapter 5, a new routing protocol based on multi-metric decisions is proposed to send video-reporting messages in VANETs. We explain each one of the considered metrics. The forwarding decision is based on a global multimetric score. Later, simulation results are shown as well as the comparison to other protocols with two different vehicles' densities.

In Chapter 6, a new routing protocol based on game-theoretical approach is proposed to send video-reporting messages in VANETs. The geographical routing protocol used is the 3MRP, which was presented in Chapter 5 (Multimedia Multimetric Map-Aware Routing Protocol) [1]. We define parameters to develop our game-theoretical model to finally calculate the probability p of sending the most important video frames (*i.e.*, I+P

frames) through the best available forwarding node. Finally, we present the comparison between the case of using our game-theoretical versus the case of non using it for 2 sources.

Finally, conclusions, publications generated from this thesis and some future work guidelines are exposed in Chapter 7.

Chapter 2

Video-streaming services over ad hoc networks

2.1 Introduction

During the last decade, the number of users who require multimedia services has increased exponentially being one of the most required services. In recent years, ad hoc networks have attracted much attention from the research community and important technical advances have arisen as a consequence. These multi-hop networks are foreseen as an important kind of next generation access networks, where multimedia services will be demanded by end users from their wireless devices everywhere.

Therefore, there is a necessity for the research community to work on proposing efficient frameworks able to provide QoS in ad hoc environments. This requirement is fundamental to success in the deployment of video-streaming services over ad hoc networks. In this Chapter we describe the employed technologies associated to the development of the different approaches proposed in this thesis. We briefly summarize the IEEE 802.11 wireless communications standard with an emphasis on its QoS extension (IEEE 802.11e), as well as on the QoS extension designed specifically for vehicular environments (IEEE 802.11p). Furthermore, we give a brief explanation about H.264, H.265 video formats and the MPEG-2 standard that we have used to compress and transmit the video frames. Later, we list and describe some applications and protocols (*e.g.*, RTP/RTCP) which give some QoS support for video-streaming services. Next, we detail the QoS parameters used to evaluate our proposals. Moreover, we describe the main video metrics to analyse the performance of our proposals.

In our framework we decided to use MPEG-2 hierarchical scalable multi-layer encoded video format [13] due to its low CPU (Central Processing Unit) decodification requirements. In any case, our framework could easily be used with other video formats after including a few changes of adaptation.

2.2 Technologies employed

In this section we briefly describe the adopted technologies associated to this thesis in the development of the different proposals.

2.2.1 Overview of infrastructureless wireless communications

In the following subsection we will summarize the IEEE 802.11 standard focusing on two specific QoS-aware extensions which are IEEE 802.11e (for MANETs) and IEEE 802.11p (for VANETs).

2.2.1.1 The IEEE 802.11 standard

The IEEE 802.11 standard [14] is the most widely used technology in wireless local area network (WLAN) since the late 90's. It introduced the basic medium access control (MAC) technique named distributed coordination function (DCF) which uses a carrier sense multiple access with collision avoidance (CSMA/CA) mechanism to transmit data packets. This mechanism is based on listening to the medium before sending the packet. If the medium is clear for a certain time DIFS (DCF Interframe Space), then a node can send its packet. Furthermore, to avoid collisions, DCF also makes use of a binary exponential backoff algorithm to minimize collisions if two nodes try to send a packet at the same time. Also, when a node senses that the medium is idle for a DIFS time, it will initiate a random wait between zero and the value of a contention window (CW) value previously defined. If during that period the medium remains idle, then the node sends the packet and waits for the corresponding acknowledgment (ACK). The ACK packet has the highest priority, and it is sent after waiting for a SIFS (Short Interframe Space) period during which the medium is idle. The SIFS period is shorter than the DIFS. If the node does not sense the ACK, it assumes that the packet did not reach the next node due to a collision. In order to minimize the probability of suffering a collision again, the node restarts the process by increasing the contention window using a binary exponential backoff algorithm (see Figure 2.1).

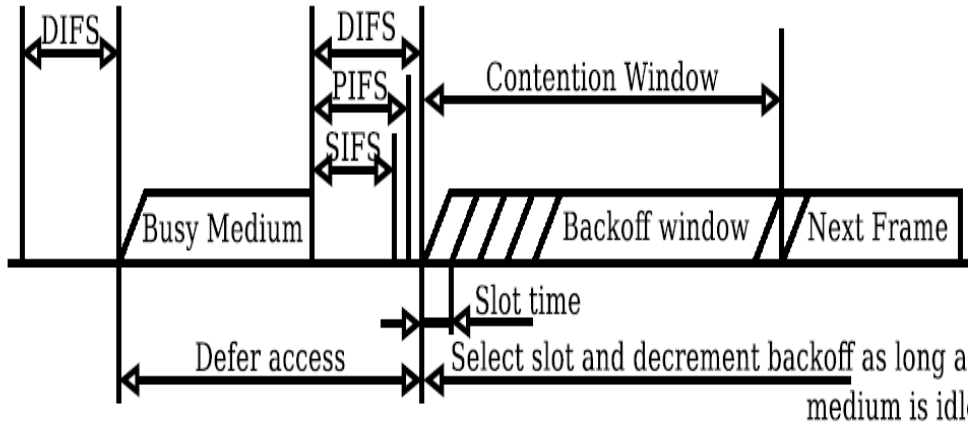

Figure 2.1: Scheme of the CSMA/CA mechanism.

IEEE 802.11 defines different network structures such as the BSS (Basic Service Set) and IBSS (Independent Basic Service Set). The BSS mode (*i.e.*, infrastructure mode) requires an Access Point (AP) to establish the network. Every node connects only with the AP and, therefore, every communication has to go through the AP. However, the IBSS mode (*i.e.*, ad-hoc mode) does not need any AP and therefore, nodes within communication range could spontaneously establish a communication.

2.2.1.2 The IEEE 802.11e standard

To provide QoS in ad hoc environments, the IEEE 802.11e [15] was proposed to provide QoS at the MAC layer. QoS in the MAC layer is fundamental in contention-based wireless networks to achieve traffic differentiation in terms of both throughput and delay. The improvement with respect the standard IEEE 802.11 is due to the substitution of the DCF function by the new enhanced distributed channel access (EDCA). EDCA is compatible with the original DCF function. Using EDCA, high-priority traffic has a higher probability to be sent than low-priority traffic. For example, a station with high priority traffic has to wait less than a station with low priority traffic before sending its packets. EDCA defines four traffic access categories (AC): background (AC_{BK}), best effort (AC_{BE}), video (AC_{VI}), and voice (AC_{VO}). Modifying both the arbitration inter-frame space (AIFS) and the contention window for each category it is possible to achieve the differentiation and prioritization of the packets corresponding to each category. Table 2.1 and Figure 2.2 show the standard values for AC.

Table 2.1: EDCA contention window values.

Access Category	CW_{min}	CW_{max}	AIFS
Background	15	1023	7
Best Effort	15	1023	3
Video	7	15	2
Voice	3	7	2

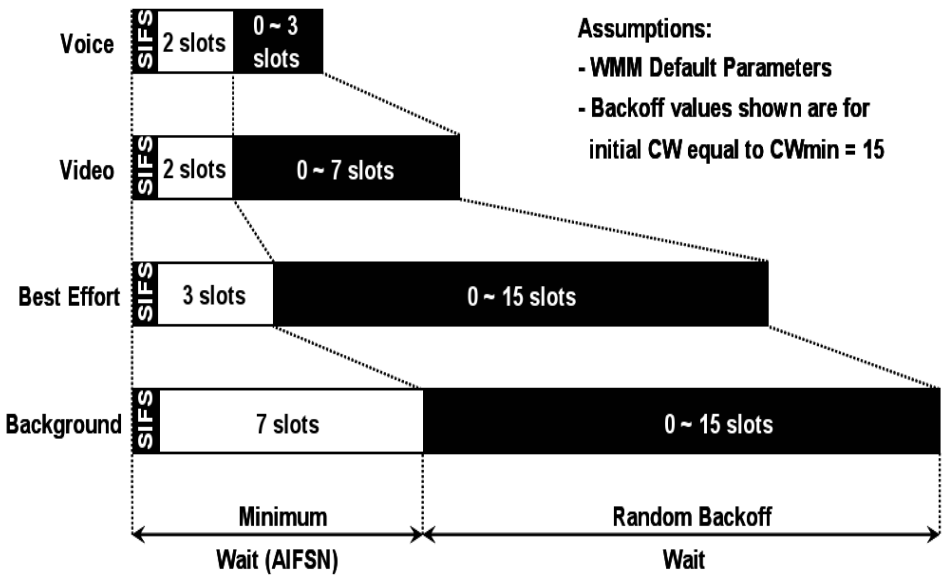

Figure 2.2: AIFS, CW_{min} and CW_{max} for each traffic category.

2.2.1.3 The IEEE 802.11p standard

VANETs have theis special wireless standards due to their special characteristics. Basically, IEEE 802.11p [16] combines IEEE 802.11a and the IEEE 802.11e QoS extensions. That is, it makes use of the same basic technology as IEEE 802.11a, and includes as a default sending mechanism the IEEE 802.11e QoS extensions. The IEEE 802.11p uses the licensed intelligent transportation system (ITS) at 5.9 GHz (5.85-5.925 GHz), which provides a free spectrum frequency band where vehicles and RSUs are allowed to transmit.

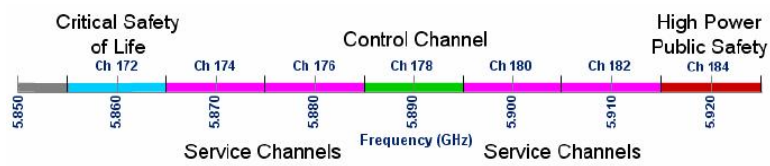

Figure 2.3: Distribution of dedicated short-range communications (DSRC) spectrum.

The dedicated short-range communications (DSRC) spectrum is divided into seven 10 MHz channels with a transmission speed ranging from 6 to 54 Mbps, see Fig. 2.3. The central one is the control channel (CCH) and is restricted to safety-critical communications only. However, the first and the last channel are reserved for special uses. The four rest channels are service channels (SCH) available for both safety and non-safety usage and a 5MHz guard band. Moreover, there are differences in DSRC regulations between Japan, Europe and U.S.A. In 2008, the electronic communications committee (ECC) reserved five channels of 10 MHz. These channels are placed in the frequency band between 5.875 and 5.925 GHz which is not exactly the same as in the US. For non-secure ITS applications, ECC recommends the use of the spectrum between 5.855 - 5.875 GHz. The transmission power in this band is limited to 33 dBm.

2.3 Overview of digital video coding techniques overview

The need to compress digital images has been clear since they were created due to the large amount of data needed to store an uncompressed image. Regarding a full resolution uncompressed image, it could seem possible to store, although storing video sequences without compression is almost a mission impossible in practice. For example, assuming a traditional frame-rate of 25 frames per second, the amount of data needed to store one hour of high definition video is about 560GB, as shown in Equation (2.1). Furthermore, if we compress each image on its own, this would reduce the previous amount, but small enough to be stored in today's typical storage mediums. Thus, to solve this problem, video compression algorithms have exploited the temporal redundancies in the video frames. This means using previously encoded or decoded frames to predict values for the next frame. In this way, data can be compressed with such a rate so that storage becomes feasible.

$$\underbrace{1920 \cdot 1080}_{\text{pixels}} \cdot \underbrace{3}_{\text{byte/pixel}} \cdot \underbrace{25}_{\text{frames/seconds}} \cdot \underbrace{3600}_{\text{seconds}} = 559.872.000 \text{ bytes} \simeq 560 \text{ GByte} \quad (2.1)$$

The development of these standards is mostly being related to two organizations which are the ISO/IEC motion picture experts group (MPEG) and the ITU-T video coding experts group (ITU-VCEG). The ISO video coding standards are indicated in this way MPEG-x (MPEG-1, MPEG-2, ...), while the ITU-T ones are indicated as H.26x (H.261, H.262, ...). This section is an overview of the two video coding standards from the ITU-T video coding experts group (ITU-VCEG), the advanced video coding (H.264/AVC) and the High Efficiency Video Coding (H.265/HEVC) standards and from the ISO/IEC Motion Picture Experts Group (MPEG) MPEG-2, which is the one used in this thesis.

2.3.1 MPEG-2 format

MPEG-2 [17] is a standard method finished at the end of the 90' to transmit digital video and audio in a compressed format using less bandwidth than with the analog method. MPEG-2 solves many of the problems found in MPEG-1, such as resolution, scalability and handling of interlaced video. It gives much better picture up to HDTV -High Definition TV- levels. It was officially adopted by the ISO (International Organization for Standardization) under the catalog number ISO 13818-1. MPEG-2 requires less CPU power than MPEG-4, although MPEG-4 is more powerful.

Three types of frames form the MPEG-2 encoded as follows:

- Intra-coded Pictures (I-Pictures).
- Predictive-coded Pictures (P-Pictures).
- Bidirectionally-predictive-coded Pictures (B-Pictures).

These three types of pictures are combined to form a GoP (*Group of Pictures*), *e.g.* 15 frames each. A GoP has three types of frames: I, P and B, and has a unique frame-pattern in a video repeated in each GoP. I (*Intra-coded*) frames encode spatial redundancy, they form the base layer, provide a basic video quality and carry the most important information for the decoding process at the receiving side. The whole GoP would be lost if the corresponding I frame was not available at decoding time. P (*Predictive-coded*) and B (*Bidirectionally-predictive-coded*) frames carry differential information from preceding (P) or preceding and posterior (B) frames, respectively. Considering these characteristics, we have assigned different priorities to the video frames according to their importance within the video flow. Therefore, I frames should have the highest priority, P frames the medium priority and B frames the lowest one. Figure 2.4 shows an example of a GoP, as well as the dependent relationship between frames at decoding time.

Furthermore, each picture is divided into slices, macroblocks and blocks (see Figure 2.5). Each slice may contain one or more adjacent macroblocks. Slices are important to manage errors. For example, if the bitstream has an error, the decoder can skip to

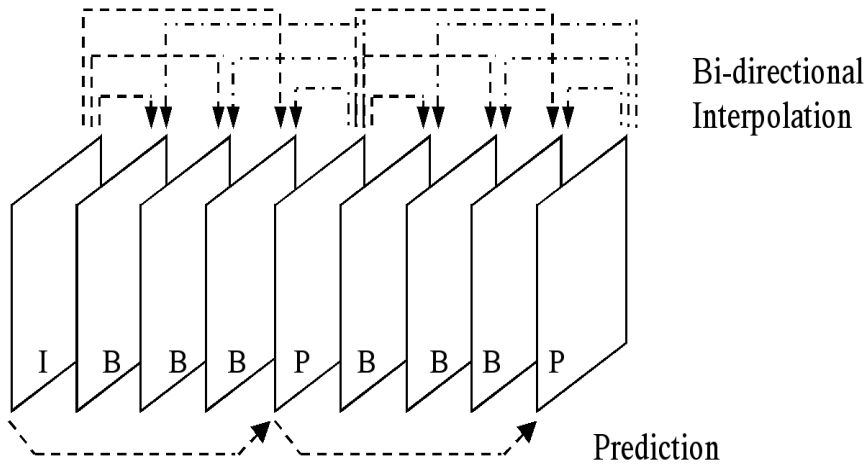

Figure 2.4: MPEG-2 GoP structure.

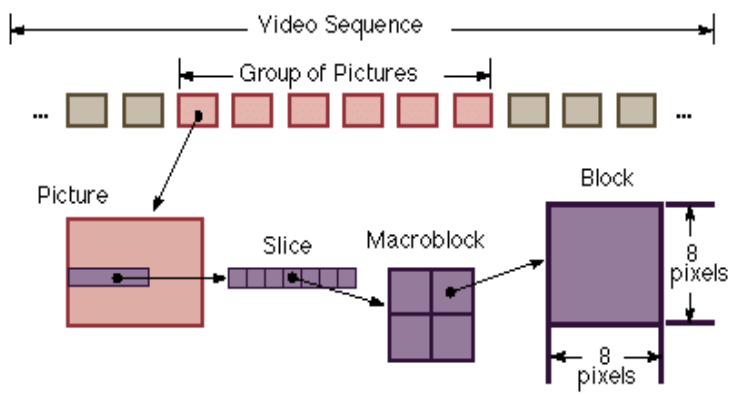

Figure 2.5: MPEG-2 Structure.

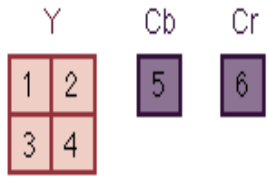

Figure 2.6: MPEG-2 Macroblock.

the beginning of the next slice. Thus, if we have more slices in the bitstream, a better error concealment can be obtained.

In the MPEG algorithm, the block represents the smallest coding unit of 8x8 pixels and can be one of those three types: luminance (Y), red chrominance (Cr), or blue chrominance (Cb). However, in MPEG2 videos are coded in YCbCr format (YUV) where the Y is the brightness (luma), Cb is blue minus luma (B-Y) and Cr is red minus luma (R-Y). A macroblock is the basic coding unit in the MPEG algorithm and is a 16x16 pixel segment in a frame. It consists of four Y, one Cr, and one Cb block as shown in Figure 2.6). These features help us to better understand the MPEG-2 video-streaming flows that we will transmit through adhoc networks.

2.3.2 H.264 (Advanced Video Coding)

H.264/AVC was developed by the MPEG together with the ITU-VCEG. The first version of the standard was completed in May 2003. Since both groups have their own way of naming new compression standards, MPEG-4 AVC is also called H.264, which is the name given by ITU-VCEG.

The MPEG-4/H.264 standard was created to offer a high compression rate, but at the cost of a high complexity. Comparing MPEG-4/H.264 standard to earlier ones, the compression gain is achieved by many small improvements, such as: better motion compensation, image segmentation into finer blocks, improved entropy encoding schemes and a new deblocking filter. The MPEG-4/H.264 standard is not a single standard, but rather a family of standards. It consists of a set of compression tools, which can be used or not, based on a selected profile. To satisfy the user's needs, several profiles have been designed. For example, the baseline profile offers a low compression rate and some error resilience, while maintaining a low complexity. On the other hand, the main profile offers high compression gain at the cost of a high complexity. As a consequence, MPEG-4/H.264 can be used in different fields from storing videos on Blu-ray discs to stream videos on websites such as Youtube or Vimeo.

2.3.3 H.265 (High Efficiency Video Coding)

H.265/HEVC, also known as MPEG-H Part 2, is a new standard for video compression that has the potential to outperform the performance than earlier standards such as H.264/AVC. The first version was presented in 2013. In comparison to AVC, HEVC offers about double data compression ratio for the same level of video quality, as well as it notably improves the video quality at the same bit rate.

The new H.265 video coding is very similar to previous standards such as H.264 and MPEG-2. The two main differences between H.264 and H.265 are: increased modes for intra prediction and refined partitioning for inter prediction. This also means that H.265 requires more computing power to encode the video.

Regarding inter prediction, the most significant change is the size of the macroblock in H.265. H.265 pictures are divided into coding tree blocks (CTBs) instead of into macroblocks. CTBs can be 64x64, 32x32 or 16x16 depending on the stream parameters. Each CTB can be divided recursively in a quad-tree structure, all the way down till 8x8. For example, a 32x32 CTB can consist of four 8x8 regions called coding units (CUs), which are the basic unit of prediction in HEVC. Those CUs can be 64x64, 32x32, 16x16 or 8x8. Due to that, H.265 ensure the highest level of compression efficiency, and support for parallel processing.

2.3.4 Video compression technique used in this thesis

As said before, video compression techniques are used to reduce the amount of data of digital video images so they can be stored in today's typical storage mediums. However, applying video compression to any video file may cause losses to the video quality, depending on the compression type used.

If the compression is *lossy*, we might have errors in the reconstructed data (*i.e.*, the original data is only reconstructed approximately) which makes it possible the achievement of high compression levels. Conversely, if the video is compressed in a *lossless* way, we will obtain the original data but te compression levels will not be high. In this thesis, we used MPEG-2 as the coded video format, due to its simplicity and enough video quality for the purpose of the video-reporting service in which we focus our research work. Nevertheless, our proposals could be easily used with MPEG-4 just after including some few adaptation changes. Nevertheless, it is not an objective of our research to go further in the kind of video coder used, since we will not investigate this topic.

2.4 QoS protocols to support video-streaming services

In this section we briefly explain some common protocols with QoS support used to assist the provision of QoS in video-streaming services.

Regarding network services, many ways are used to characterize the QoS. QoS refers to the ability of a network element (*e.g.*, an application or a router) to provide some level of assurance to a consistent data delivery.

Moreover, all protocols that were thought to be used over wired networks can not be directly applied in wireless ad hoc networks due to its inherent dynamism which produces frequent link breakages. Due to that, providing QoS over ad hoc networks generates challenges to those developers of new proposals where all the OSI layers of the protocol stack could cooperate between each other, which is known as cross-layer design.

2.4.1 RTP/RTCP (Real Time Protocol/Real Time Control Protocol)

RTP/RTCP [18] is one of the most widely used transport protocols to provide some QoS support to multimedia services. Video data is encapsulated in RTP packets and then sent over the network using UDP. Normally, RTP/RTCP is usually used over UDP/IP.

RTCP packets carry control information regarding the streaming of media. RTP packets contain various fields listed in the following:

- **CSRC** (*Contributing SouRCe Identifier*) 0 to 15 items, 32 bits each. The CSRC list identifies the contributing sources for the payload contained in this packet. The CC field gives the number of identifiers. When a number of RTP streams pass through a mixer, the CSRC is used. A mixer can be used, for example, in a conference to combine data received from different sources and send it as a single stream to reduce the needed bandwidth.

- **SSRC** (*Synchronization Source Identifier*) (32 bits). This field represents the RTP packet stream source. SSRC is unique and randomly chosen. Sources must calculate new SSRCs in case of collision. In order to identify the stream of RTP packets for each media of the same session, different SSRC numbers should be used.

- **CC (CSRC count)** (4 bits). The CSRC count contains the number of CSRC identifiers that follow the fixed header. This number is higher than one if the payload of the RTP packet contains data from several sources.

- **PT, (Payload Type)** (7 bits). This field indicates the encoding type for audio (*e.g.*, PCM) or video (*e.g.*, MPEG2, H.264, etc.). Furthermore, it describes the data format in detail such as the coding method implemented in the audio and video streams.

- **SN, (Sequence Number)** (16 bits). This field is increased in each packet. With this field, the application can detect losses and also can recover the synchronism between the audio and the video flows. The temporary space and the sequence numbers space are the same for all the packets that belong to the same synchronized source.

- **Time Stamp** (32 bits). In each RTP packet, the timestamp is increased. The application may use this field to synchronize a stream or to synchronize several streams among themselves (*e.g.*, audio and video streams for the same session).

RTCP control protocol provides QoS information about an RTP session. RTCP distinguishes several types of packets as following:

- Packets to report about the data reception quality (RR, *Receiver Report*)

- Packets to inform about the data delivery (SR, *Sender Report*)

- Packets to inform about the session participants (SDES, *Source Description*)

RTCP-RR packets are sent periodically to the source from the destination node. The feedback information is given to each source, and it consists on:

- **Fraction Lost:** Fraction of packets lost in the RTP stream since the last report.

- **Cumulative number of RTP packets lost:** Total number of RTP packets lost.

- **Extended highest sequence number received:** The highest RTP packet sequence number received.

- **Interarrival Jitter:** It informs about the network congestion state.

- **Timestamp** of the last SR packet received by that source.

- **Last SR timestamp:** The elapsed time between the last SR packet received from a source and the moment of the current transmission of the RR relative to the same source.

Regarding the RTCP traffic, it should be lower than the 5% of total session bandwidth, according to the RFC-3550 [18]. In our simulations RTCP packets were sent each 1 second to fulfill that recomendation.

2.5 Network performance metrics

In this section, we list the most common parameters typically used to measure the performance of an ad hoc network when multimedia services (*e.g.*, video-streaming) are transmitted.

2.5.1 Delay

Average packet delay is defined as how long it takes for a packet in average to travel from source to destination. This delay is due to several reasons:

- **Processing delay:** It represents the time that nodes take to process the packet headers.
- **Queuing delay:** It represents the time that a packet spends in the queues of the routers along the forwarding path.
- **Transmission delay:** It represents the time to send the packet's bits through the wireless link.
- **Propagation delay:** It represents the time it takes for the signal to reach its destination.

In the simulations we run during the research work of this thesis, the packet delay is measured by analyzing the trace file generated by NS-2 at each simulation.

2.5.2 Delay jitter

Delay jitter (also known as *Packet Delay Variation* (PDV) [19]) is defined as the mean variation in packet delay of consecutive packets being transmitted through the same network. The effects of PDV that may disturb the video quality when a required video frame is not available to be decoded can be reduced by a properly sized buffer at receiver. Nonetheless, this buffer will add an extra delay before the media starts playing. For interactive real-time applications (*e.g.*, VoIP) PDV can be a serious issue and therefore those applications may need QoS-aware enabled networks to provide a high quality channel.

In our framework we include a delay jitter computation algorithm in the RTCP protocol. It is an estimation of the statistical variance of the inter-arrival time of incoming RTP packets, measured in timestamp units. For example, if we transmit audio sampled at 8000 hertz, the unit is 1/8000 seconds. The interarrival jitter $Jitter_{new}$ is defined as the smoothed mean absolute value of the difference between the sending interval at a source and the interarrival time at a receiver. The value of $instantaneousjitter$ can be computed using Equation (2.2) where $sent_i$ is the RTP timestamp from packet i, rec_i is the time of arrival in RTP timestamp units for packet

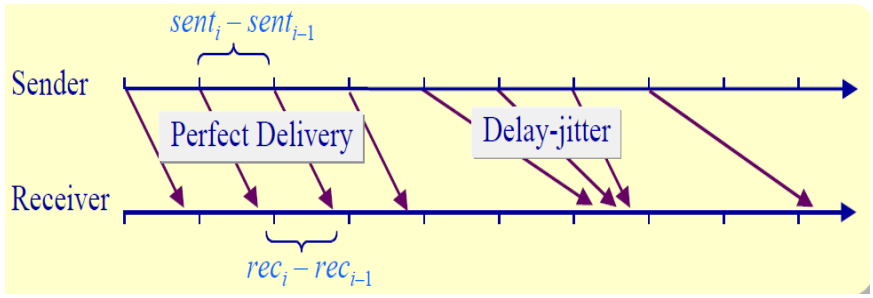

Figure 2.7: Jitter calculation.

i, $sent_{i-1}$ is the RTP timestamp from packet $i-1$ and rec_{i-1} is the time of arrival in RTP timestamp units for packet $i-1$.

$$instantaneous\ jitter = |(rec_i - rec_{i-1}) - (sent_i - sent_{i-1})| \tag{2.2}$$

$$Jitter_{new} = Jitter_{old} + (instantaneous\ jitter - Jitter_{old})/16 \tag{2.3}$$

The current value of $Jitter_{new}$ is sampled each time a reception report is released. It is proposed that the change in this jitter estimate could indicate congestion before it leads to packet loss. The RTP/RTCP implementation of our framework computes the delay jitter using Equations (2.2) and (2.3), according to the RFC-3550 for RTP [18].

2.5.3 Packet losses

In wireless networks different reasons could lead to lose packets, such as: saturated network links, collision, link breakages, poor signal power strength, among others. Packet losses are defined as the percentage of packets lost (P_{sent} - $P_{received}$) divided by the total number of packets sent (P_{sent}) by the source, according to Equation (2.4). Here, $P_{received}$ is the number of packets received. In this thesis, we have also computed the packet losses of each type of video frame, *i.e.*, I, P and B frames. This is due to the different priorities that each type of video frames have according to their importance in the video stream.

$$\%P_{loss} = \frac{P_{sent} - P_{received}}{P_{sent}} \cdot 100 \tag{2.4}$$

2.6 Video performance metrics

To measure the video quality obtained at the receiver side (*i.e.*, the destination node), objective and subjective measures may be used. Objective measures use algorithms to compute numerical values over the received video sequences, whereas subjective video quality methods are able to measure the video quality that is perceived by the human visual system (HVS). The subjective video quality methods are based on groups of trained/untrained users that watch the video content and provide ratings for quality [20]. In addition, to meet the ITU-T recommendations for subjective quality evaluation, the tests must follow strict evaluation conditions such as including conditions on viewing distance, room illumination, test duration, and evaluators' selection [21]. Basic subjective measures have also been provided in our research work, used in Chapter 3 and explained in details in Appendix A.

In the following, we list some of the most used video performance metrics:

- **MSE (Mean Square Error):** It is the mean of the squared differences between the values of pixels in two images.
- **PSNR (Peak Signal to Noise Ratio):** The only difference between MSE and PSNR is that PSNR is the logarithmic representation of MSE. This metric is used in our performance evaluations. In the next subsection, we explain in detail its description.
- **VQM (Video Quality Measure):** VQM was developed by the institute for telecommunication science (ITS). It provides an objective measurement for perceived video quality by measuring the perceptual effects of video impairments including blurring, jerky/unnatural motion, global noise, block distortion and color distortion to combine them into a single metric.
- **SSIM (Structural Similarity Index):** SSIM was first presented in [22]. The difference between the previously described methods and SSIM is that SSIM uses structural distortion measurement instead of the error-based method. SSIM was designed to improve traditional methods such as PSNR and MSE, which have proven to be quite inconsistent with human visual perception. However, SSIM is more complex to b obtain compared to PSNR.

All these metrics described above, were mainly designed to test video compression codecs, where only degradation of the compressed data is presented. Nonetheless, in our framework frame losses are also present due to congestion in the network, collisions and other effects. Due to that, we have implemented a basic forward error correction (FEC) technique that consists on substituting a last frame by another previously received. Basically, we identify each one of the lost frames and substitute them by the last received one of the same type (*i.e.*, I, P or B). In the next subsection we will describe briefly PSNR, as a video performance metric used in our thesis due to its simplicity.

2.6.1 Peak Signal to Noise Ratio (PSNR)

Over years, the image and video processing research community has been using the mean squared error (MSE) and the peak signal-to-noise ratio (PSNR) as basic metrics to measure the subjective quality of experience of users. PSNR is the logarithmic representation of MSE. The reasons for the popularity of these two metrics is due to the simplicity for computing their formulas. Both are simple to understand and implement to be computed. Basically, the higher the PSNR, the better the quality of the reconstructed picture. The lower the value of MSE, the lower the error. Furthermore, to compute the PSNR, we first must calculate the mean-squared error between an original picture, $P_{original}$, and its corresponding decoded picture, $P_{decoded}$, both of size MxN pixels, following these Equations:

$$MSE = \left(\frac{1}{M \cdot N}\right) \sum_{m=0}^{M-1} \sum_{n=0}^{N-1} (P_{original}(m,n) - P_{decoded}(m,n))^2 \tag{2.5}$$

$$PSNR(db) = 10 \cdot \log \frac{R^2}{MSE} \tag{2.6}$$

Where R is the maximum possible pixel value of the input picture. For example, R is 255 in our case ($R = 2^8$-1) when the pixels are represented using 8-bits per sample.

2.7 Conclusions

The number of users of multimedia services is expected to continue increasing and due to that it is essential to develop architectures able to provide QoS over ad hoc networks, which is still an open challenging issue. In our framework we decided to work with video format MPEG-2 due to its simplicity and enough video quality for video-reporting messages about incidents in the city. In this Chapter, digital video coding techniques and QoS support for video-streaming have been explained. The protocol stack with QoS support RTP/RTCP has been described. In addition, the most important network performance metrics have been defined and the way to compute them as well. Due to its simplicity, PSNR has been selected to take measures of the video quality in our simulations. In addition, the typical QoS metrics (*e.g.*, losses, delay and jitter) to carry out the performance evaluation of our proposals, have been described.

Chapter 3

A Multi-User Game-Theoretical Multipath Routing Protocol to Transmit Video-Reporting Messages over Mobile Ad Hoc Networks

In this Chapter we propose a multipath routing protocol to provide video-reporting messages over MANETs using a novel multi-user game-theoretical approach. This new approach could be used in smart cities where management and prevention of accidents is one of its most important goals. Finally, simulations show the benefits of our proposal, taking into account the mobility of the nodes and the presence of interfering traffic. The content of this Chapter has been published in [23] and [24].

3.1 Introduction

A Mobile Ad hoc NETwok (MANET) is a group of self-organized wireless mobile nodes (MNs) able to communicate with each other without the need of any fixed network infrastructure nor centralized administrative support. MANETs suffer from link breakages due to nodes that move and have limited battery life, which produce changes in the network topology. In addition, the transmission range (TR) in such mobile devices is limited, so multi-hop paths as well as efficient routing protocols will be needed. Each MANET node will operate both as a terminal host and as a forwarding node. MANETs should adapt dynamically to be able to maintain communications despite of these issues [25].

MANETs have attracted much attention from the research community over the last years and important technical advances have risen. These multi-hop networks are foreseen as an important kind of next generation access networks, where multimedia services will be demanded by end users from their wireless devices everywhere. In many situations and areas, users may spontaneously form an infrastructureless operation ad hoc network to share their resources and contents. Besides, MANETs can be used together with existing cellular networks forming a hybrid cellular ad hoc network as MANETs can extend the coverage, capacity and interconnectivity of current cellular networks [26].

Multimedia services require Quality of Service (QoS) provision. The special characteristics of MANETs, such as mobility, dynamic network topology, energy constraints, infrastructureless and variable link capacity, make the QoS provision over these networks an important challenge. In particular, instead of using fixed network configuration parameters, a better solution would be to adjust the framework parameters according to the current environmental conditions.

Our research in this Chapter focuses on the deployment of an efficient multipath routing protocol to provide video-reporting messages over MANETs. In this Chapter, we aimed to design a dynamic selection of data forwarding paths using a game-theoretical forwarding algorithm in a multipath multimedia routing protocol MMDSR that we present in section 3.3. Our contribution seeks to enhance the overall performance of the video-reporting service.

The rest of the Chapter is structured as follows. Section 3.2 includes some relevant related work. In section 3.3 we summarize the features of our multipath routing protocol. Section 3.4 gives a brief explanation of the game-theoretical proposal. Section 3.5 describes analytically our novel game-theoretical model to transmit video-reporting messages over MANETs. Section 3.6 describes a method to calculate a specific parameter of the model. Simulation results are shown and analyzed in section 3.7. Finally, conclusion is given in section 3.8.

3.2 Related Work

Routing is the process of selecting the best path or paths in a network through which data will be forwarded. Forwarding paths are not necessarily the shortest ones, but rather they could be selected seeking to improve the service performance. Proposals of routing protocols for ad hoc networks similar to our work can be classified in four categories: (a) single path routing; (b) general multipath routing; (c) multipath routing used to transmit video; and (d) game-theoretical algorithms used in the routing. In the following we summarize some representative works related to our proposal for each category.

(a) Regarding single path routing, many protocols were designed in the last years for MANETs [27, 28, 29, 30, 31, 32, 33] based on improvements of basic and widely referenced ad hoc routing protocols such as ad hoc on-demand distance vector (AODV) [34] and dynamic source routing (DSR) [12]. Based on AODV, [27] incorporates an admission control scheme and a feedback scheme to satisfy the QoS-requirements of real-time applications; [28] adds a route fragility coefficient (RFC) as a metric to find stable routes; [29] proposes an efficient algorithm to balance energy consumption among all participating nodes; and [30] provides n backup routes in case of link failure instead of one. On the other side, based on DSR, [31] presents a pragmatic scheme to establish and sustain trustworthy routes in the network; [32] introduces a new route maintenance strategy called distance based route maintenance (DISTANCE) to prevent link failure; and [33] uses the ant colony optimization (ACO) algorithm producing a significantly improvement in terms of packet losses, end-to-end delay, routing overhead and energy consumption.

(b) Some works like [35, 36, 37, 38, 39] tackle the congestion problem present when the MANET is heavily loaded, since this factor negatively affects the packet losses. To cope with this issue, multipath routing protocols were proposed to alleviate congestion, optimize the use of the scarce MANET resources, increase the packet delivery ratio and improve the offered quality of service. For example, authors in [35] proposed the congestion-adaptive routing protocol (CRP) to prevent congestion. Simulation results show that CRP improves significantly the packet loss rate and the end-to-end delay compared to AODV and DSR. In [36], the authors introduced a type of service aware routing protocol (TSA) which uses both the packet type of service and the traditional hop count as route selection metrics. This proposal tries to avoid congestion by distributing the load over a potentially greater area. A linear load balancing protocol using multiple paths is proposed in [37], where n routes are sorted in increasing order of their hop count and have assigned priority values so that the shorter the path the higher the priority of the path to be selected to distribute

the transmitted packets. In [38], the authors introduced a mechanism to find a primary forwarding route using the basic AODV engine and an alternative backup path to be used when the main route is broken. The backup path excludes nodes already used in the primary path, so that they are node-disjoint paths. The work [39] presented the Fibonacci multipath load balancing protocol (FMLB) for MANETs to distribute transmitted packets over multiple paths through the mobile nodes using an algorithm based on the Fibonacci sequence.

(c) Multipath routing protocols offer interesting benefits to increase the available bandwidth, which is suitable to transmit video over ad hoc networks where the bandwidth is a scarce resource. Several works such as [40, 41, 10, 42, 43] presented interesting approaches to transmit video flows over multipath frameworks. In [40], the authors analyzed the topic of multipath routing for multiple description video coding in wireless ad hoc networks. They found that genetic algorithms (GAs) are effective to address this type of cross-layer optimization problems. They demonstrate using numerical results the superior performance of their GA-based approach. In [41] the authors proposed an optimal routing algorithm to distribute video over multiple paths seeking to minimize congestion and to improve the video quality. In [10] the authors designed an adaptive multipath multimedia dynamic source routing (MMDSR) protocol able to self-configure dynamically depending on the state of the network while taking into account the special features of the video frames to distribute them over the multipath scheme. The authors in [42] proposed an extension of multipath optimized link state routing protocol (MP-OLSR) named fuzzy-based quality of service MP-OLSR (FQ-MP-OLSR) integrating two fuzzy systems. The first is used to calculate a multi-constrained QoS metric based on delay, throughput and signal to interference plus noise ratio (SINR) while the second is applied to adapt cost functions used to penalize paths previously computed by the Dijkstra's algorithm. Simulation results showed that FQ-MP-OLSR achieves a significant improvement in terms of QoS and quality of experience (QoE). The work in [43] presented a QoS-aware routing framework combining three QoS mechanisms, *i.e.*, cross-layer communication mechanism, session admission control and QoS-aware multipath routing to achieve an efficient video transmission over MANETs. Simulation results showed the improvement obtained in terms of video quality.

(d) Concerning the application of game theory in the routing for ad hoc networks, works in the literature deal mainly with two important issues: proposals that include incentives to *encourage nodes to cooperate* [44, 45] and proposals that apply game theory *to attain a QoS-aware framework*

[46, 47, 48]. In the case of MANET nodes that do not belong to a single authority, nodes do not have a common goal and seek to maximize their own utility trying to save their limited resources by reducing packet forwarding for others. Besides, mobility in MANETs causes hard challenges in the provision of the QoS required to distribute multimedia data. In [44], an analysis of cooperation incentives provided by reputation systems, price-based systems and an incentive strategy using game theory was presented. Also, the authors proposed an integrated system combining the previous strategies. Results clearly prove the benefits of the integrated system over the individual reputation system and the price-based system in terms of cooperation's effectiveness as well as in selfish node detection. In [45], the authors presented a novel incentive scheme for probabilistic routing which stimulates selfish nodes to participate. Results showed a 75.8% gain in delivery ratio compared to the case of a probabilistic routing providing no incentive. In [46], a dynamic probabilistic protocol based on game theory, called forwarding game routing protocol (FGRP), was introduced for the selection process of the forwarding nodes. In this protocol, a node is a player of the forwarding game and takes the forwarding decision upon the reception of a flooding packet. Each node tries to maximize its utility by selecting an appropriate strategy. Simulations show the benefits of FGRP in terms of end-to-end delay and packet delivery ratio. Current works in the literature that are similar to ours are [47, 48]. In [47] the authors use game theory to design a self-optimizing algorithm to minimize the end-to-end delay in a multi-class MANET. The approach consists of a fully distributed algorithm based on AODV for which they analytically prove that it reaches an optimal routing for each user in terms of delay, and which also minimizes the overall delay in the network. They apply a potential game that meets the principle of *individual optimization provides a global optimal configuration*. They include a numerical evaluation that shows improvement compared to AODV. In our case, we use a multipath (instead of only one path) forwarding scheme to transmit real video (instead of Poisson traffic) and we use several metrics (instead of only using the delay) to arrange the paths. The work [48] studies the optimal forwarding problem in MANETs based on a generalized two-hop relay (the source node replicates copies of its packets to other relaying nodes so that each packet travels at most two hops to reach its destination) with limited packet redundancy f (f-cast, each packet can be replicated to at most f different relaying nodes) for packet routing. They propose a forwarding game where each node i individually decides a probability p_i to send its own traffic and helps to forward other traffic with probability $1-p_i$. The payoff for a node is the achievable throughput capacity of its own traffic. They obtain the optimal forwarding strategy

that each node should adopt to ensure the optimum per node throughput capacity. Similarly to us they also mathematically derive a per node forwarding probability using game theory, although in their case it is used by a node to send/forward or not a packet, whereas in our case it is used by a node to decide if it sends a video frame through the best path or through the second best one. Besides, we use different forwarding schemes.

In this present Chapter, we deal with the issue of QoS provision and leave cooperation encouragement for future work. After analyzing the multipath routing protocols presented in this section, for our purpose of distributing video messages over MANETs and VANETs, the most suitable approaches as a reference are our previous proposals Multipath Multimedia Dynamic Source Routing (MMDSR) [10] and game-theoretical MMDSR (g-MMDSR) [49]. MMDSR is a QoS-aware self-configured multipath routing protocol that dynamically adapts to the changing environment, whereas g-MMDSR enhances MMDSR by including a 2-player game-theoretical algorithm in the forwarding scheme. To the best of our knowledge, the aim to apply together a QoS-aware multipath routing scheme and a multi-user game-theoretical approach that includes the particular features of the video frames into the game model to efficiently distribute video reporting messages over mobile ad hoc networks, is novel. In this Chapter, the multipath routing scheme of MMDSR is enhanced by including a multi-user game-theoretical algorithm so that competing nodes share the scarce resources in a more suitable and efficient way. Our previous proposal [49] introduced a 2-player game-theoretical routing scheme to improve MMDSR, and in this present Chapter we will develop a general multi-player game-theoretical routing protocol. In the next section, we summarize MMDSR in a nutshell.

3.3 Multipath Multimedia Dynamic Source Routing (MMDSR)

In this section, we give the main features of the MMDSR routing protocol. We further improve the routing scheme by designing a novel game-theoretical model to provide video-streaming in MANETs. The framework is able to provide video-streaming services over IEEE 802.11e [50] MANETs and to dynamically adapt to the changing network conditions inherent in MANETs.

3.3.1 Basics of the General Framework

The multipath routing scheme of MMDSR is based on the DSR (Dynamic Source Routing) protocol [12] to find available paths from source to destination. Video is distributed using RTP/RTCP (Real-time Transport Protocol/Real-time Control

Protocol) [18] over UDP as transport protocols. Our system uses a layered MPEG-2 VBR coding of the video flow, which is formed by sets of frames, usually 4 to 20 frames, called GoP (Groups of Pictures), see Figure 3.1. A GoP has three types of frames: I, P and B, and has a unique frame-pattern in a video repeated in each GoP. I (Intra) frames encode spatial redundancy, they form the base layer, provide a basic video quality and carry the most important information for the decoding process at the receiving side. The whole GoP would be lost if the corresponding I frame were not available at decoding time. P (Predicted) and B (Bi-directional) frames carry differential information from preceding (P) or preceding and posterior (B) frames, respectively. Considering these characteristics, we assign different priorities to the video frames according to their importance within the video flow. Therefore, I frames should have the highest priority, P frames the medium priority and B frames the lowest one.

In the MAC (Media Access Control) layer, we use the IEEE 802.11e [50] standard, which provides QoS support. It consists of four different Access Categories (AC), each with their own configuration parameters, *i.e.* contention window minimum (CW_{min}) and maximum (CW_{max}), arbitration interframe space (AIFS) and transmission opportunity (TxOp). The values of (CW_{min}), maximum (CW_{max}), arbitration interframe space (AIFS) and transmission opportunity (TxOp) are shown in 2.1 of Chapter 2. Each packet from the higher layers arrives at the MAC layer with a specific priority value and is mapped into the proper AC. We defined the mapping of the different packets into each one of the four AC_s as follows:

- AC0: signaling.
- AC1: high priority packets (I frames).
- AC2: medium priority packets (P frames).
- AC3: low priority packets (B frames + other best effort traffic).

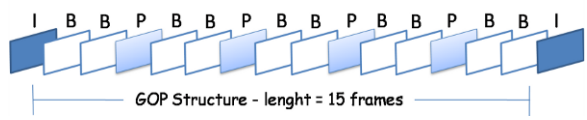

Figure 3.1: MPEG-2 GoP structure.

3.3.2 Multipath Routing Scheme in MMDSR

MMDSR is a previous proposal developed by member of our research group, of a multipath routing protocol that uses the standard DSR as the engine to search for available paths. MMDSR uses up to three paths through which the three types of video

frames will be sent. As Figure 3.2 shows, traditionally the most important video frames (I frames) would be sent through the best available path, P frames through the second best path and B frames through the third best path (worst one). In our results, we obtained that there are notable benefits in arranging two or three paths to transmit the video frames. However, arranging more than three paths in a multipath scheme does not provide a big improvement, while increases unnecessarily the management. Similar results were obtained in [51].

Figure 3.2: Multipath routing scheme using three paths.

The user requirements are negotiated using QoS parameters to provide the required image quality. We use the following parameters: minimum expected bandwidth (BW_{min}), maximum percentage of packet losses (L_{max}), maximum delay (D_{max}) and maximum delay jitter (J_{max}).

$$user\_req \equiv \{BW_{min}, L_{max}, D_{max}, J_{max}\} \tag{3.1}$$

3.3.3 MMDSR Control Packets

Decisions such as path selection or tuning of configuration parameters are operated from the source. MMDSR periodically discovers AP available paths between source and destination by sending monitoring *Probe Message* (PM) packets. After that, a *Probe Message Reply* (PMR) packet is generated at destination to carry the collected information about the quality of the available paths. The reduced size of these packets (around 64 bytes, depending on the number of paths found out) and the low frequency of sending them (every 3–18 s depending on the network state, see Equation (3.4))

makes the incurred overhead almost negligible. Figure 3.3 shows PM and PMR packets which are periodically interchanged between source and destination.

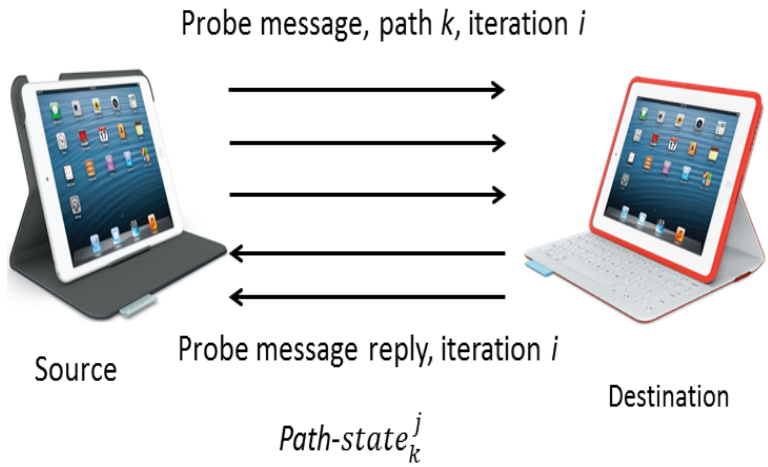

Figure 3.3: PM and PMR packets.

Then, a score is given to each one of the paths after analyzing the feedback information at the source node to classify them accordingly. That score is updated continuously after the reception of each PMR packet. Looking at the QoS parameters of the paths, the source selects three paths (if it is possible, or less if it is not) to compose the multipath scheme. The vector $path - state_k^j$ contains all the quality parameters calculated for each one of the available paths:

$$path - state_k^j \equiv \{BW, L, D, J, H, RM, MM\}_k^j \tag{3.2}$$

where j is the iteration number of the algorithm and k refers to each one of the paths (with $k \leq AP$). The QoS parameters are: available bandwidth (BW_k^j), percentage of packet losses (L_k^j), delay (D_k^j), delay jitter (J_k^j), hop distance (H_k^j), reliability metric (RM_k^j) calculated from the SNR (Signal to Noise Ratio) of the links involved in each path, and mobility metric MM_k^j calculated from the relative mobility of the neighboring nodes within each path. The last two metrics were previously proposed in [49].

This process is repeated periodically to refresh the paths since the topology of MANETs vary and might produce link breakages. The routing period depends on the network state, as it is explained in section 3.3.5.

3.3.4 Path Classification in MMDSR

Once the source has selected a set of paths that fulfil the requirements depicted in Equation (3.1), the classification of those paths is done by checking sequentially the qualifications of the QoS parameters, according to the following list:

1. $RM_k^j + MM_k^j$
2. H_k^j
3. BW_k^j
4. $L_k^j + J_k^j$
5. D_k^j

We first arrange the available paths looking at the metrics *RM* and *MM*, since we prefer the most reliable *RM* and stable *MM* paths to distribute video over MANETs. In case of draw, the decision is taken depending on the hop-count metric (H) which decides the shortest path. In case of another draw, we consider bandwidth (BW), then losses (L) and delay jitter (J), and finally delay (D). Nonetheless, other alternative algorithms to arrange the available paths could also be considered. Finally, the source selects k paths (with $k \leq AP$) to compose the multipath routing scheme. In our case, $k = 3$ paths. Notice that if only two paths were available, we still could differentiate both paths (*i.e.*, the best and the medium-quality path), but if only one was available then all the packets would be sent through that single path. Notice that we arrange the k paths dynamically through time, in each iteration j. This way, the multipath scheme adapts to the changing environment of MANETs.

3.3.5 MMDSR Self-Configuration

Due to the highly variable network topology of MANETs, any proposed routing protocol should be dynamic. Having this in mind, MMDSR is able to self-configure. Here, we will just point out the basics of the self-configuration operation.

Our framework monitors the current state of the network and in case of changes, the algorithm modifies the routing period of the algorithm and the thresholds to classify paths. We adjust those parameters dynamically depending on a parameter called *NState*, which brings information about the global network state and is updated by the algorithm iteration by iteration. *NState* for iteration j is computed as follows:

$$\begin{aligned} NState^j &= w_{RM} \cdot \overline{RM^j} + w_{MM} \cdot \overline{MM^j} + w_{BW} \cdot \overline{BW^j} + \\ &\quad w_L \cdot \overline{L^j} + w_D \cdot \overline{D^j} + w_J \cdot \overline{J^j} + w_H \cdot \overline{H^j} \end{aligned} \tag{3.3}$$

In Equation (3.3), the upper bars denote averages and the ws are the weights assigned to each metric. When the source receives the feedback from the network

by means of PMR packets, it calculates the *NState* using Equation (3.3) from the QoS parameters of all the k paths (see Equation (3.2)) on that itereation j.

The routing period ($T_{routing}$) to refresh the multipath scheme also varies dynamically and is calculated according to Equation (3.4), so that when the network is behaving well (*i.e.*, $NState$ is high), $T_{routing}$ is also high and the paths that form the multipath scheme will be used longer. Conversely, if the network is behaving bad (*i.e.*, $NState$ is low) then $T_{routing}$ is low and the paths are refreshed sooner.

$$T_{routing}^{j+1} = \gamma \cdot NState^{j} + \theta \tag{3.4}$$

To obtain the previous Equation, a high number of simulations were conducted under a wide range of network conditions where the network performance was good, normal and bad. For the scenario under consideration (also used in the present paper), the obtained values were $\gamma = 10$ and $\theta = 3$.

Till now, we have summarized the basics of the QoS-aware adaptive multipath routing protocol. Next, we introduce our novel game-theoretical routing scheme to further improve the transmission of video over MANETs.

3.4 A Game-Theoretical Routing Protocol for MANETs

Game Theory is a branch of applied mathematics that has been used basically in economics to model competition between companies. During the last years, Game Theory has also been used in networking to solve routing and resource allocation problems in a competitive environment. MANET nodes take decentralized decisions, and resource management mechanisms can help those nodes to behave constructively improving the network performance as a whole [52]. In our approach we apply Game Theory in the multipath routing protocol to further improve our proposal. We assume that each source node has a set of I, P and B video frames of a video flow to be sent; also, we assume that each source has three paths through which those frames will be sent. Nodes *play* a *routing game* to distribute the video flows seeking their own best performance. The *players* of the game are the MANET nodes and the *action* of the game is to select the proper route to forward their video-streams. In the following section, we will introduce the game-theoretical proposal included in the multipath routing scheme.

3.4.1 The Bases of Our Proposal

Figure 3.4 shows the proposed architecture. We assume N connections (S_1-D_1, S_2-D_2, ..., S_N-D_N) and three paths. It is likewise possible to apply the proposal to any MANET independently of the number of connections, nodes and paths.

So far, nodes always try to send the most important video frames through the best available path obtained by the multipath routing protocol. This means that I frames, which are the biggest ones and carry the most important video information, will be

sent through the best path, whereas the least important frames (*i.e.*, B frames) will be sent through the worst one. Nevertheless, if each node sends the most important frames through the best path, this path could get congested. As a consequence, that best path could suffer more losses than the others, which would lead to classify it as a worse path. This behavior could produce an oscillatory performance that might affect the video experience of users if it happened frequently.

To cope with this issue, users could *play a game* such that the best two paths (best, medium) could be selected by each player to transmit the most important video frames (*i.e.*, I+P frames). That is, each user could prefer to send sometimes the most important frames through the medium-quality path. Just for simplicity, B frames are considered always to be sent through the third path, which is the worst one. Also, I and P frames belonging to the same video stream are going to be sent through the same path to make more evident the inconveniences of sharing the same path, since there are more P frames than I frames per flow.

In our game, in each iteration, users select paths for their respective video flows. As it is shown in Figure 3.5, we have three possible situations. Without playing the game, all users would always send the important frames through the best path (Figure 3.5(a)). Alternatively, they could play our routing game. Notice that the second case (Figure 3.5(b)) is worse than the first case(Figure 3.5(a)) for all users since they are sending their frames together through the medium-quality path instead of together through the best path. Nevertheless, this should not happen often. In the third case (Figure 3.5(c)), I+P frames will be sent through the available best path by each user with a certain probability p and through the second best path available with a probability $1 - p$.

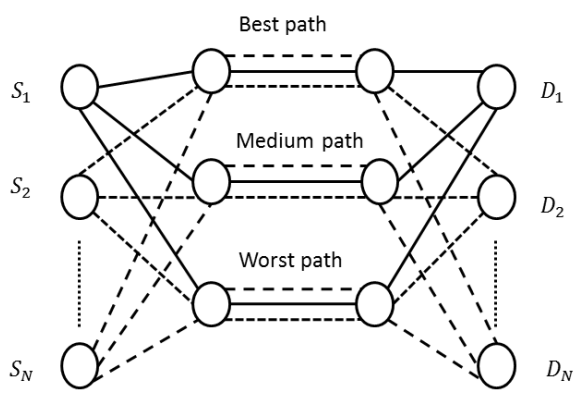

Figure 3.4: Proposed framework to send the video frames.

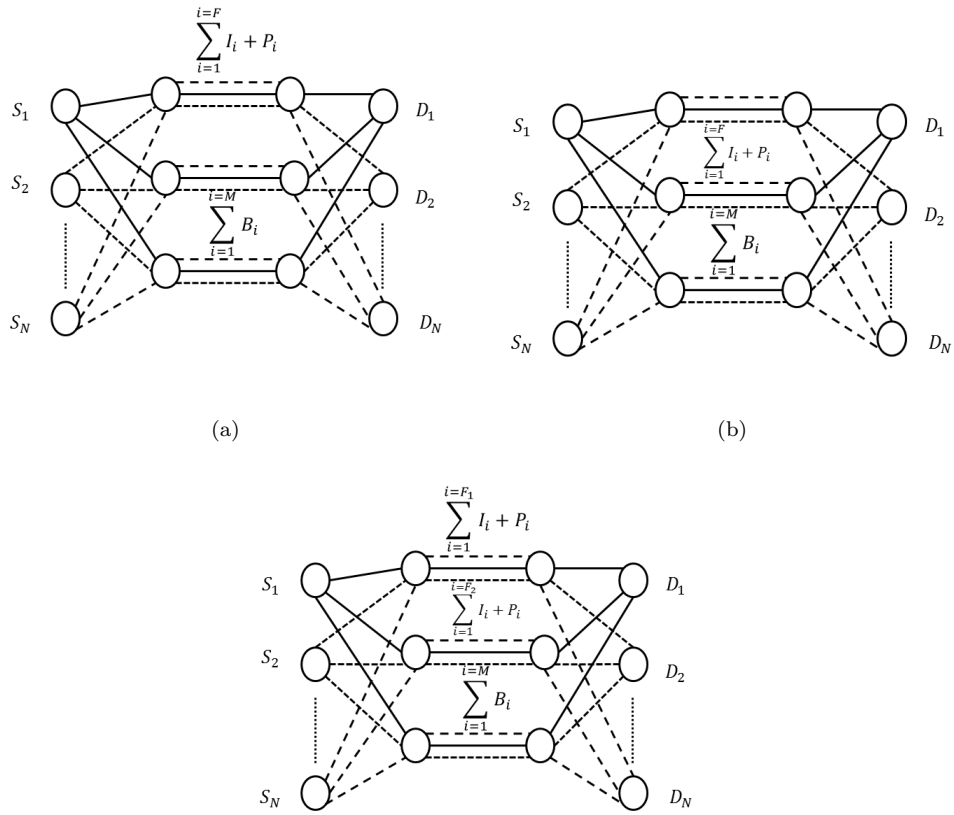

Figure 3.5: Three possible allocation situations after playing the game. F and M represent the number of (I+P) and B frames to be sent, respectively. All the B frames are always sent through the worst path. (**a**) All the I+P frames are sent through the best path; (**b**) All the I+P frames are sent through the medium-quality path; (**c**) I+P frames will be sent through the best path with a certain probability p and through the second best path with a probability *1-p*. F_1 and F_2 represent the number of (I+P) frames sent through the best path and through the medium-quality path, respectively, being $F = F_1 + F_2$.

Notice that players (users) must decide their choices (*i.e.*, their corresponding probability p) simultaneously and without communicating with each other. If we have a number of I+P frames to be sent equal to F, depending on the p value, a number of I+P frames equal to F_1 will be sent through the best path and a number of I+P frames equal to F_2 will be sent through the medium-quality one, being $F = F_1 + F_2$. M is the number of B frames to be sent, always through the worst path.

In the next section we will compute the optimal probability p (called p^*) of sending I+P frames through the best path that produces the best outcome for each player.

3.5 Game-Theoretical Routing Scheme for Video-Streaming in MANETs

In this section we first state the description of our basic game applied for our framework. We the develop the game-theoretical scheme for MANETs analyzing the benefit to transmit I+P video frames through the best path, Finally, we design the utility function of our game-theoretical approach.

3.5.1 General basis of our game-theoretical approach

A *game* can be described by listing the players participating in the game, a set of strategies for those players, and a specification of payoffs for each combination of strategies. Let S be a finite set of N players $1, ..., N$. Each player i has a finite set of available actions A_i. Let $a_i \in A_i$ be each particular action chosen by player i. The action space, A, is the cartesian product of all A_i, *i.e.*, $A = A_1 \times A_2 \times ... A_N$. An N-tuple action, a, is a point in the action space A. A *pure strategy* provides a complete definition of how a player will play a game. In particular, it determines the move a player will make for any situation it could face. A *mixed strategy* of player i, α_i, is an assignment of a probability, $p_i \in P = [0, 1]$, to each pure strategy. This allows a player to randomly select among the set of pure strategies. Let $\alpha = (\alpha_1, \alpha_2, ..., \alpha_N)$ be the mixed strategy profile, then the probability that a particular N-tuple action, $a = (a_1, a_2, ..., a_N)$, will occur, $p(a)$, is formed from the product of the probabilities assigned to a by α. Let u_i be the *utility function* of player i in the strategic form game occurring in each stage. The utility function is a mathematical description of preferences that maps the action space to a set of real numbers. A utility function for a given player assigns a real number for every possible outcome of the game, so that a higher number implies that the outcome is more preferred.

$$u_i : A \rightarrow R \tag{3.5}$$

$U_i(\alpha)$ is the expected utility for player i for the mixed strategy profile α, and has

the following expression:

$$U_i(\alpha) \equiv \sum_{a \in A} p_a \cdot u_i(a) \tag{3.6}$$

A strategic game G can be expressed using three primary components: the set of players S, the action space A, and the set of individual utility functions for player i, u_i.

$$G = (S, A, u_i) \tag{3.7}$$

A mixed strategies extension to G is given by the next expression, where $\Delta(A_i)$ is the set of all probability distributions over A_i and U_i is the set of all expected utilities to i.

$$G' = (S, \Delta(A_i), U_i) \tag{3.8}$$

A *best response* is a strategy which produces the most favorable outcome for a player, taking other players' strategies as given. A *Nash Equilibrium* (NE) [53] is a solution in which each player plays a best response to the strategies of other players. Each player is assumed to know the strategies of the other players, and no player has incentive to unilaterally change their current strategy while the other players keep theirs unchanged. Players are in equilibrium if a change in strategies by any one of them would lead that player to earn less than if they remained with their current strategy. It is a mathematical fact that every mixed extension of a strategic game has at least one *mixed strategy Nash equilibrium* [53].

To define best responses more generally, we need a notation for the set of strategies used by all players other than player i, named α_{-i}:

$$\alpha_{-i} = (\alpha_1, ..., \alpha_{i-1}, \alpha_{i+1}, ..., \alpha_N) \tag{3.9}$$

Strategy α_i^* is a best response for player i to the strategies of all players except i, α_{-i}^*, if:

$$U_i(\alpha_i^*, \alpha_{-i}^*) \geq U_i(\alpha_i, \alpha_{-i}^*), \ \ \forall\, \alpha_i \ \in \ \Delta(A_i) \tag{3.10}$$

This means that if α_i^* is a best response for player i to the assumed set of strategies α_{-i}^* played by the other *N-1* players, then it must give player i a payoff at least as large as the player would get if they placed any other strategy α_i from their set of allowed strategies. Equivalently, a best response (BR) correspondence to player i is given by :

$$\alpha_i^* \ \in \ BR_i(\alpha_{-i}) = argmax_{\alpha_i \in \Delta(A_i)} U_i(\alpha_i, \alpha_{-i}) \tag{3.11}$$

Let us remark that $argmax_x F(x)$ is the value of x for which $F(x)$ has the largest value. A joint strategy $\alpha^* = (\alpha_1^*, ..., \alpha_N^*)$ is a NE if, for each player i, α_i^* is a best response to α_{-i}^*.

Remember that every finite game (finite number of players, each of which with a finite set of strategies) has Nash equilibria in either mixed or pure strategies [54, 55].

3.5.2 The Benefit of Using a Particular Path to Transmit I+P Video Frames

Before defining the player's utility of the game, we will define a parameter that evaluates the benefit of using a particular path. As we have mentioned before, we assume that we always have at least two available paths (best and medium-quality paths) to send packets. Each path will have its own benefit as we describe next.

Definition: *The benefit of a path$_k$ is:*

$$\beta_k = \begin{cases} \phi_k, & \text{if the path fulfills the QoS requirements (see Equation(3.1))} \\ 0, & \text{otherwise} \end{cases} \tag{3.12}$$

where $\phi_k \in \mathbb{R}^*$.

Let us assign $\phi_k = \phi_b$ as the benefit for the best path and $\phi_k = \phi_m$ as the benefit for the medium-quality path, where ϕ_b and $\phi_m \in \mathbb{R}^*$. Later, we will relate ϕ_b and ϕ_m with the subjective QoS experienced by the users regarding the video frames received from each path (see Equation (3.23)). Strategy α_i is defined as follows:

$$\alpha_i = \begin{cases} \text{Transmit using the best path.} \\ \text{Transmit using the medium-quality path.} \end{cases} \tag{3.13}$$

Probability p is the probability of sending (I+P) frames through the best path and probability $(1-p)$ is the probability of sending those frames through the medium-quality path.

3.5.3 Design of the Utility Function

The utility function U_i designed for our game-theoretical routing protocol aims at achieving two goals: Minimizing the rate of (I+P) frames lost and minimizing the delay jitter, since these two parameters are most significant in video-streaming services. An initial short delay can be easily bearable by the user. Part of that delay would be produced after gathering frames in the reception buffer to reorder frames before the decoding process. The proposed utility function for player i is the following:

$$U_i = \underbrace{\left(\frac{n_{rb,i} - n_{sb,i}}{n_{sb,i}}\right) \cdot \phi_{b,i} \cdot \frac{p_i^2}{J_{b,i}}}_{\text{Best path}} + \underbrace{\left(\frac{n_{rm,i} - n_{sm,i}}{n_{sm,i}}\right) \cdot \phi_{m,i} \cdot \frac{(1-p_i)^2}{J_{m,i}}}_{\text{Medium path}} \tag{3.14}$$

All variables presented in Equation (3.14) are defined in Table 3.1.

Table 3.1: Definitions of the variables presented in Equation (3.14).

Variable	Definition
$i = 1, 2, 3..., N$	generic player, being N the number of players.
p_i	Player's i probability of sending the (I+P) frames through his/her best path.
$\phi_{b,i}$	Player's i benefit for the best path.
$\phi_{m,i}$	Player's i benefit for the medium-quality path.
$n_{s,i}$	Number of (I+P) frames sent by player i through the best and the medium-quality path.
$n_{sb,i}$	Number of (I+P) frames sent by player i through the best path.
$n_{rb,i}$	Number of (I+P) frames received from player i through the best path.
$n_{sm,i}$	Number of (I+P) frames sent by player i through the medium-quality path.
$n_{rm,i}$	Number of (I+P) frames received from player i through the medium-quality path.
$J_{b,i}$	Delay jitter of player i through the best path.
$J_{m,i}$	Delay jitter of player i through the medium-quality path.

Now let us relate $n_{sb,i}$ and $n_{sm,i}$ with $n_{s,i}$:

$$n_{sb,i} = p_i \cdot n_{s,i} \tag{3.15}$$

$$n_{sm,i} = (1 - p_i) \cdot n_{s,i} \tag{3.16}$$

where $n_{s,i} = n_{sb,i} + n_{sm,i}$.

Substituting Equations (3.15) and (3.16) in Equation (3.14) we get the following:

$$U_i = \underbrace{\left(\frac{n_{rb,i} - p_i \cdot n_{s,i}}{p_i \cdot n_{s,i}}\right) \cdot \phi_{b,i} \cdot \frac{p_i^2}{J_{b,i}}}_{\text{Best path}} + \underbrace{\left(\frac{n_{rm,i} - (1 - p_i) \cdot n_{s,i}}{(1 - p_i) \cdot n_{s,i}}\right) \cdot \phi_{m,i} \cdot \frac{(1 - p_i)^2}{J_{m,i}}}_{\text{Medium path}} \tag{3.17}$$

Notice that each player makes his/her own path classification, *i.e.*, each player might have different best and medium-quality paths.

In Equation (3.14), we have made our utility function U_i be proportional to the negative of the amount of I+P frames losses. This way, the utility increases as the losses decrease, for both the best and the medium-quality paths. In Equation (3.14), $\left(\frac{n_{rb,i} - n_{sb,i}}{n_{sb,i}}\right)$ is the negative of the amount of I+P frame losses through the best path, whereas $\left(\frac{n_{rm,i} - n_{sm,i}}{n_{sm,i}}\right)$ is the negative of the amount of I+P frame losses through the

medium-quality path. In addition, U_i is a concave function so that we ensure to have a p value that produces the maximum utility.

Besides, U_i is proportional to the benefit of the path (β_k, expressed in Equation (3.12)), that equals ϕ_b and ϕ_m for the best and the medium-quality path, respectively. Finally, U_i is inversely proportional to the jitter delay, so that the utility increases as the jitter delay decreases. This is reflected with the factors $(\frac{1}{J_{b,i}})$ and $(\frac{1}{J_{m,i}})$, for the best and the medium-quality paths, respectively. We can see a numerical example of the utility function in section (3.7.2.3).

Depending upon the values of the utilities, pure strategies may not exist, but in that case there are always mixed strategies [54, 55]. The mixed strategy α_i^* is a Nash equilibrium (NE) if the utilities $U_i(i = 1, ..., N)$ satisfy Equation (3.11). If there exists a mixed Nash equilibrium, player i will have a best response. To obtain it, U_i must be maximized:

$$\frac{\partial U_i}{\partial p_i} = 0 \tag{3.18}$$

For the sake of a clearer writing we will omit the i index to refer the user in the previous variables shown in Table 3.1. Thus, we will use n_{sb} instead of $n_{sb,i}$, and so on.

Then, applying Equation (3.18) in Equation (3.17) we obtain:

$$\frac{\partial U_i}{\partial p_i} = -2 \cdot p_i \cdot \left(\frac{\phi_b}{J_b} + \frac{\phi_m}{J_m}\right) + \frac{\phi_b}{J_b} \cdot \frac{n_{rb}}{n_s} - \frac{\phi_m}{J_m} \cdot \frac{n_{rm}}{n_s} + 2 \cdot \frac{\phi_m}{J_m} \tag{3.19}$$

To simplify the previous Equation, we assume that J_b, J_m, n_{sb}, n_{sm} and n_s are higher than zero. This assumption has sense since a jitter equal to zero is very improbable and at least one frame should have been sent as well. We define the following variables:

$$\hat{\phi}_b = \frac{\phi_b}{J_b},\ \hat{\phi}_m = \frac{\phi_m}{J_m},\ \hat{n}_b = \frac{n_{rb}}{n_s},\ \hat{n}_m = \frac{n_{rm}}{n_s} \tag{3.20}$$

Next, we substitute Equation (3.20) in Equation (3.19) and we get:

$$\frac{\partial U_i}{\partial p_i} = -2 \cdot p_i \cdot \left(\hat{\phi}_b + \hat{\phi}_m\right) + \hat{\phi}_b \cdot \hat{n}_b - \hat{\phi}_m \cdot \hat{n}_m + 2 \cdot \hat{\phi}_m \tag{3.21}$$

Then, by combining both Equations (3.18) and (3.21), we attain the solution for the best probability of sending (I+P) frames through the best path, that gives a NE in the utility function U_i. This is called as the best response of the game. Thus, using p_i^* to compute the probability of sending I+P frames through the best path, is a strategy which produces the most favorable outcome for player i, taking the other players' strategies as given.

$$p_i^* = \frac{\hat{\phi}_b \cdot \hat{n}_b + \hat{\phi}_m \cdot (2 - \hat{n}_m)}{2\left(\hat{\phi}_b + \hat{\phi}_m\right)} \tag{3.22}$$

This way, each player i will continuously update his/her best response p_i^* using Equations (3.22) and (3.20). To do so, the user easily obtains from the RTCP feedback

packets: the number of I+P frames received so far from the best and the medium-quality paths (n_{rb} and n_{rm}, respectively), the number of I+P frames sent so far (n_s) and the jitter delay through the best and the medium-quality paths (J_b and J_m, respectively). In the next section, we explain how the user computes the benefits for the best and the medium-quality paths.

3.5.4 Computation of the benefit of using a path

We have designed the value of the benefit of a path to be proportional to the subjective video quality perceived by the user regarding the video frames received from that path. In this work, we use the MOS (Mean Opinion Score) as a measure of the subjective QoS.

Accordingly, we define the following Equations to compute the benefits of the best and medium-quality paths, ϕ_b and ϕ_m, respectively:

$$\phi_b = k_b \cdot MOS_b \;\; and \;\; \phi_m = k_m \cdot MOS_m \tag{3.23}$$

where k_b and k_m are constants, $[k_b\ ,\ k_m] \in \mathbb{R}^*$.

Notice that k_b and k_m cannot equal zero because in this case, ϕ_b and ϕ_m would be zero too, which means that both paths would not satisfy the QoS parameters (see Equation (3.12)). The first condition for a path to be used by the sources is Equation (3.12); otherwise that path would not be taken into consideration.

Substituting Equation (3.23) in Equation (3.20), we get:

$$\hat{\phi}_b = \frac{\phi_b}{J_b} = \frac{k_b \cdot MOS_b}{J_b} \;\; and \;\; \hat{\phi}_m = \frac{\phi_m}{J_m} = \frac{k_m \cdot MOS_m}{J_m} \tag{3.24}$$

Next, using Equation (3.24) in Equation (3.22) we have this expression for the best response probability, p_i^*:

$$p_i^* = \frac{\left(\frac{k_b \cdot MOS_b}{J_b}\right) \cdot \hat{n}_b + \left(\frac{k_m \cdot MOS_m}{J_m}\right) \cdot (2 - \hat{n}_m)}{2 \cdot \left(\frac{k_b \cdot MOS_b}{J_b} + \frac{k_m \cdot MOS_m}{J_m}\right)} \tag{3.25}$$

Let $\frac{k_b}{k_m} = k_{b/m}$. As k_m is different from zero, we can divide the whole Equation (3.25) by k_m. After substituting, we obtain the Nash Equilibrium strategy for player i:

$$p_i^*(k_{b/m}) = \frac{\left(\frac{k_{b/m} \cdot MOS_b}{J_b}\right) \cdot \hat{n}_b + \left(\frac{MOS_m}{J_m}\right) \cdot (2 - \hat{n}_m)}{2 \cdot \left(\frac{k_{b/m} \cdot MOS_b}{J_b} + \frac{MOS_m}{J_m}\right)} \tag{3.26}$$

We designed U_i to be a concave function, so that there is one p^* value where U_i is on its maximum value. Due to that, $\frac{\partial^2 U_i}{\partial^2 p_i}$ must be less than zero. This way, deriving

Equation (3.21) we obtain:

$$\frac{\partial^2 U_i}{\partial^2 p_i} = -2 \cdot \left(\hat{\phi}_b + \hat{\phi}_m\right) \tag{3.27}$$

Since we need that $\frac{\partial^2 U_i}{\partial^2 p_i} < 0$,

$$\hat{\phi}_b + \hat{\phi}_m > 0 \ ; \ \forall \ [\phi_b, \ \phi_m] \in \ \mathbb{R}^*, \quad [J_b, \ J_m] \in \ \mathbb{R}^*_+ \tag{3.28}$$

Concluding, if player i adopts the strategy to send his/her (I+P) frames through the best path with a certain probability that equals p_i^* (see Equation (3.26)), his/her own benefit and the whole benefit of the network will be the highest.

All the values that are needed to compute p_i^*, except $k_{b/m}$, can be obtained during normal network operation from the feedback information given by the RTCP packets. This way, users will update the probability p_i^* with the current QoS parameters carried in the last received RTCP packet. Thus, $k_{b/m}$ is the single pending parameter to be obtained in Equation (3.26). In the next section, we will give a method to calculate analytically this parameter.

3.6 A Method to calculate $k_{b/m}$

MOS_b and MOS_m are the mean opinion score values measured in the best and the medium-quality path, respectively. They can take any value between 1 and 5, where 5 means *Excellent*, 4 means *Good*, 3 *Fair*, 2 *Poor* and 1 *Bad*. After carrying out a video-streaming test, we obtained the following results shown in Table 3.2 and Figure 3.6. Notice that these values depicted in Table 3.2 seem too high. The reason is that we focus on video-reporting messages for emergency services in smart cities. In this environment the goal is a fast alert of the authorities using a light and short video-reporting messages despite the fact that the video quality is not too good. For further information about the test please see the Appendix A.

Table 3.2: Mapping the mean opinion score (MOS) with the fraction of packet losses (FPL) for (I+P) frames in a general MANET scenario.

MOS	**FPL**
5-Excellent	FPL<20%
4-Good	20% $\leq$ FPL $<$ 30%
3-Fair	30% $\leq$ FPL $<$ 40%
2-Poor	40% $\leq$ FPL $<$ 50%
1-Bad	FPL $\geq$ 50%

Now, our goal is to calculate $k_{b/m}$ so we can compute the value of p_i^* using Equation (3.26). Three conditions will limit the computing of $k_{b/m}$: $0 \leq p_i \leq 1$ and U_i being a concave function. Below, we will study separately those three conditions.

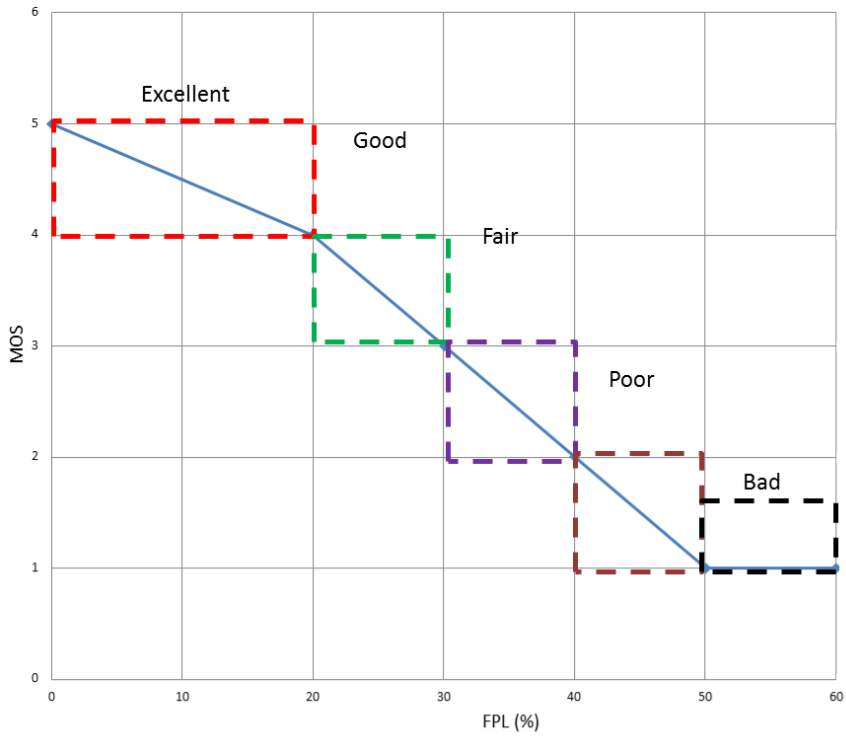

Figure 3.6: Subjective video quality measured by means of the mean opinion score (MOS) as a function of the fraction of packet losses (FPL).

3.6.1 Condition 1: $p_i \geq 0$

Combining Equation (3.22) with $p_i \geq 0$, we get that:

$$\frac{\hat{\phi}_b \cdot \hat{n}_b + \hat{\phi}_m \cdot (2 - \hat{n}_m)}{2\left(\hat{\phi}_b + \hat{\phi}_m\right)} \geq 0 \tag{3.29}$$

Remember that Equation (3.28), which is the denominator of Equation (3.29) must also be fulfilled.

Thus, we need:

$$\hat{\phi}_b \cdot \hat{n}_b + \hat{\phi}_m \cdot (2 - \hat{n}_m) \geq 0 \tag{3.30}$$

After that, we substitute Equation (3.24) in Equation (3.30) to get the following first condition to be fulfilled by $k_{b/m}$:

$$\frac{k_b \cdot MOS_b \cdot \hat{n}_b}{J_b} + \frac{k_m \cdot MOS_m \cdot (2 - \hat{n}_m)}{J_m} \geq 0 \tag{3.31}$$

Now, if we multiply the whole inequation (3.31) by $\frac{1}{k_m}$ ($\forall\ k_m\ \in\ \mathbb{R}^+$) and rename $\frac{k_b}{k_m}$ by $k_{b/m}$:

$$\frac{k_{b/m} \cdot MOS_b \cdot \hat{n}_b}{J_b} + \frac{MOS_m \cdot (2 - \hat{n}_m)}{J_m} \geq 0 \tag{3.32}$$

$$\frac{k_{b/m} \cdot MOS_b \cdot \hat{n}_b}{J_b} \geq \frac{MOS_m \cdot (\hat{n}_m - 2)}{J_m} \tag{3.33}$$

$$k_{b/m} \geq \frac{MOS_m \cdot J_b \cdot (\hat{n}_m - 2)}{MOS_b \cdot J_m \cdot \hat{n}_b} \tag{3.34}$$

Equation (3.34) needs to be fulfilled by $k_{b/m}$.

3.6.2 Condition 2: $p_i \leq 1$

Combining Equation (3.22) with $p_i \leq 1$ leads to:

$$\frac{\hat{\phi}_b \cdot \hat{n}_b + \hat{\phi}_m \cdot (2 - \hat{n}_m)}{2 \cdot \left(\hat{\phi}_b + \hat{\phi}_m\right)} \leq 1 \tag{3.35}$$

Looking at Equation (3.28), we can write:

$$\hat{\phi}_b \cdot \hat{n}_b + \hat{\phi}_m \cdot (2 - \hat{n}_m) \leq 2 \cdot \left(\hat{\phi}_b + \hat{\phi}_m\right) \tag{3.36}$$

Now, we substitute Equation (3.24) in Equation (3.36) to get:

$$\frac{k_b \cdot MOS_b \cdot \hat{n}_b}{J_b} + \frac{k_m \cdot MOS_m \cdot (2 - \hat{n}_m)}{J_m} \leq 2 \cdot \left(\frac{k_b \cdot MOS_b}{J_b} + \frac{k_m \cdot MOS_m}{J_m}\right) \tag{3.37}$$

Again, we multiply the whole inequation by $\frac{1}{k_m}$ ($\forall\ k_m\ \in\ \mathbb{R}^+$) and rename $\frac{k_b}{k_m}$ by $k_{b/m}$:

$$\frac{k_{b/m} \cdot MOS_b \cdot \hat{n}_b}{J_b} + \frac{MOS_m \cdot (2 - \hat{n}_m)}{J_m} \leq 2 \cdot \left(\frac{k_{b/m} \cdot MOS_b}{J_b} + \frac{MOS_m}{J_m}\right) \tag{3.38}$$

and removing $2 \cdot \left(\frac{MOS_m}{J_m}\right)$ from both sides of Equation (3.38), we reach to:

$$\frac{k_{b/m} \cdot MOS_b \cdot (\hat{n}_b - 2)}{J_b} \leq \frac{MOS_m \cdot \hat{n}_m}{J_m} \tag{3.39}$$

Now, we will find out which is the sign of the expression $(\hat{n}_b - 2)$. $\hat{n}_b$ was defined in Equation (3.20) as the relation between the number of I+P frames received from the best path (n_{rb}) and the total number of I+P frames sent (n_s).

$$\hat{n}_b = \frac{n_{rb}}{n_s} = \frac{n_{rb}}{n_{sb} + n_{sm}} \leq 1 \tag{3.40}$$

since $n_{rb} \leq n_{sb}$ (some I+P frames might have been lost through the best path) and $min(n_{sm}) = 0$ (that minimum value is obtained when no frame was sent through the medium-quality path).

Therefore,

$$\hat{n}_b - 2 \leq -1 \tag{3.41}$$

Finally, the second inequation to be fulfilled by $k_{b/m}$ is:

$$k_{b/m} \geq \frac{MOS_m \cdot J_b \cdot \hat{n}_m}{MOS_b \cdot J_m \cdot (\hat{n}_b - 2)} \tag{3.42}$$

3.6.3 Condition 3: Concave Function U_i

For U_i to be a concave function, Equation (3.28) must be fulfilled. Substituting Equation (3.24) in Equation (3.28), we get:

$$\frac{k_b \cdot MOS_b}{J_b} + \frac{k_m \cdot MOS_m}{J_m} > 0 \tag{3.43}$$

If we multiply the whole inequation by $\frac{1}{k_m}$ $(\forall\, k_m \in \mathbb{R}^+)$ and rename $\frac{k_b}{k_m}$ by $k_{b/m}$, we get:

$$\frac{k_{b/m} \cdot MOS_b}{J_b} > -\frac{MOS_m}{J_m} \tag{3.44}$$

Finally, we obtain Equation (3.45) as the third condition to be fulfilled by $k_{b/m}$:

$$k_{b/m} > \frac{-MOS_m \cdot J_b}{MOS_b \cdot J_m} \tag{3.45}$$

3.6.4 The Three Inequations to Be Fulfilled by $k_{b/m}$

We first rewrite the three inequations to be satisfied by $k_{b/m}$: Equations (3.34), (3.42) and (3.45). Besides, we will rename the thresholds of the three inequations as α_0, α_1 and α_2, respectively.

$$\begin{aligned} k_{b/m} &> \frac{-MOS_m \cdot J_b}{MOS_b \cdot J_m} = \alpha_0 \\ k_{b/m} &\geq \frac{MOS_m \cdot J_b \cdot (\hat{n}_m - 2)}{MOS_b \cdot J_m \cdot \hat{n}_b} = \alpha_1 \\ k_{b/m} &\geq \frac{MOS_m \cdot J_b \cdot \hat{n}_m}{MOS_b \cdot J_m \cdot (\hat{n}_b - 2)} = \alpha_2 \end{aligned} \tag{3.46}$$

We need to find a value for $k_{b/m}$ that satisfies the three inequations. First of all, the range of solutions for $k_{b/m}$ is $]K_{b/m}, +\infty)$, where $K_{b/m}$ will be the maximum value among α_0, α_1 and α_2. The probability $p_i^*(k_{b/m})$ of sending (I+P) frames through the best path is depicted in Figure 3.7. The limit of $p_i^*(k_{b/m})$ when $k_{b/m} \to \infty$ (horizontal asymptote) can be obtained from Equation (3.26) and it has the following value:

$$\lim_{k_{b/m} \to \infty} p_i^*(k_{b/m}) = \frac{\hat{n}_b}{2} \tag{3.47}$$

The vertical asymptote occurs at $k_{b/m}$-value that makes the denominator zero (*i.e.*, $k_{b/m} = \alpha_0$). We should find a value for $k_{b/m}$ in the range $]K_{b/m}, +\infty)$ with which $p_i^*(k_{b/m})$ changes softly throughout time. This way, the transition in the selection between the best and the medium-quality paths will be smooth producing a more stable system. For that, we calculate the first derivative $\frac{\partial p_i^*(k_{b/m})}{\partial k_{b/m}}$, which represents the slope value for each $k_{b/m} > K_{b/m}$ (*i.e.*, Zone of interest).

$$\begin{aligned} \frac{\partial p_i^*(k_{b/m})}{\partial k_{b/m}} = & \frac{\left(\frac{\hat{n}_b \cdot MOS_b}{J_b}\right) \cdot \left(\frac{2 \cdot k_{b/m} \cdot MOS_b}{J_b} + \frac{2 \cdot MOS_m}{J_m}\right)}{4 \cdot \left(\frac{k_{b/m} \cdot MOS_b}{J_b} + \frac{MOS_m}{J_m}\right)^2} \\ & - \frac{\left(\frac{2 \cdot MOS_b}{J_b}\right) \cdot \left(\frac{k_{b/m} \cdot MOS_b \cdot \hat{n}_b}{J_b} + \frac{MOS_m \cdot (2 - \hat{n}_m)}{J_m}\right)}{4 \cdot \left(\frac{k_{b/m} \cdot MOS_b}{J_b} + \frac{MOS_m}{J_m}\right)^2} \end{aligned} \tag{3.48}$$

After simplifying the Equation, we obtain:

$$\frac{\partial p_i^*}{\partial k_{b/m}} = \frac{\frac{MOS_b}{J_b} \cdot \frac{MOS_m}{J_m} \cdot (\hat{n}_b + \hat{n}_m - 2)}{2 \cdot \left(\frac{k_{b/m} \cdot MOS_b}{J_b} + \frac{MOS_m}{J_m}\right)^2} \tag{3.49}$$

Now, we isolate $k_{b/m}$ from Equation (3.49) in terms of $\frac{\partial p_i^*(k_{b/m})}{\partial k_{b/m}}$ and we get the following expression:

$$k_{b/m} = \frac{\pm\sqrt{\frac{\frac{MOS_b}{J_b}\cdot\frac{MOS_m}{J_m}\cdot(\hat{n}_b+\hat{n}_m-2)}{2\cdot\frac{\partial p_i^*(k_{b/m})}{\partial k_{b/m}}}} - \frac{MOS_m}{J_m}}{\frac{MOS_b}{J_b}} \tag{3.50}$$

Here, we can see that $(\hat{n}_b + \hat{n}_m - 2) \leq 0$, since $\hat{n}_b = \frac{n_{rb}}{n_s} = \frac{n_{rb}}{n_{sb}+n_{sm}} \leq 1$, and $\hat{n}_m = \frac{n_{rm}}{n_s} = \frac{n_{rm}}{n_{sb}+n_{sm}} \leq 1$. Look at Equation (3.40) to see the easy justification for both expressions.

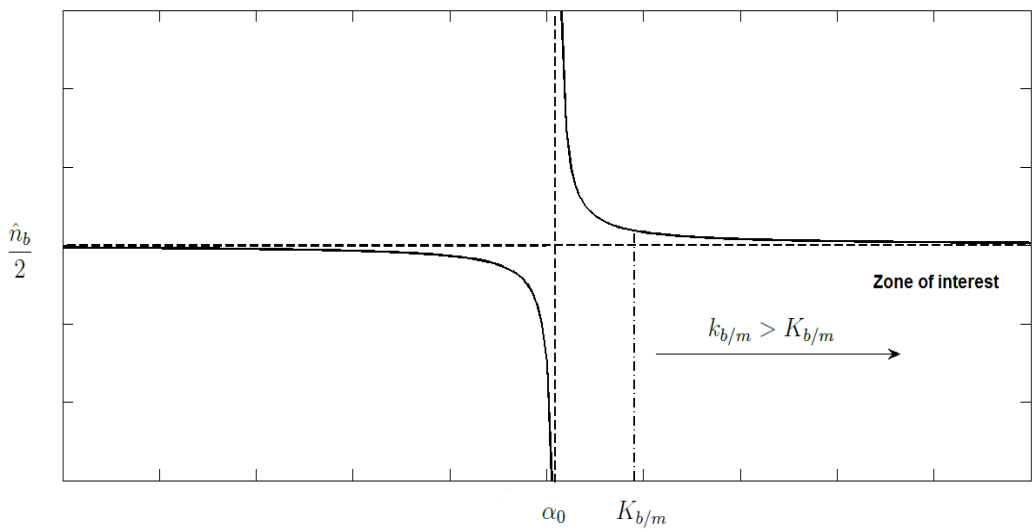

Figure 3.7: Best response probability p_i^* as a function of $k_{b/m}$, see Equation (3.26).

Consequently, we need that $\frac{\partial p_i^*}{\partial k_{b/m}} \leq 0$ to compute a proper $k_{b/m}$ value.

The parameters of Equation (3.50) that can be calculated by the nodes themselves during operation time are: the number of I+P frames received from the best path (n_{rb}) and the number of I+P frames sent through the best path (n_{sb}) to compute $\hat{n}_b = \frac{n_{rb}}{n_{sb}}$; the number of I+P frames received from the medium-quality path (n_{rm}) and the number of I+P frames sent through the medium-quality path (n_{sm}) to compute $\hat{n}_m = \frac{n_{rm}}{n_{sm}}$; the jitter delay through the best and the medium-quality paths (J_b and J_m, respectively)

computed from the RTCP packets; and the MOS of the best and the medium-quality paths, computed with Equation (A.1) presented in the Appendix A.

The only variable in Equation (3.50) that is not defined yet is $\frac{\partial p_i^*(k_{b/m})}{\partial k_{b/m}}$. To design a proper value for $\frac{\partial p_i^*(k_{b/m})}{\partial k_{b/m}}$, we carried out a high amount of simulations under different network conditions and with different values of $\frac{\partial p_i^*(k_{b/m})}{\partial k_{b/m}}$ and we noticed that with a value of $\frac{\partial p_i^*(k_{b/m})}{\partial k_{b/m}} = -0.2$, the variation of p_i^* throughout time was soft enough without sharp changes. From Equation (3.50), we see that we have two possible values for $k_{b/m}$, one of them is higher than $K_{b/m}$ and the other one is lower than $K_{b/m}$, so we take the one which belongs to the range $]K_{b/m}, +\infty)$.

To conclude with, Algorithm 1 summarizes the methodology to compute the best response probability p_i^* for player i to send his/her I+P frames through the best path, and with probability $(1 - p_i^*)$ through the medium-quality path.

Algorithm 1 Calculation of p_i^*, the best response probability for player i that maximizes his/her utility function U_i.

Require: Obtain updated QoS values from the periodically received RTCP packets.

1: Obtain the values of (MOS_b, MOS_m, J_b, J_m, $\hat{n}_b$, $\hat{n}_m$)

2: Compute the $k_{b/m}$ parameter designed that fulfills the requirements.

$$k_{b/m} = \frac{\pm\sqrt{\frac{\frac{MOS_b}{J_b}\cdot\frac{MOS_m}{J_m}\cdot(\hat{n}_b+\hat{n}_m-2)}{2\cdot\frac{\partial p_i^*}{\partial k_{b/m}}} - \frac{MOS_m}{J_m}}}{\frac{MOS_b}{J_b}}$$

3: Calculate the probability p_i^* to send I+P frames through the best path, that maximizes the utility function U_i

$$p_i^*(k_{b/m}) = \frac{\left(\frac{k_{b/m}\cdot MOS_b}{J_b}\right)\cdot\hat{n}_b + \left(\frac{MOS_m}{J_m}\right)\cdot(2-\hat{n}_m)}{2\cdot\left(\frac{k_{b/m}\cdot MOS_b}{J_b} + \frac{MOS_m}{J_m}\right)}$$

3.7 Simulation Results

In this section, we first depict a case study in a smart city about which we will set the NS2 simulation scenarios. The case study involves an emergency situation in MANETs

and VANETs to transmit a multimedia reporting message to the closest emergency unit and to alert other citizens around. After that, we present a performance evaluation in a MANET scenario in Subsection 3.7.2, and in a VANET scenario in Subsection 3.7.3.

3.7.1 A Case Study in a Smart City

We focus this work on two realistic smart city scenarios. A mobile adhoc network (MANET) and a vehicular ad hoc network (VANET), where emergency prevention and response are key issues. In the two scenarios under consideration, we assume that in a given moment an accident happened. Most of the citizens nowadays carry mobile phones or tablets. In the MANET/VANET scenario, we assume that a smart citizen/driver witnesses the situation, makes a short video-reporting message about the accident (the driver will just push a button that will make a small exterior car-mounted camera shoot the video, or alternatively the sensors deployed in the car will trigger the record of that video). The video-reporting message is sent through the MANET/VANET to the nearest emergency unit (e.g., police, ambulances, hospitals). Authorities will respond upon receiving the video and will take proper actions. This way, with a video-reporting message the emergency can be evaluated much better than with a simple text. It would be easier to ensure an accurate interpretation of the situation and the accident could be treated with the adequate level of seriousness. The smart citizen/driver sends a multimedia message which includes different information regarding the incident, e.g., the GPS location, a voice message and a short video of the incident. A suitable kind of smart-112 (911 in U.S.A) application in the citizen's mobile/vehicle sends the multimedia message to the smart-112 emergency center, who manages the proper actions for that incident. For instance, ambulances and paramedical will be sent there, traffic lights will turn to red around the accident, a green wave of traffic lights will help the ambulances get there sooner, the nearest hospital is warned, the doctors wait for the injuries, *etc.* A video of the incident facilitates a preliminary evaluation of the wounded people as well as helps to better determine the requirements needed to manage the dangerous situation. Our purpose in this work is to design a game-theoretical multipath routing protocol suitable to transmit those video-reporting messages over MANETs/VANETs in this kind of smart city scenarios. In the next section, a detailed performance evaluation in the MANET scenario will be studied, whereas a preliminar brief performance evaluation in a VANET scenario is done in section 3.7.3. Two proposals specifically designed for VANETs will be presented in Chapters 5 and 6.

3.7.2 Performance Evaluation in a MANET Scenario

We implemented our proposal in the open source network simulator NS2 [56] where we conducted simulations to evaluate the benefits of our approach. The MANET scenario was generated with the Bonnmotion tool [57]. The same quantity of

interfering CBR traffic was generated in each simulation to constrain the paths. For instance, for 2 players, we generated interfering CBR traffic at 300 Kbps, 200 Kbps for 3 players, 150 kbps for 4 players and 120 kbps for 5 players. This way, a total interference CBR raffic of 600 Kbps was sent whatever the number of players was. The simulation settings of the scenario are shown in Table 3.3. All the Figures show confidence intervals (CI) of 90 percent obtained from 20 simulations per point, each simulation with an independent Bonnmotion scenario.

The scenario used to test the proposal consists of a set of 50 mobile nodes distributed in a MANET of 520 $\times$ 520 m^2. The transmission range of the nodes is 120 m. Nodes move with a speed up to 2 m/s. Video flows are transmitted from nodes S_i to nodes D_i, $1 \leq i \leq N$ where N is the number of players (sources). The paths discovered by the MMDSR routing protocol are classified by each user using the MMDSR path classification described in section 3.3.4. Each source decides the path to route packets according to the game-theoretical routing algorithm presented in section 3.5 and depicted in Figure 3.5.

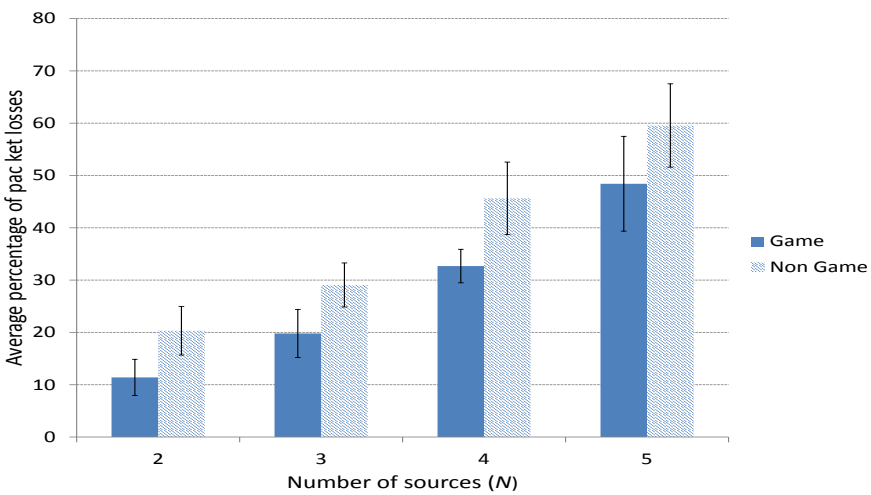

Figure 3.8: Average percentage of packet losses.

Figure 3.8 shows the average percentage of packet losses when using the game-theoretical scheme for a variable p value calculated using Algorithm 1 against the case of non using it (Non game option). We can clearly notice how including the game-theoretical routing scheme, the average video packet losses are reduced around 10% for $N = 2$ to 5 users. The average packet losses decreases due to the optimal selection of paths based on a probability value (*i.e.*, p^*) that optimally balances the load among the two paths at stake (*i.e.*, the best and the medium-quality paths). Figure 3.9 depicts the (I+P) packet losses throughout simulation time. In this case, we see how using the

game-theoretical model, losses are around 20% lower than non using it.

Table 3.3: Simulation settings of the MANET scenario.

Area	**520 × 520 m^2**
Number of nodes	50
Average node speed	2 m/s
Transmission range	120 m
Mobility Pattern	Random Waypoint
MAC specification	IEEE 802.11e, EDCF
$CW_{i,min}$, i ∈ (0,1,2,3)	(7, 15, 31, 63)
$CW_{i,max}$, i ∈ (0,1,2,3)	(15, 31, 1023, 1023)
$AIFS_i$, i ∈ (0,1,2,3)	(34 μs, 43 μs, 52 μs, 61 μs)
$(BW_{min}, L_{max}, D_{max}, J_{max})$	(50 Kbps, 35 %, 0.125 s, 0.004 s)
Nominal bandwidth	11 Mbps
Simulation time	1000 s
Video encoding	MPEG-2 VBR
Video bit rate	150 Kbps
Video sources	2 to 5
Video sequence sent	Traffic accidents [58]
Routing protocol	Game-theoretical algorithm + MMDSR
Transport protocol	RTP/RTCP/UDP
Maximum packet size	1500 Bytes
Multipath scheme	K=3 paths
Weighting values (Equation (3.3))	1/7
Queue sizes	50 packets
Interfering CBR traffic	(300, 200, 150 and 120) Kbps
Channel noise	−92 dBm
Mobility pattern generator	Bonnmotion

Figure 3.10 depicts the average end-to-end packet delay. We can see that the case including the Game scheme improves the delay compared to the Non Game case. This is specially notable (around half a second) for a high number of sources $N = 4$ or 5,

since in those cases, the amount of traffic is much higher and a smart selection of the forwarding paths gains importance.

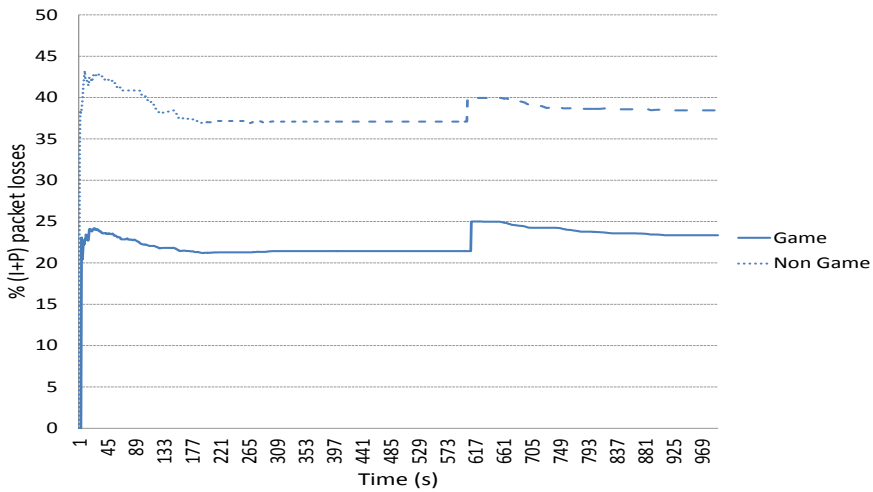

Figure 3.9: Percentage of packet losses *vs.* time ($N = 3$ users).

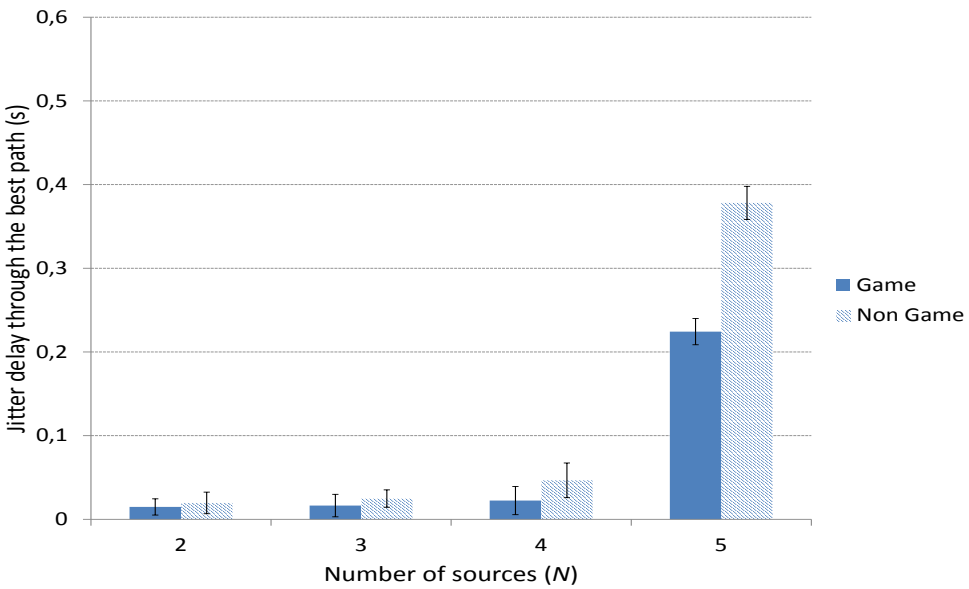

Figure 3.11: Delay jitter through the best path.

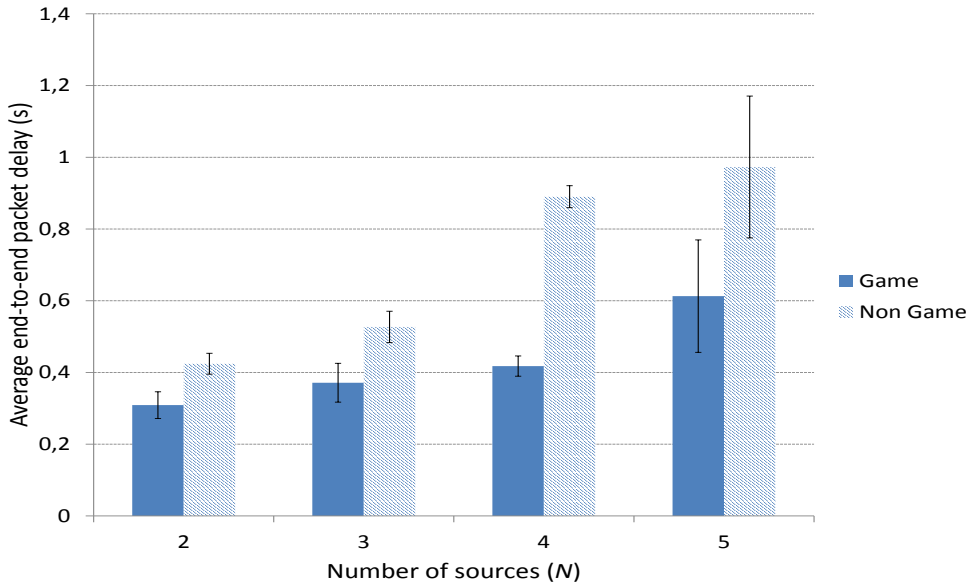

Figure 3.10: Average end-to-end packet delay.

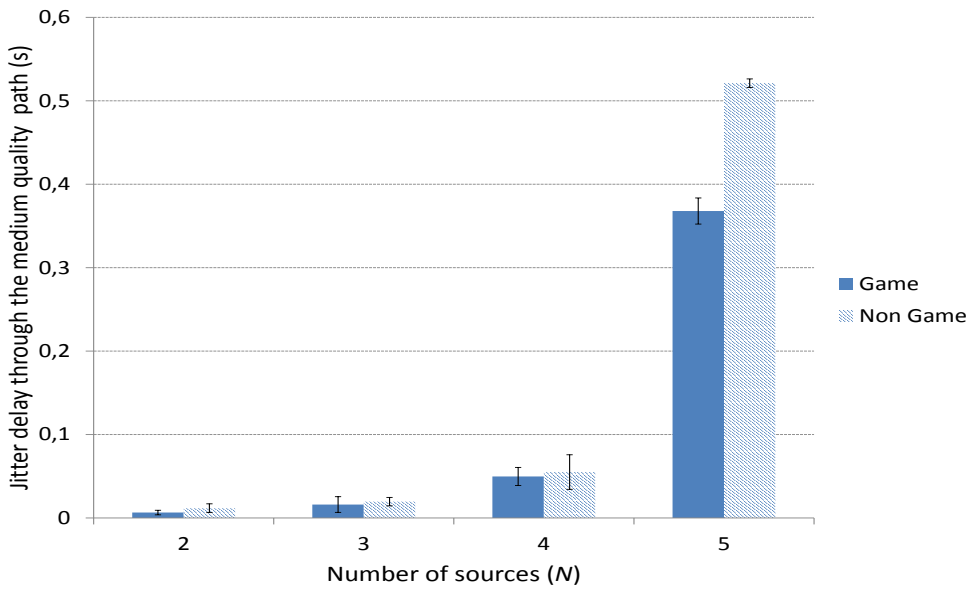

Figure 3.12: Delay jitter through the medium-quality path.

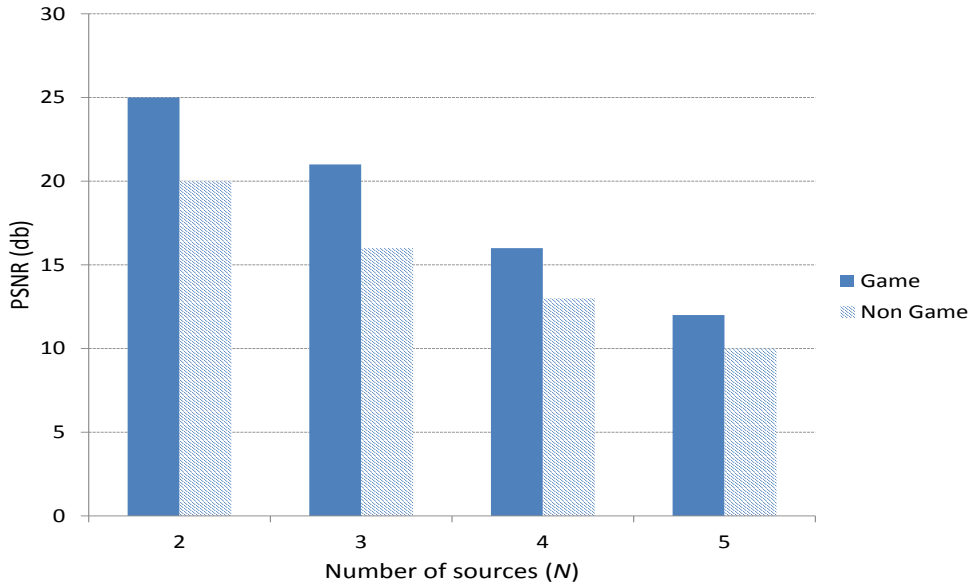

Figure 3.13: Peak Signal to Noise Ratio (PSNR).

Figures 3.11 and 3.12 depict the average delay jitter suffered by packets through the best and the medium-quality path, respectively. In both cases, the jitter using the game-theoretical scheme shows a slightly better result against the Non Game case for 2 to 4 players. The improvement is notably higher for 5 sources, when the jitter is also higher due to the high traffic that produces a higher variation in the packet delays.

Figure 3.13 depicts the peak signal-to-noise ratio (PSNR) obtained for 2, 3, 4 and 5 players. We can see that the case including the Game scheme improves the PSNR compared to the Non Game case. Also, PSNR decreases as N increases. This is because as N increases, the number of video frames to be sent increases, causing more packet losses and as a result a lower PSNR.

3.7.2.1 Gain for I and P Frames

To better see separately the gain obtained for I and P frames, we define the following parameters:

$$\%GainI_i = \left(\frac{ILNG_i - ILG_i}{ILNG_i} \right) \cdot 100 \tag{3.51}$$

$$\%GainP_i = \left(\frac{PLNG_i - PLG_i}{PLNG_i} \right) \cdot 100 \tag{3.52}$$

where

- i: 2, 3, 4 and 5 sources (players).
- $ILNG_i$: percentage of packet losses for I frames when the game-theoretical scheme is not used.
- ILG_i: percentage of packet losses for I frames when the game-theoretical scheme is used.
- $PLNG_i$: percentage of packet losses for P frames when the game-theoretical scheme is not used.
- PLG_i: percentage of packet losses for P frames when the game-theoretical scheme is used.
- $GainI_i$: Gain obtained for I frames using the game-theoretical scheme with respect to not using it.
- $GainP_i$: Gain obtained for P frames using the game-theoretical scheme with respect to not using it.

Figure 3.14 shows the average of all the simulation results for $\%GainP_i$ and $\%GainI_i$. We can see that when the game-theoretical scheme is applied, the gain is 11%, 18%, 25%, 32% for I packets (dark bars) and 95%, 83%, 75%, 69% for P packets (light bars), for 2, 3, 4 and 5 players, respectively. As we can observe, $\%GainP_i > \%GainI_i$ in all the cases. This is because there are much more P frames than I frames (see Figure 3.1) per player so the benefits are more noticeable for P frames. When N increases, the difference is lower, since the number of I frames increases.

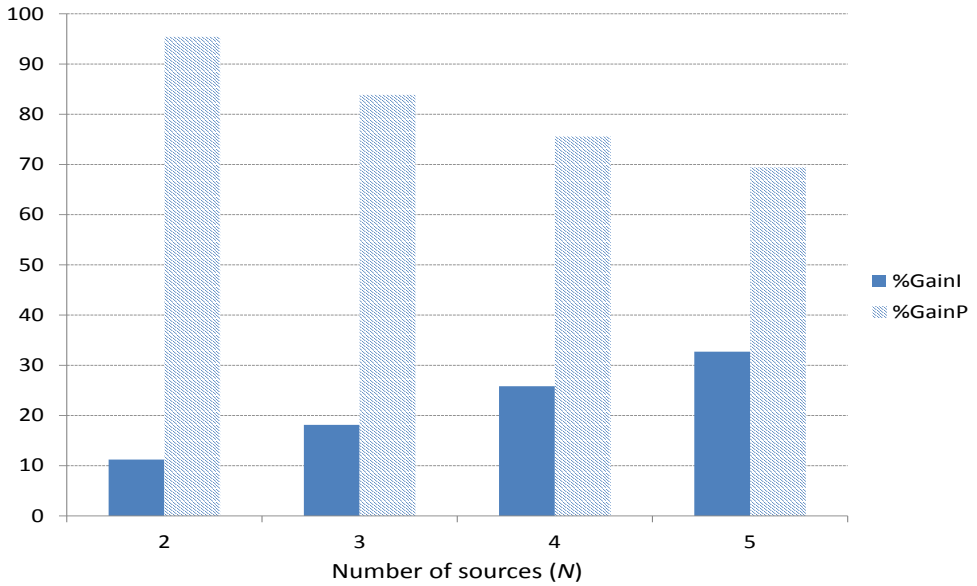

Figure 3.14: Gain in terms of packet losses for I and P video frames using the game-theoretical scheme with respect to not using it.

In addition, we observe a slightly increment for $\%GainI_i$ (dark bars) as N increases. This is because as N increases, the number of I frames increases and this makes the game-theoretical scheme benefits more noticeable. On the other hand, $\%GainP_i$ decreases as N increases. The reason is that as N increases, there are too many P frames (more collisions), higher loads to be balanced and as a result we obtain a lower benefit. Nonetheless, $\%GainP_i$ is still high (around 70% for 5 sources). This does not affect I frames since they represent a lower number of the traffic, in this scenario.

3.7.2.2 Utility Function Values

In this section, we will compute the gain of our game-theoretical routing scheme. Let us define U_{G_i} as the utility function for player i when the game-theoretical scheme is used and U_{NG_i} as the utility function when it is not used. Both utility function values will be computed using Equation (3.17). G_i is the gain obtained for player i by using the game-theoretical scheme with respect to not using it, $0 \leq G_i \leq 1$.

$$G_i = \frac{U_{G_i} - U_{NG_i}}{U_{G_i}} = \frac{U_{p=p_i^*} - U_{p=1}}{U_{p=p_i^*}} \tag{3.53}$$

Using Equation (3.17) in Equation (3.53) we obtain:

$$G_i = \frac{U_{G_i} - U_{NG_i}}{U_{G_i}} = 1 - \frac{\left(\frac{n_{rb,i} - n_{s,i} \cdot 1}{n_{s,i} \cdot 1}\right) \cdot \phi_{b,i} \cdot \frac{1}{J_{b,i}}}{\left(\frac{n_{rb,i} - n_{s,i} \cdot p_i^*}{n_{s,i} \cdot p_i^*}\right) \cdot \phi_{b,i} \cdot \frac{(p_i^*)^2}{J_{b,i}} + \left(\frac{n_{rm,i} - n_{s,i} \cdot (1-p_i^*)}{n_{s,i} \cdot (1-p_i^*)}\right) \cdot \phi_{m,i} \cdot \frac{(1-p_i^*)^2}{J_{m,i}}} \tag{3.54}$$

3.7.2.3 A Numerical Example

In this section, we show a numerical example to calculate the gain obtained with our proposal for $N = 2$ users using Equation (3.54), *i.e.*, G_1 and G_2. To do that, we use the values obtained during simulation from the RTCP packets. They are shown in Table 3.4.

Table 3.4: Simulation output values for $N = 2$ users.

$J_{b,1}$, $J_{b,2}$	(0.021067 s, 0.008867 s)
$J_{m,1}$, $J_{m,2}$	(0.011379 s, 0.010136 s)
$\hat{n}_{b,1}$, $\hat{n}_{b,2}$	(0.6, 0.45)
$\hat{n}_{m,1}$, $\hat{n}_{m,2}$	(0.2, 0.4)
$MOS_{b,1}$, $MOS_{b,2}$	(5, 5)
$MOS_{m,1}$, $MOS_{m,2}$	(4, 5)

We calculate the variables $k_{b/m,1}$ and $k_{b/m,2}$ for players 1 and 2 using Equation (3.50) and the simulation output values shown in Table 3.4. Results are shown in Table 3.5.

Table 3.5: Best response probabilities p_i^* for $N = 2$ users.

$k_{b/m,1}$, $k_{b/m,2}$	(0.6268, 0.7111)
p_1^*, p_2^*	(0.72, 0.54)

After that, we simplify $\left(\frac{n_{rb,i} - n_{sb,i}}{n_{sb,i}}\right)$ and $\left(\frac{n_{rm,i} - n_{sm,i}}{n_{sm,i}}\right)$ as seen in Equations (3.55) and (3.56) in order to be easily calculated later using Table 3.4.

$$\left(\frac{n_{rb,i} - n_{sb,i}}{n_{sb,i}}\right) = \frac{n_{rb,i} - n_{s,i} \cdot p_i^*}{n_{s,i} \cdot p_i^*} = \frac{\hat{n}_{b,i}}{p_i^*} - 1 \tag{3.55}$$

$$\left(\frac{n_{rm,i} - n_{sm,i}}{n_{sm,i}}\right) = \frac{n_{rm,i} - n_{s,i} \cdot (1 - p_i^*)}{n_{s,i} \cdot (1 - p_i^*)} = \frac{\hat{n}_{m,i}}{(1 - p_i^*)} - 1 \tag{3.56}$$

Next, we calculate ϕ_b and ϕ_m for each player using Equation (3.23) so they can be substituted in Equation (3.17).

$$\phi_{b,1} = k_{b,1} \cdot MOS_{b,1} = k_{b/m,1} \cdot k_{m,1} \cdot MOS_{b,1} = 3.134 \cdot k_{m,1} \tag{3.57}$$

$$\phi_{b,2} = k_{b,2} \cdot MOS_{b,2} = k_{b/m,2} \cdot k_{m,2} \cdot MOS_{b,2} = 3.555 \cdot k_{m,2} \tag{3.58}$$

$$\phi_{m,1} = k_{m,1} \cdot MOS_{m,1} = 4 \cdot k_{m,1} \tag{3.59}$$

$$\phi_{m,2} = k_{m,2} \cdot MOS_{m,2} = 5 \cdot k_{m,2} \tag{3.60}$$

Finally, substituting Equations (3.55) to Equation (3.60) in Equation (3.54), we obtain that $G_1 \approx 0.65$ and $G_2 \approx 0.85$.

These values mean that for player 1 the gain is 65% more using the game-theoretical model instead of not using it. In the same way, for player 2 the gain is 85%. Figures 3.15 and 3.16 show the utility functions U_1 and U_2 and their maximum values obtained for $p_i = p_i^*$ for players 1 and 2, computed with Equation (3.26).

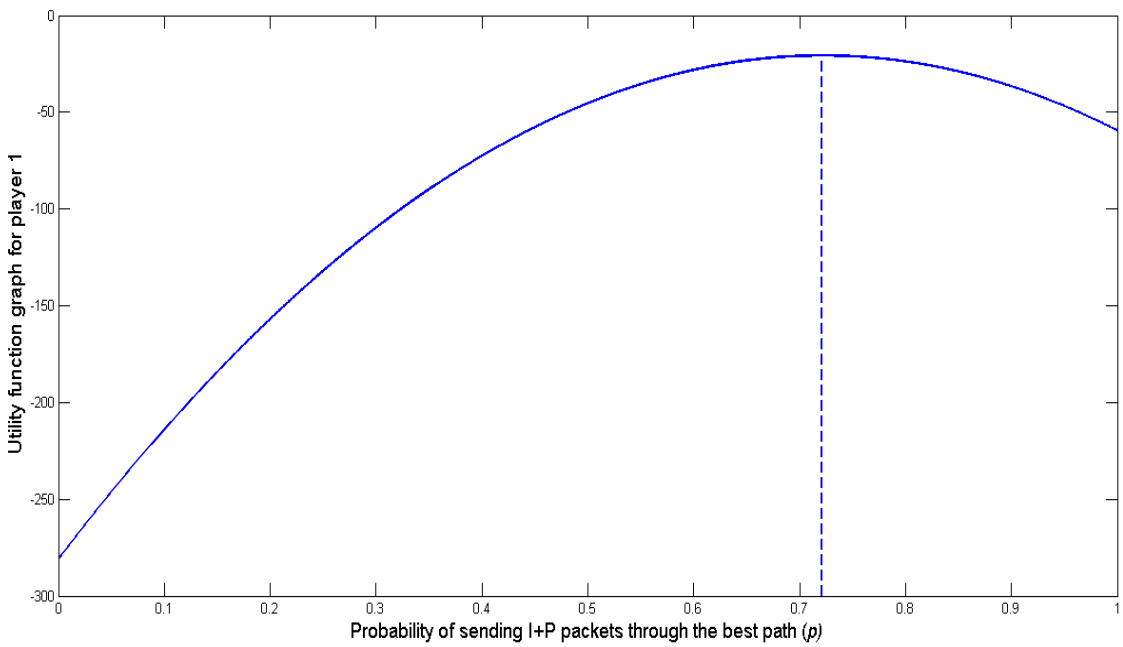

Figure 3.15: Utility function graph for player 1.

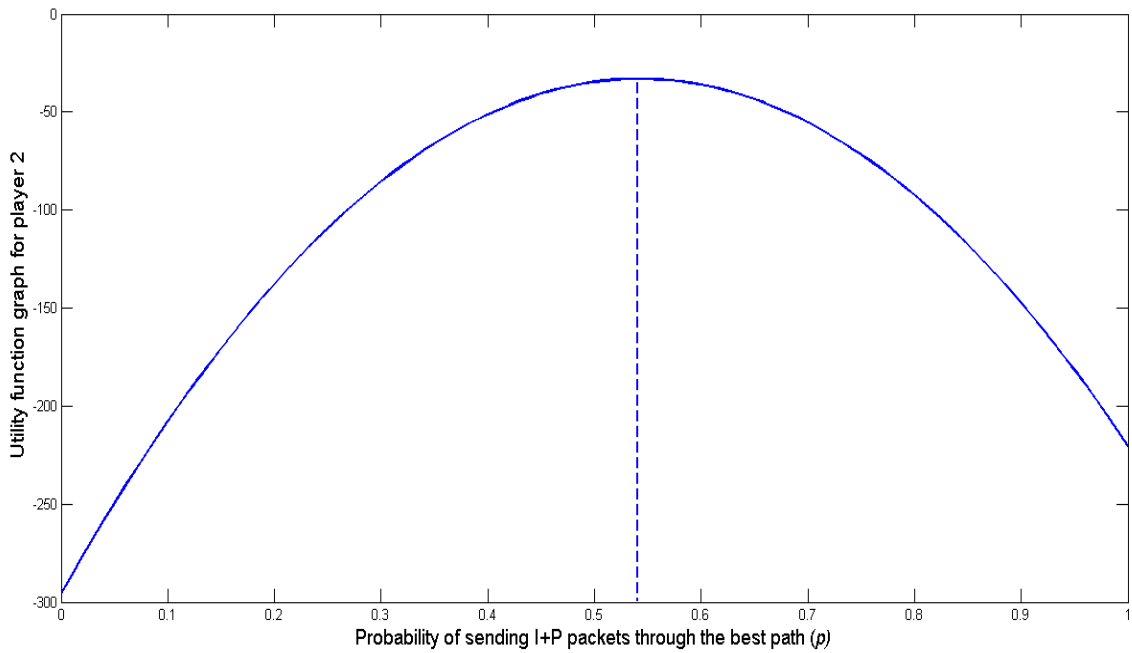

Figure 3.16: Utility function graph for player 2.

3.7.2.4 Behaviour of p_i^*

It is important to analyze the behavior of p_i^* when the fraction of packet losses (FPL) through the best or through the medium-quality paths (FPL_b or FPL_m) changes. We can easily guess that if the packet losses through the best path (*i.e.*, FPL_b) increases, the probability to sent (I+P) frames through that best path p_i^* should decrease, so more (I+P) packets would be sent through the medium-quality path. On the other hand, if the packet losses through the medium path (*i.e.*, FPL_m) increases, p_i^* should increase, so more (I+P) packets would be sent through the best path.

A way to check this logical behavior is to analyze an interval of time of a simulation where jitter and losses behave almost constant in one path (best or medium-quality path) and see how jitter and losses in the other path behave. However, it was impossible to find such an interval. Due to that, we decided to prove it mathematically taking some values of our simulations as inputs. This will help us to analyze the p_i^* behavior when FPL_b or FPL_m changes, which are shown in Figures 3.17 and 3.18. As we can see, we only study the behavior of p_i^* as a function of the FPL till 40% of packet losses since above that threshold it is considered as a non interest range. We show the average results of three different simulations.

Figure3.17 depicts the behavior of the best response probability p_i^* of sending I+P frames through the best path for player i when the FPL through the medium-quality path FPL_m increases. It is important to mention that as FPL_m increases, p_i^* increases as well. The reason is that when FPL_m increases that means that we are loosing more packets in the medium-quality path, so we should better send the packets through the best path (*i.e.*, increase p_i^*) in order to alleviate the congestion in the medium-quality path.

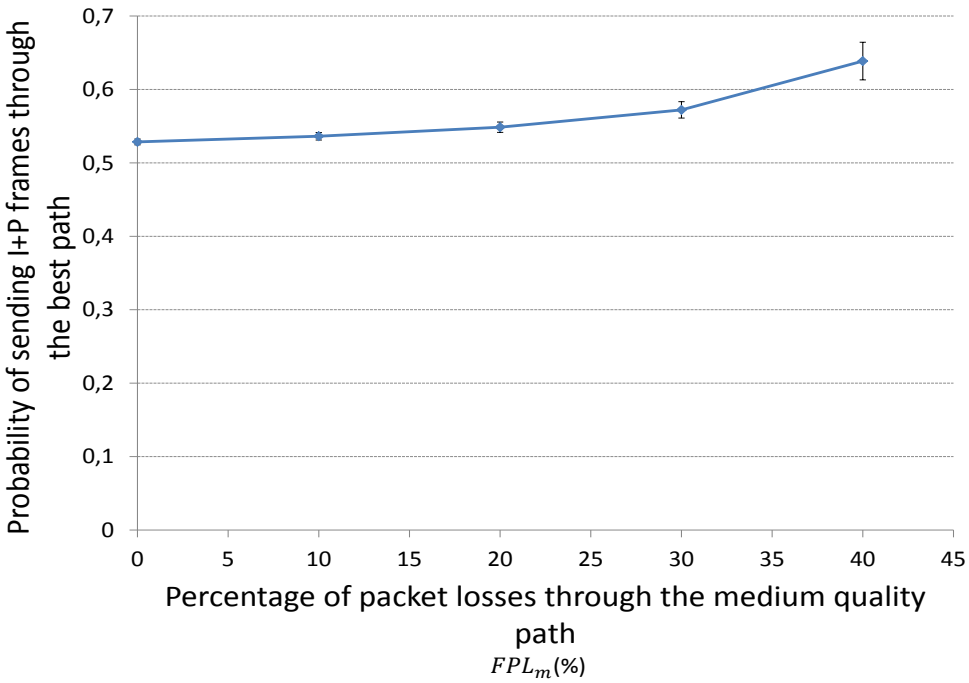

Figure 3.17: Behaviour of p_i^* as the fraction of packet losses (FPL) through the medium-quality path (FPL_m) increases. Here the FPL through the best path remains quite constant.

In the same way, Figure 3.18 depicts the behavior of the best response probability p_i^* of sending I+P frames through the best path for player i (*i.e.*, p_i^*) when the FPL through the best quality path FPL_b increases. We can see that when FPL_b increases, p_i^* decreases. The reason is that when FPL_b increases that means that we are loosing more packets in the best path, so we should send more packets through the medium-quality pat (*i.e.*, decrease p_i^*) in order to avoid congestion in the best path. For further information about how we obtained Figures 3.17 and 3.18, please see the Appendix A.

In the next section, we present an initial performance evaluation of our proposal in a VANET scenario to show the benefits of our approach in this kind of vehicular scenario. As pointed out in section 3.8, a multi-user game-theoretical geographic routing protocol specifically designed to cope with the inherent issues of VANETs, and based on this current work as a starting point, will be presented in Chapter 6.

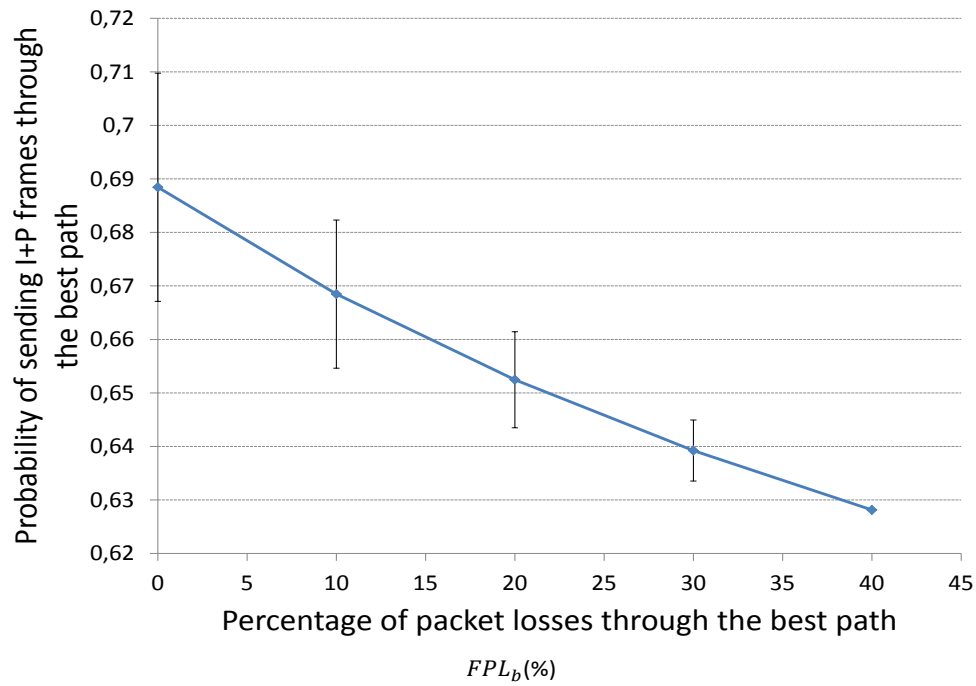

Figure 3.18: Behaviour of p_i^* as the fraction of packet losses (FPL) through the best path (FPL_b) increases. Here the FPL through the medium-quality path remains quite constant.

3.7.3 Performance Evaluation in a VANET Scenario

In this subsection we introduce a brief performance evaluation of our proposal in a VANET scenario, where we proved the MMDSR protocol improved by including the multi-user game-theoretical forwarding algorithm described in section 4. Video flows are transmitted from two vehicles to two access points AP1 and AP2 (see Figure 3.19), respectively. AP1 is the Ana Torres Institute (a surgery clinic) and AP2 is the Hospital Clinic of Barcelona, which represent two emergency units where vehicles will send their multimedia reporting messages upon the event of a traffic accident. Each vehicle will

send its multimedia reporting message to the closest AP. We carried out ten simulations per point using the NS2 [56]. Figures 3.20, 3.21 and 3.22 show the results with confidence intervals (CI) of 90 percent and 20 repitions per point using independent Simulation of Urban MObility (SUMO) scenarios in each.

In the simulations, we used a real city area obtained from the example district of Barcelona, Spain (see Figure 3.19). In order to simulate a realistic scenario, the CityMob for Roadmaps (C4R) [59] simulator was used to obtain the mobility model. C4R is a mobility generator that uses the SUMO engine [60]. Besides, C4R imports maps directly from OpenStreetMap [61] and generates NS2 compatible files to specify the mobility model for the vehicles through the city along the whole simulation. The simulation settings of the VANET scenario are shown in Table 3.6.

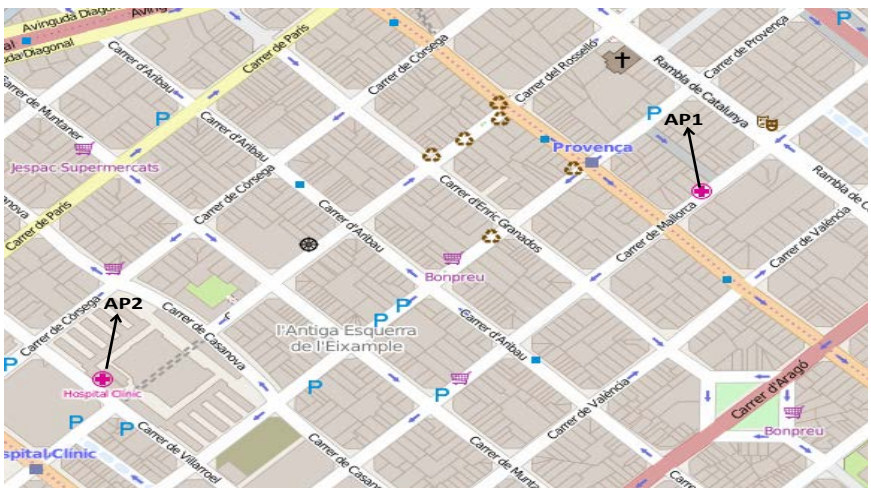

Figure 3.19: Simulation scenario of Barcelona, Spain ($N = 2$ source vehicles out of 50 vehicles). It includes two emergency units: AP1 (Ana Torres surgery clinic) and AP2 (Hospital Clinic of Barcelona).

Figure 3.20 shows the average percentage of packet losses for $N = 2$ players (source vehicles) out of 50 vehicles, when using the game-theoretical scheme (*game* option) against the case of non using it (*Non game* option). We can see how including the game-theoretical routing scheme, the average video packet losses are reduced from 26% to 11%. This decrement of the average packet losses is due to the optimal selection of paths based on a probability value (*i.e.*, p^*) that optimally balances the load among two paths at stake (*i.e.*, the best and the medium-quality paths) depending on the quality of the paths. Figure 3.21 depicts the average end-to-end packet delay. We can see that the case including the *Game* scheme improves the delay compared to the *Non Game*

case. It is reduced from 0.09 s to 0.04 s. Figure 3.22 depicts the average jitter delay suffered by the packets. Here, we observe that the jitter using the game-theoretical scheme shows slightly better result compared to the *Non Game* case for 2 players.

This has been a first performance evaluation of our game-theoretical routing approach applied in vehicular ad hoc networks. Results show clear benefits after including our game-theoretical approach in a multipath location-based routing protocol over VANETs. Based on these incipient results, in Chapter 6 we will further develop a multi-hop geographical routing protocol for VANETs based on a multi-user game-theoretical approach to send video reporting messages in a smart city following a similar work strategy made in this Chapter. The main difference with this Chapter 3 will be the design of the game-theoretical forwarding algorithm based on a hop-by-hop strategy instead of on an end-to-end forwarding path strategy as we did in this Chapter. We foresee enhanced results for VANETs after including this improvement.

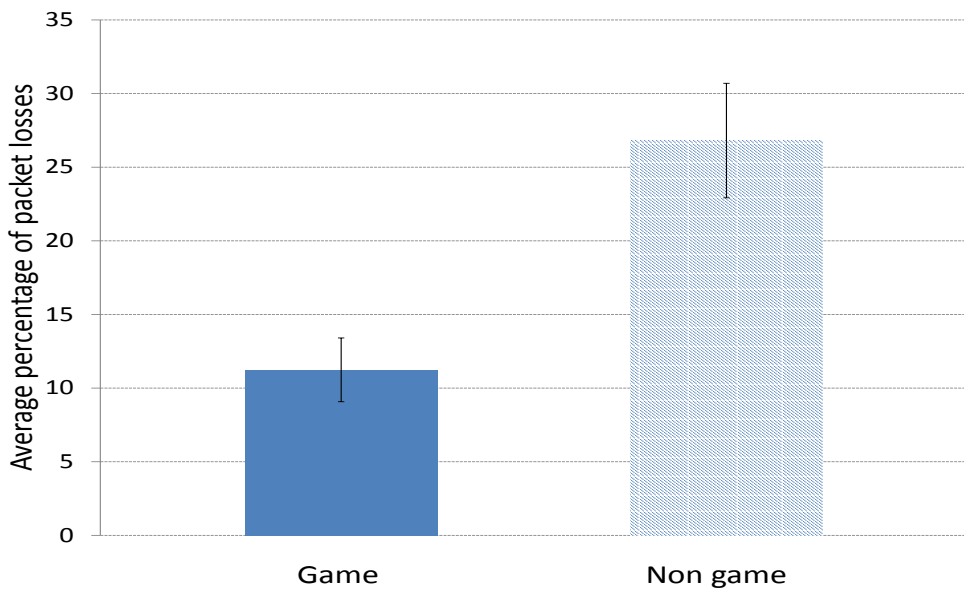

Figure 3.20: Average percentage of packet losses for $N = 2$ players (source vehicles).

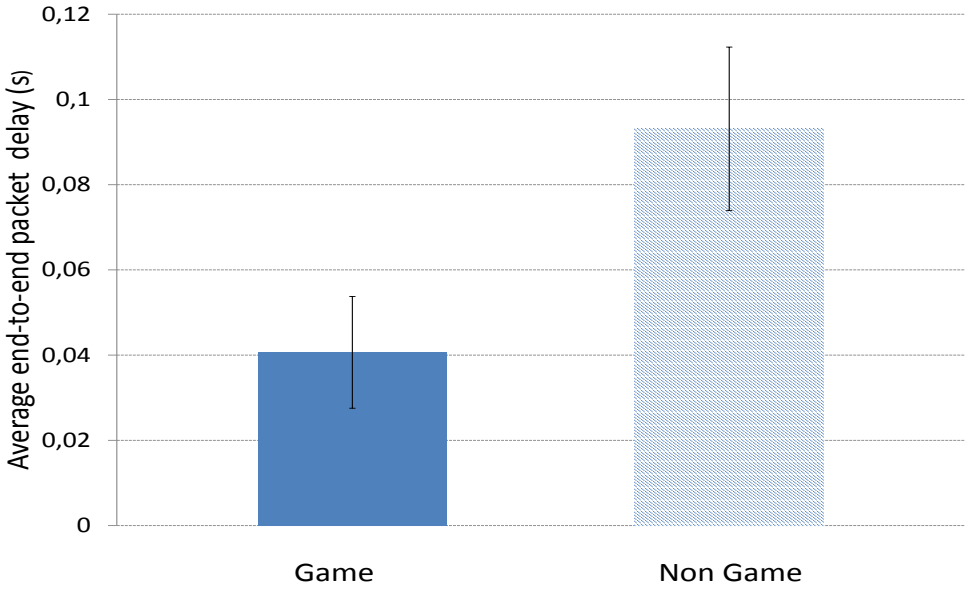

Figure 3.21: Average end-to-end packet delay for $N = 2$ players (source vehicles).

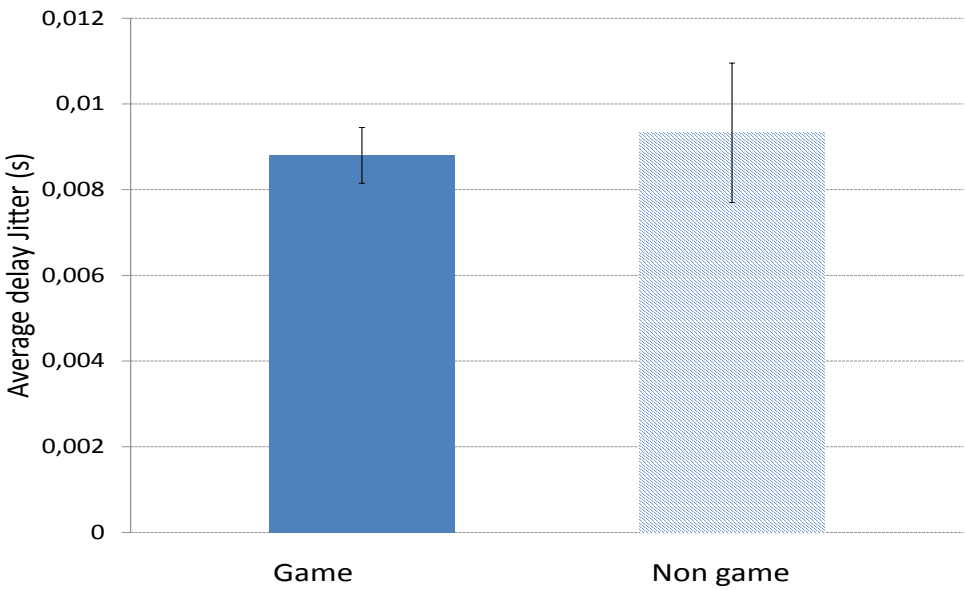

Figure 3.22: Average delay jitter for $N = 2$ players (source vehicles).

Table 3.6: Simulation settings of the VANET scenario.

Map Zone	**Example District of Barcelona**
Area	850×580 m^2
Number of nodes	50
Transmission range	120 m
Mobility generator	SUMO [60]/C4R [59]
MAC specification	IEEE 802.11p
Nominal bandwidth	11 Mbps
Simulation time	250 s
Video encoding	MPEG-2 VBR
Video bit rate	150 Kbps
Video sources	2
Video sequence sent	Traffic accidents [58]
Routing protocol	Game-theoretical algorithm + MMDSR
Transport protocol	RTP/RTCP/UDP
Maximum packet size	1500 Bytes
Multipath scheme	$K = 3$ paths
Weighting values (Equation (3.3))	1/7
Queue sizes	50 packets
Interfering CBR traffic	100 Kbps

3.8 Conclusions and Future Work

In this Chapter, we have designed a new routing protocol for MANETs to send video-reporting messages in a smart city. The routing protocol is based on a game-theoretical scheme for N users. Our framework could be used in smart cities where prevention of accidents is an important goal. We understand that with a video message, the level of seriousness of the accident could be much better evaluated by the authorities allowing a fast warning of the incident to emergency units, which potentially could save lives.

The users of the framework could be any dynamic sensor such as citizens with

smart phones or tablets that could participate in the MANET to send the video to the competent authorities. Also, smart citizens would easily be warned by other citizens about any situation in the city, which would improve the quality of life in the smart cities.

In our framework, the probability p of sending the most important video frames (*i.e.*, I+P frames) through the best available path varies depending on some network characteristics. This way, instead of sending the I+P video frames always through the best available path, users play a strategic routing game where these frames will be sent through one of the two best paths according to a certain probability p^*.

Simulation results in the MANET scenario show the benefits of our proposal by outperforming the results compared to the case of non using our game-theoretical routing. In terms of packets losses, delay and jitter, results notably improve for $N = 2$, 3, 4 and 5 users (players), due to the new way of selecting the forwarding path based on p^*. Our proposal makes the network more efficient as well as achieves a higher degree of satisfaction of the users by receiving much more (I+P) frames with a lower average end-to-end delay and jitter. This definitively will improve the quality of the video perceived by the end user. Moreover, improvements are also shown for $N = 2$ users in simulation results of a VANET scenario, in terms of percentage of packet losses, average packet delay and average delay jitter. A multi-user game-theoretical geographic routing protocol specially designed for VANETs will be presented in Chapter 6.

Chapter 4

Realistic environment for VANET simulations (REVsim)

In this Chapter we present a tool named REVsim (Realistic Environment for Vanets simulation) able to analyse the presence of obstacles in a real map. Parameters such as α, β, road resolution and transmission range have been defined and used in our proposed algorithm. Finally, a validation of our algorithm is shown. The content of this Chapter has been published in [3].

4.1 Introduction

With the aim to attain realistic results in our simulations to test our proposals, we have tackled the issue of detecting the presence of obstacles in real maps [3] so that each time a node is going to send a packet, a previous check is done to ensure that no obstacles are found between the current and the next forwarding node; otherwise, the packet is dropped. This way we mimic what would happen in real life.

In this Chapter we focus on the analysis of the presence of buildings in a real map where a VANET operates. In this part, we aimed to design an algorithm able to detect obstacles in a real map of a city. This contribution seeks to further enhance the realism and efficiency of our VANET simulations to attain more confident and trusted results. In Figure 4.1, we can see that vehicle A will not be able to receive any packet from vehicle B due to the presence of a building. In this example A and C are in Line of Sight (LOS), whereas A and B are not. In most simulators, if vehicle B is within the

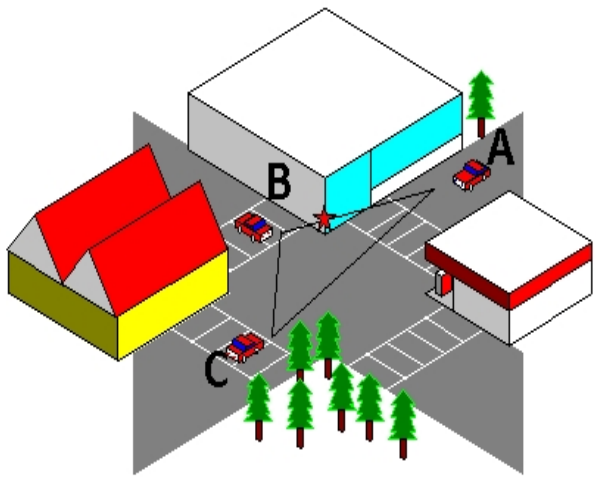

Figure 4.1: Example of the modelling of obstacles.

transmission range of vehicle A, A can receive packets from vehicle B despite being there a building in the middle, which in real life would block the transmission.

The rest of the Chapter is structured as follows. Section 4.2 presents a general view about mobility model generators for VANETs. In section 4.3 we explain our proposal to detect buildings in cities. In section 4.4 we validate our proposal and give threshold values for our parameters. In section 4.5, we summarize how to use our program REVsim. Finally, conclusions are given in section 4.6.

4.2 Mobility model generators for VANETs

Mobility model generators for VANETs are used to generate travel paths of vehicles in a vehicular scenario. In most cases, the movement traces generated can be saved and imported into a network simulator to study the performance of VANET scenarios with the impact of specific movements of the nodes that will determine the connectivity of the network. It is essential to generate realistic movement traces in order to obtain correct evaluations of VANET protocols. We can find many mobility model generators, and we will focus on two well known by the research community, VANETMOBISIM [62] and C4R [59]. We will give a brief explanation about each one of them. For our proposal, we employed the Citymob for Roadmaps (C4R) mobility generator able to

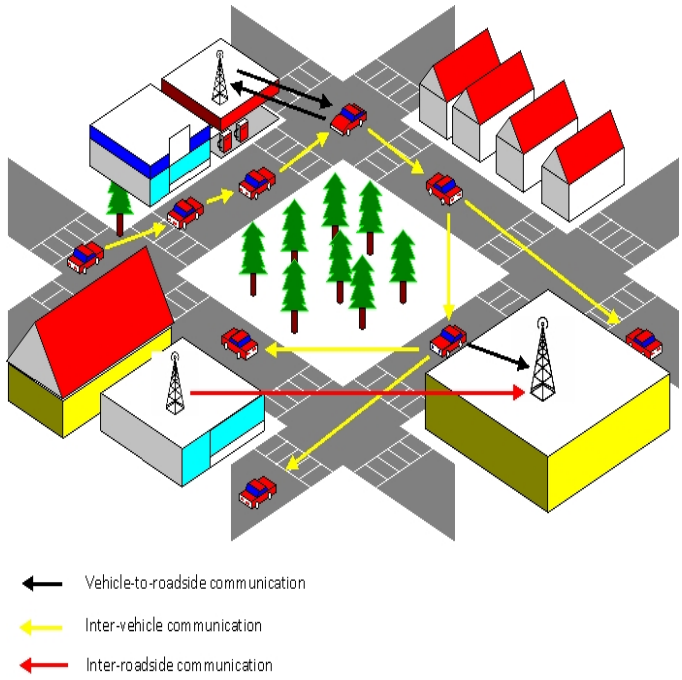

Figure 4.2: Different types of communications in VANETs.

import maps directly from OpenStreetMaps [61]. We decided to use C4R because we wanted to use Barcelona real maps taken by C4R from OpenStreetMaps (OSM).

4.2.1 C4R

The C4R simulator has been created to simulate more realistic vehicular scenarios using real road maps from all over the world. C4R is based on the OpenStreetMap tool [61] to download real road maps, C4R also uses SUMO [60] to generate the vehicles and their movements within those scenarios (real maps). OpenStreetMap (OSM) is a collaborative project creating a free editable map of the world, which is being built largely from many collaborators, and released with an open content license. On the other side, the Simulation of Urban MObility (SUMO) is an open source, microscopic, space-continuous traffic simulator created to manage large road networks.

4.2.2 VANETMOBISIM

VanetMobiSim [62] focuses on vehicular mobility with realistic automotive motion models at both macroscopic and microscopic levels. The framework includes several mobility models, as well as analysers of geographic data sources in various formats, and a visualization module. The set of extensions provided by VanetMobiSim consists mainly of the two following: a vehicular spatial model and a set of vehicular-oriented mobility models. Vehicular spatial model is composed of spatial elements (such as traffic lights or multi-lane roads), their attributes and the relationships that link these spatial elements to describe vehicular areas. The spatial model is created from topological data obtained in four different ways: user-defined, random, Geographic Data Files (GDF) and based on the TIGER/line files from the U.S.A Census Bureau [63].

As we can see, VanetMobiSim can offer many possibilities and features to create realistic scenarios. In addition, VanetMobiSim trace files can be imported into NS-2 [56], GloMoSim [64] or QualNet network simulators [65].

4.3 Detecting the presence of obstacles in real maps

In this section, we give a brief summary of the main features of our program REVsim [3] which is able to detect obstacles at each time-stamp in real maps, e.g., taken from the OpenStreetMaps [61].

4.3.0.1 Motivation

To trust the results of any performance evaluation of a new proposal using a network simulator, a realistic environment should be used. Buildings as obstacles present in a real map could attenuate or even block the signal. Due to this fact, it is extremely important to take into account obstacles that can actually be found in any real city map. Therefore, two nodes that belong to the same transmission range will actually be able to communicate with each other depending on the presence or absence of obstacles between them. Common traffic simulators do not take into account this transcendent issue. These facts lead us to design a program called REVsim [3] to detect if two nodes within the same transmission range could actually interchange packets or not during simulation due to the presence of buildings. REVsim is able to detect the presence of buildings in the cities that could avoid the communication between two vehicles. Furthermore, this detection is done efficiently and fast, as we will explain in the following.

4.3.0.2 Program scheme

In Figure 4.3, we illustrate the scheme used to develop REVsim. Below, we explain in detail all the input files, the input parameters as well as the output files of our tool.

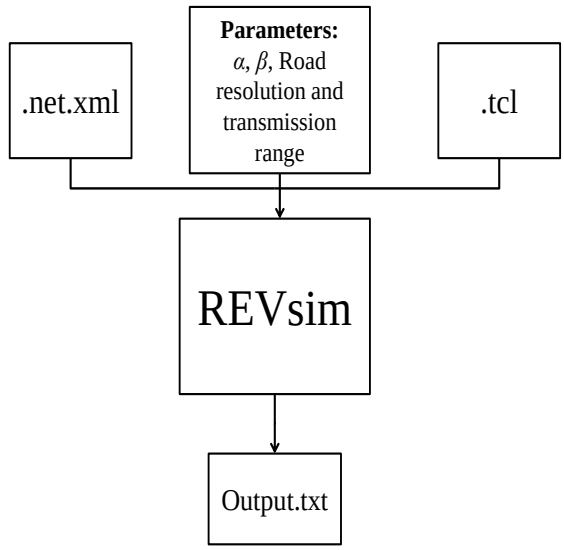

Figure 4.3: Proposed scheme of our REVsim tool to detect buildings efficiently in real maps.

4.3.0.3 Input files

The program has two input files:

- A file *.net.xml* that contains the output format provided by the C4R simulator [59] with the transformed coordinates of the map downloaded from OpenStreetMaps [61]. From that file we extract different kind of objects that define a map, such as a simple 2D point location, or a discrete line reaching a junction. These parameters with information about the map are extracted from the file *.net.xml* using java code and are saved in arrays in order to use them efficiently later by our program REVsim.

- A file *.tcl* that contains the output of the C4R simulator. This file contains the information about nodes, positions and their movements at each moment during the simulation.

Figure 4.4 shows a simple example at a given moment. The blue line means that vehicle B is on road 1. The green line means that any node that belongs to road 1 (*e.g.*, vehicle B) can establish a communication with any vehicle from the green-color road (*e.g.*, vehicle C in road 2). Furthermore, vehicle B can not establish a communication

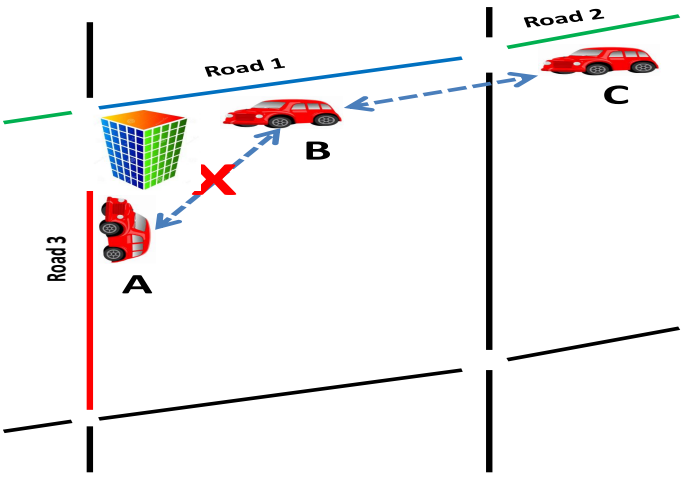

Figure 4.4: Color code for junction and lines.

with any vehicle from the red-colour road (*e.g.*, vehicle A in road 3) due to presence of a building between roads 1 and 3.

4.3.1 Input Parameters

We define four parameters to help the forwarding algorithm to determine if two nodes (*i.e.*, two vehicles) in the same transmission range could establish a communication or not due to the presence of buildings between them. These parameters are α, β, road resolution and transmission range.

4.3.1.1 The α parameter of our algorithm to detect buildings

As it is depicted in Figure 4.5, the α parameter is defined as the angle that relates two roads (road A and road B in Figure 4.5) starting from a common junction. An obstacle is assumed to be between those roads. The α parameter is used to determine till which angle α we can still consider that vehicles in road A can establish communication with vehicles in road B. In this way, the visibility between two vehicles is true or false depending on the value of α, which is calculated using Equation (4.1).

$$\alpha = 180° - \arccos\left(\frac{\vec{U}\cdot\vec{V}}{\|\vec{U}\|\cdot\|\vec{V}\|}\right) \tag{4.1}$$

where α is the angle between the two vectors $\vec{U}$ and $\vec{V}$ that define roads A and B, respectively. $\| \vec{U} \|$ is the magnitude of vector $\vec{U}$ and $\| \vec{U} \| \cdot \| \vec{V} \|$ is the scalar product

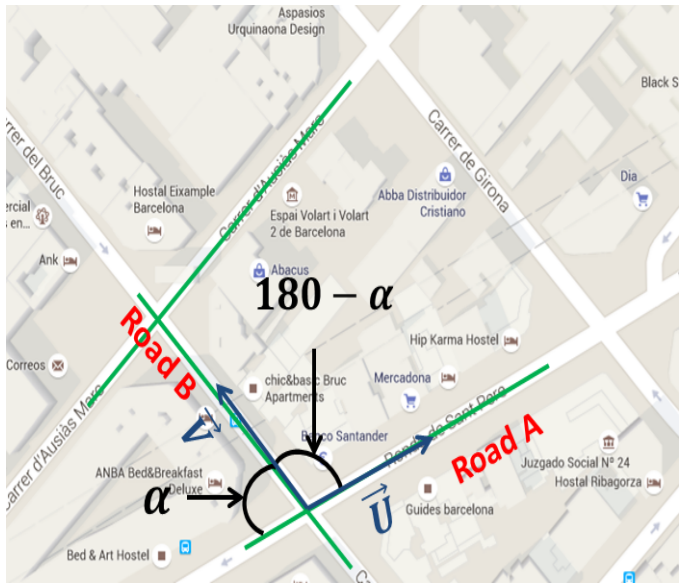

Figure 4.5: The α parameter to detect if two vehicles are in line of sight or not.

of both vectors. A node in the street A can establish communication with another node in the street B if $\alpha < \alpha_t$ where α_t is a threshold value for α.

4.3.1.2 The β parameter of our algorithm to detect buildings

As it can be seen in Figure 4.6, the β parameter is defined to establish the relationship between two or more lines that are part of a same curved road. In this way, we determine the grade of curvature as a vehicle travels through the consecutive lines of a same curved road. Besides, β is used to efficiently determine the relationship of two related curved roads by means of the lines that compose both roads. Notice that related roads means that any two nodes in those roads could establish communication.

Our algorithm begins analysing the value of α as a first step and then the value of β as a second step, locating the points in the map using lines instead of roads. We consider that roads are formed by lines so for each single point (vehicle) in the map, its associated line is determined. That is, the algorithm determines on which line of the road the vehicle is located. Mathematically, β is the sum of a set of small betas obtained between two vehicles A and B (see Figure 4.7), $\beta_{\phi,K} - \beta_{\phi,J}$, $\phi \leq J \leq K \leq L$, being J the line number of vehicle A, being K the line number of the vehicle B and L the total number of lines in that road. Those small betas define the curvature between the two vehicles A and B, according to Figure 4.7. The parameter β is calculated as

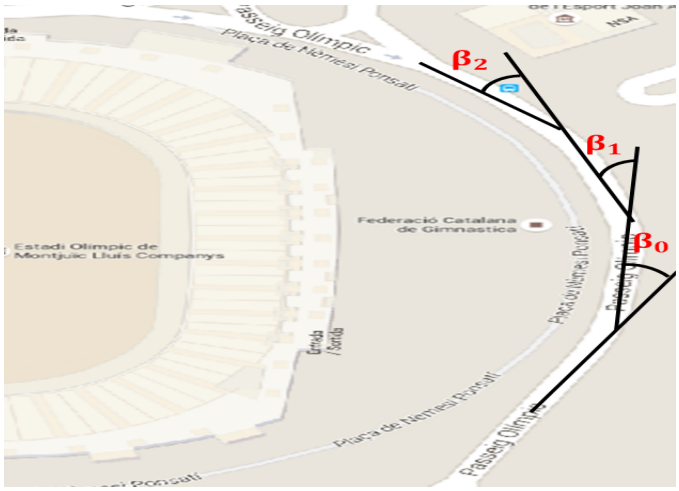

Figure 4.6: The β parameter used by the REVsim algorithm in curved roads.

seen in Equation (4.2).

$$\beta = \sum_{i=\phi}^{i=K} \beta_i - \sum_{i=\phi}^{i=J} \beta_i \tag{4.2}$$

Two vehicles in that road can establish communication with each another if $\beta < \beta_t$ where β_t is a threshold value for β.

4.3.1.3 Road Resolution

Every line of a road is sampled into discrete points that describe that line. This raises a trade-off between the processing time and the precision of the algorithm, knowing that increasing the number of samples per line means a higher precision in the location of vehicles, but also an increment in the processing time. In Figure 4.8, we show two different values of road resolution where we can notice that the high road resolution generates more samples than the low road resolution, so the positions of vehicles are more accurate if the road resolution is higher.

4.3.1.4 Transmission Range

For every vehicle in the urban scenario, the algorithm only analyses the presence of buildings in the line formed with every neighbour vehicle within its transmission range. This way we reduce the analysis only for those vehicles with which the vehicle could establish a communication. This is done for every simulation moment, analyzing the snapshot of every vehicles' location and the interaction with the buildings in the real

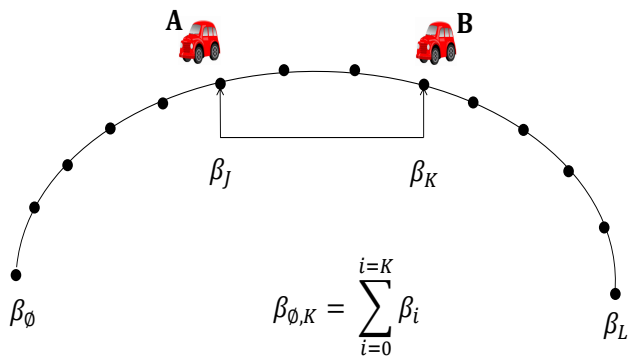

$$\beta_{\emptyset,K} = \sum_{i=0}^{i=K} \beta_i$$

$$\beta_{\emptyset,J} = \sum_{i=0}^{i=J} \beta_i$$

$$\beta = \beta_{\emptyset,K} - \beta_{\emptyset,J}$$

Figure 4.7: An example of how the β parameter is computed between two vehicles A and B located on a curved road.

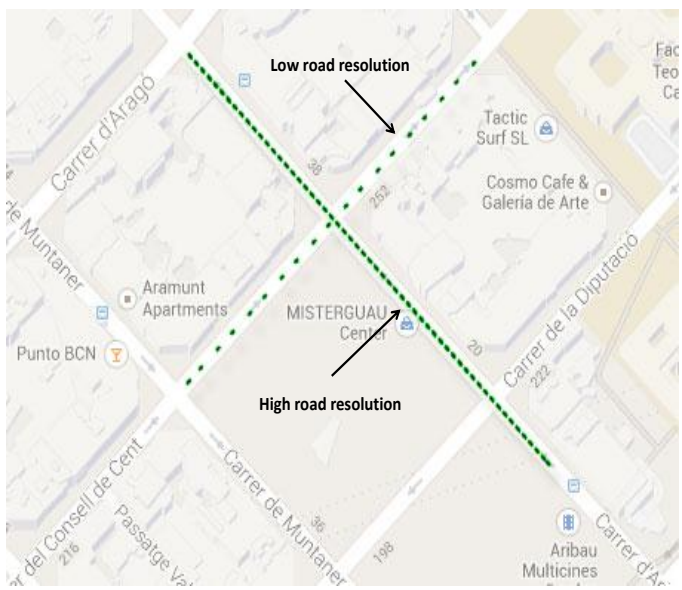

Figure 4.8: Two different road resolution.

map. It is important to highlight that this analysis is done off-line, once we select the piece of real map, from OpenStreetMaps [61], that will feed the NS-2 simulator.

4.3.2 The output building-aware file

As Figure 4.3 shows, after REVsim processes all its inputs, it obtains an output file named *output.txt*, whose format can be seen in Table 4.1. During simulation the forwarding algorithm will look at this file to quickly find out if two nodes are in line of sight (LOS) or not in case of having a building between them. This will be done each time a node needs to select a next hop among its neighbours to forward a packet towards destination.

The first row of the *output.txt* file contains the trio D T N, where D signals the beginning of the file, T is the simulation time in seconds and N is the number of nodes. These specific header information will help us to determine each value of the file (1 or 0) regarding each combination of two nodes in each timestamp of the simulation. Values of $b_{1,2,1}$, $b_{1,2,2}$, ..., $b_{N-1,N,T}$ will be set to 0 or 1, where 0 means that both nodes cannot communicate each other due to the presence of a building between them, whereas 1 means that they can communicate. For example, $b_{1,2,3}$ represents the relation between node 1 and node 2 in timestamp 3 second. If $b_{1,2,3} = 0$ means that node 2 cannot receive any packet from node 1 in timestamp 3 second. Conversely, if $b_{1,2,3} = 1$ means that it is possible that node 2 receives packets from node 1 in timestamp 3 second. We can notice that $b_{1,2,T}$ is the last value of the relation between sender 1 and receiver 2 in the last time-stamp T (*i.e.*, the simulation time). After $b_{1,2,T}$, the file follows with $b_{2,3,1}$ and not $b_{2,1,1}$ because the relation between nodes 2 and 1 in timestamp 1 (*i.e.*, $b_{2,1,1}$) is the same as $b_{1,2,1}$ which is found above in the file, so there is no need to repeat it again. We generate this format of output file because it allows a very fast look up of the $b_{i,j,k}$ value to know if there is a building ($b_{i,j,k} = 1$) or not ($b_{i,j,k} = 0$) between vehicles i and j in the moment k.

Figure 4.1 shows a snapshot of the scenario in a given moment t in which nodes A and C are in LOS, therefore their associated $b_{A,C,t}$ value for that moment is 1. However, nodes A and B have an obstacle between them, so they cannot establish a communication. For that reason, the associated $b_{A,B,t}$ value is 0 in that moment.

If the routing protocol needs to know during simulation if any two nodes can communicate or not, the algorithm can easily calculate the position of the binary answer of the output file *output.txt* using Algorithm 2 and go directly to the proper position to read the value. Algorithm 2 explains how to compute the row where the answer is found using simple information such as source node, destination node, number of nodes, simulation time and the specific time-stamp we want to check. Let us see a simple example: The simulation time is 10 seconds ($T = 10$), there are 10 nodes ($N = 10$) and we want to know if in time-stamp 3 second node 4 can receive packets from node 1 or not. For that, we need to go to find the value of $b_{1,4,3}$. As the source is 1, we use the Equation written in line 7 which is

$Position = (Destination - Source - 1) \cdot Simulationtime + Timestamp$ and as a result, $Position = 23$. This means that we have to go directly to row 23 of the file *output.txt* to find the binary answer $b_{1,4,3}$. Depending on the binary answer, the receiver node 4 will be able to receive the packet ($b_{1,4,3} = 1$) sent by node 1 or will have to drop it ($b_{1,4,3} = 0$). This way, we emulate what would have happened actually in real life, so our simulations are more realistic and we can trust our results.

Moreover, using this efficient external file obtained offline for the specific simulation map, we save a lot of processing time which is an important factor when we are carrying out many simulations. It is important to highlight that with this proposal it is not necessary to check online during simulation if two nodes are in LOS or not, which would add delay to the simulation. With this method, it is only necessary to make a fast look-up to a text file previously obtained for the real map taken from OSM.

Algorithm 2 Calculate the position value of the REVsim output file for (*Source*, *Destination*) in a specific *Timestamp*.

Require: Input data (*Source*, *Destination*, Total simulation time, Number of nodes, *Timestamp*)

Require: $i = 1$, $pos = 0$

1: **if** *Source* > *Destination* **then**
2: *tmp* = *Destination*
3: *Destination* = *Source*
4: *Source*=*tmp*
5: **end if**
6: **if** *Source* = 1 **then**
7: *Position* =(*Destination* - *Source* - 1) * Simulation time + *Timestamp*
8: **end if**
9: **while** $i <$ *Source* **do**
10: *Pos* = *Pos* + (Number of nodes -i) * Simulation time
11: *Position* = *Pos* + (*Destination* - *Source* - 1) * Simulation time + *Timestamp*
12: $i = i+1$
13: **end while**

To sum up, Algorithm 2 is used to compute a position in the file *output.txt*. That position corresponds to the binary answer of the communication checking between nodes *Source* and *Destination* at time *Timestamp*. If the positions of *Source* and *Destination*

are not in increasing order, the algorithm interchanges the role of both nodes (lines 1 to 4). After that, the initial position, *Pos*, is computed for the recorded values corresponding to node *Source* (line 10). Finally, the algorithm computes the offset value *Position* (line 7 or 11) associated with the destination *Destination* node at time *Timestamp*.

Table 4.1: Building-aware output file *output.txt*.

D T N
$b_{1,2,1}$
$b_{1,2,2}$
.....
$b_{1,2,T}$
$b_{1,3,1}$
$b_{1,3,2}$
.....
$b_{1,3,T}$
.....
$b_{1,N,T}$
$b_{2,3,1}$
$b_{2,3,2}$
.....
$b_{2,3,T}$
.....
$b_{2,N,T}$
.....
.....
$b_{N-1,N,1}$
$b_{N-1,N,2}$
.....
$b_{N-1,N,T}$

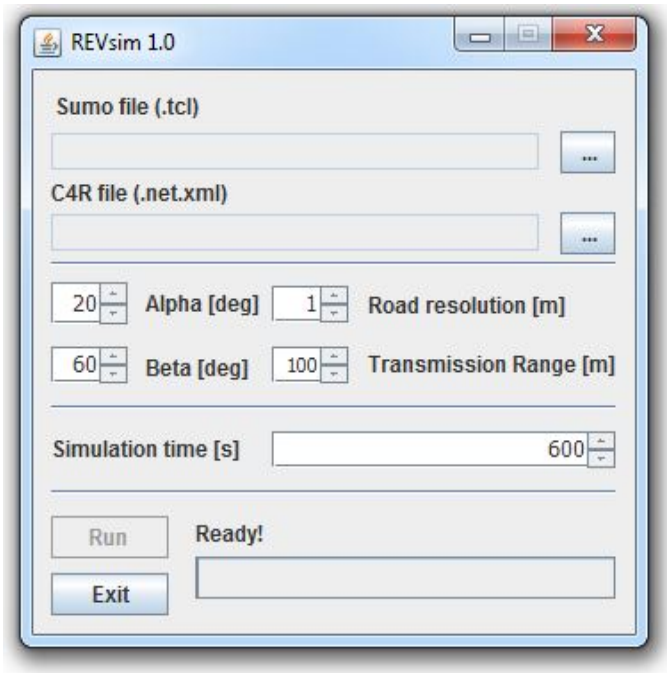

Figure 4.9: The user interface of the REVsim tool to find out if every two nodes will be in LOS or not during the whole simulation.

4.3.3 The REVsim user interface

A friendly user interface has been created using Java to provide all the user inputs, so that any one can use the program easily. The REVsim user interface is shown in Figure 4.9. It is important to mention that the simulation time shown in the interface graph is set by the user and it is necessary to be the same value as the simulation time used in the mobility model C4R to generate the output *tcl* file that feeds the network simulator NS-2. This will ensure the correct operation of the simulations.

4.3.4 Tuning the REVsim parameters for a generic scenario

To obtain the building-aware output file *output.txt* we need to tune the REVsim parameters α, β, road resolution and transmission range, so that the program is able to detect the presence of every building in the map that may block the signal between every pair of vehicles during the whole simulation. To do this, we have used a representative enough generic map from Barcelona (see Figure 4.10) that includes either curved and

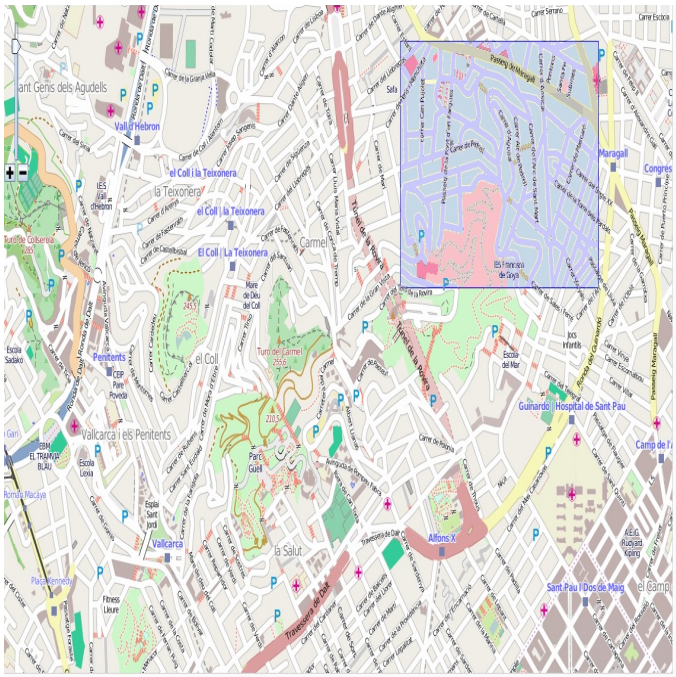

Figure 4.10: Generic map of the city of Barcelona, Spain, used in our tests.

straight roads, a highway and a Manhattan-style area with a grid of streets.

4.4 Validation and tuning of parameters

To validate our proposal, we must calculate the threshold for the alpha, beta and road resolution parameter. Anyway, we leave to the users the option to modify each one of them depending on their criteria. To carry out our validations, we used the mixed map of Figure 4.10 that combines all the usual characteristics that can be found in any map such as curves, highways and Manhattan-style areas.

In Figure 4.11(a), we took a snapshot of the scenario using $\alpha_t = 10$. The red point describes the position of the vehicle in a specific time-stamp while the blue road represents the road to which this vehicle belongs. In this specific case the threshold for alpha is $\alpha_t = 10$ degrees and the real alpha between segments A and B is $\alpha = 90$ degrees. This means that this red point (the vehicle) can interchange packets with any vehicle found in the green roads F and G. These green roads F and G are considered related to the blue road A since both angles $(\vec{A} \measuredangle \vec{F})$ and $(\vec{A} \measuredangle \vec{G})$ are lower than α_t.

On the contrary, the red point (the vehicle) cannot send nor receive packets from any vehicle found on roads B, E, C and D since all the angles ($\vec{A} \measuredangle \vec{B}$), ($\vec{A} \measuredangle \vec{E}$), ($\vec{A} \measuredangle \vec{D}$) and ($\vec{A} \measuredangle \vec{C}$) are 90 degrees, which is higher than α_t.

In Figure 4.11(b), we took a snapshot of the scenario using $\alpha_t = 100$. In this case, we are making an error as we will explain later. Between roads A and B, $\alpha = 90°$, then $\alpha < \alpha_t$ meaning that the red point can send or receive packets from any vehicle found in roads B, E, C and D. However, this is an error because between roads (A and B) or (A and E) or (A and C) or (A and G) an obstacle is found. So this $\alpha_t = 100$ would not be a proper threshold value of α for this scenario.

Now, we take another piece of our mixed map where α_t will take the following values: 10, 20 and 60 degrees.

In Figure 4.12(a), α_t is 10 degrees. The red point represents the vehicle in a specific time-stamp, the blue road H means that this red point belongs to this road and the green roads G, A and E mean that any vehicle in road H can interchange packets with any vehicle found on roads G, A and E. Notice that the angle α between roads H and D is higher than 10 degrees and therefore, any vehicle found in road D cannot interchange packets with any vehicle found on road H due to the presence of an obstacle which is a true situation.

In Figure 4.12(b), α_t is 20 degrees. Here, no changes happen with respect to Figure 4.12(a). However, in Figure 4.12(c), α_t is 60 degrees and here we see another mistake due to that vehicles found in roads D and B can send or receive packets to or from any vehicle found on road H knowing that there is an obstacle between roads H and D as well as between roads H and B.

Related to β_t (β threshold), we took 2 pieces of our mixed map, one is similar to a curve shape as in Figure 4.13 and the other is a kind of S-shaped curve which is shown in Figure 4.14. The reason to take these special curves is that if with these kind of curves β_t is calculated showing no or little errors in detecting if two nodes in the same transmission range and in the same road can actually see each other or not, thus for any other simple curves with this β_t no errors will be committed.

As we go increasing beta, see Figs. 4.13(a), 4.13(b) and 4.13(c), the visibility between the red point (vehicle) and any node found in next lines will decrease.

Taking another S-shape group of curves, shown in Figs. 4.14(a), 4.14(b) and 4.14(c), we see that as we go passing from line to line in the road, β is coming higher rapidly due to presence of such a sharp curve.

4.4.1 Alpha threshold

To obtain which is the proper range of values for the threshold α_t, we carried out many simulations with different values of α_t, using many snapshots of the vehicles' positions in different time-stamps. We analysed if all the vehicles in a specific road would see or not other vehicles in other roads within their transmission range throughout simulation. For each α_t tested, we concluded if using that threshold α_t the blocking buildings would be

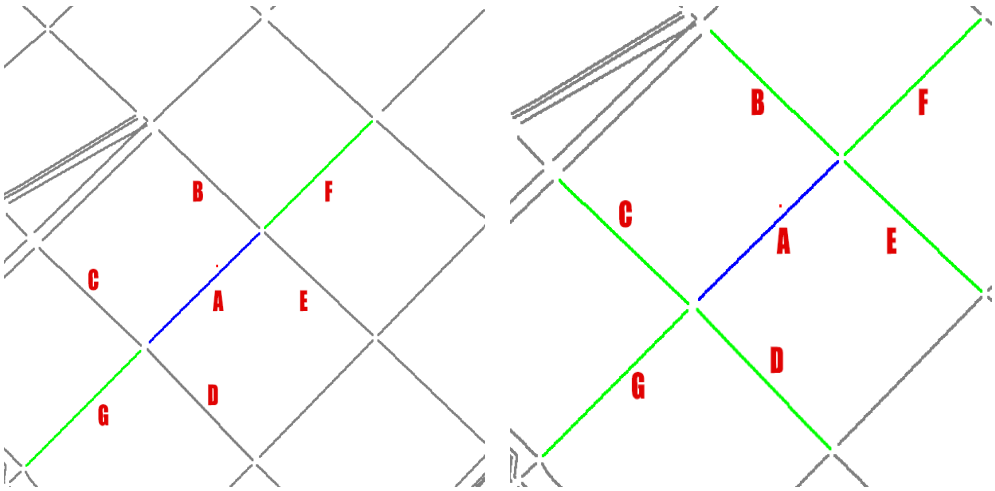

(a) $\alpha_t = 10$ degrees (b) $\alpha_t = 100$ degress

Figure 4.11: α_t values

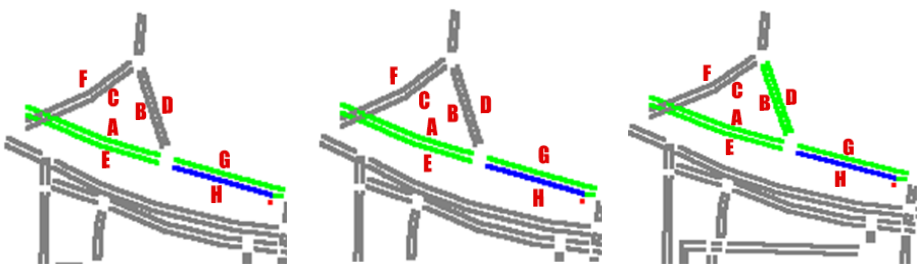

(a) $\alpha_t = 10$ degrees (b) $\alpha_t = 20$ degrees (c) $\alpha_t = 60$ degrees

Figure 4.12: α_t from 10 to 60 degrees

detected or not. After many tests, $\alpha_t = 20°$ showed to be an optimal value for different generic city maps like the one shown in Figure 4.10. Therefore, any α angle lower than 20° means that nodes found on those roads will be able to send and receive packets without any problem caused by a blocking building.

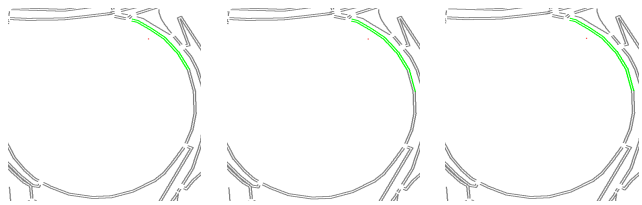

(a) $\beta_t = 40$ degrees (b) $\beta_t = 50$ degrees (c) $\beta_t = 60$ degrees

Figure 4.13: β_t from 40 to 60 degrees

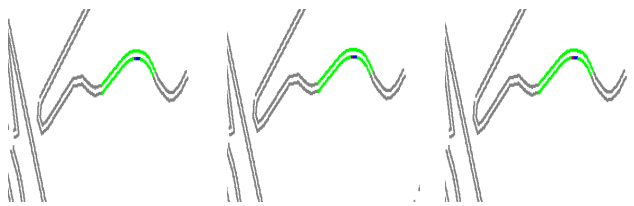

(a) $\beta_t = 40$ degrees (b) $\beta_t = 50$ degrees (c) $\beta_t = 60$ degrees

Figure 4.14: β_t from 40 to 60 degrees

4.4.2 Beta Threshold

After many simulations, we obtained that $\beta_t = 60°$ was the optimal threshold value below which all the blocking buildings located in curved roads were detected. Basically, β depends on how long and how curved is the road. The longer and curvier the road, the higher the value of β should be.

4.4.3 Road Resolution

After making many tests varying the road resolution value, we got that using a road resolution equal to 1m produced a good trade-off between precision and processing time.

4.4.4 Transmission Range

Here, we just put the transmission range value of each vehicle. This value as we have explained before will allow us to make a pre-filter step of the number of nodes to be analysed. The reason is that it has no sense to check nodes that are outside the transmission range of the node under study.

Concluding this section, our REVsim [3] tool allows the forwarding algorithm to

quickly find out which are the actual neighbours of a node with which the node is in LOS (*i.e.*, both nodes could actually communicate) in every moment. In the following, we will validate our proposal.

4.5 How to use REVsim

In order to use REVsim you should follow the following steps:

1. Open C4R [59]
   (a) Select a map.
   (b) Add vehicles randomly, specify a simulation model, choose simulation time.
   (c) Begin the simulation, C4R will give us (*.tcl*) file and a (*.net.xml*) file.
2. Open REVsim [3]
3. Select the files (*.tcl* and *.net.xml* files), browsing them from the outputs created by C4R.
4. Specify the simulation time (must be the same as C4R)
5. Specify the values of other parameters such as α_t, β_t, road resolution and transmission range.
6. Click Run
7. When it finishes, an output file (*.txt* file) will be created in the same file directory.

4.6 Conclusions

The importance of taking into account the presence of obstacles in VANET simulations has become an important issue to get trusted results. In this Chapter, we present a program named REVsim [3] able to analyse the presence of obstacles in a real map in such a way that at each instant of time we can check if two nodes (*i.e.*, vehicles) in the same transmission range can establish communication between them or not (due to the presence of an obstacle) by checking the output file generated by REVsim. Our program depends on some parameters such as α, β, road resolution and transmission range to take its decision.

Chapter 5

Multimedia Multimetric Map-Aware Routing Protocol (3MRP)

In this Chapter we propose a multimedia multimetric map-aware routing protocol (3MRP)[1] to provide video-reporting messages over VANETs in smart cities. Furthermore, a realistic scenario is created by using real maps with SUMO [60] including buildings that may interfere the signal between sender and receiver. Also, we use our REVsim [3] tool explained in Chapter 4 that allows vehicles to be able to prevent vehicles behind buildings to be chosen as next forwarding nodes. Simulations show the benefits of our proposal, taking into account the mobility of the nodes and the presence of interfering buildings.

5.1 Introduction

The special requirements and the unique characteristics of VANETs (*e.g.*, special mobility patterns, short life links, rapid topology changes) generate challenges for the research community. Among these challenges, it is necessary to develop new routing protocols specially designed for VANETs that are able to provide promising multimedia services for smart cities. In this Chapter, a new proposal of a multimetric geographical routing protocol for VANETs to transmit video-reporting messages is presented. Our

proposal considers several quality of service (QoS) metrics to select the best next forwarding vehicle for each packet in each hop towards its destination. These metrics are properly weighted to obtain a multimetric score for each vehicle in transmission range so that the current forwarding node can take the best next hop forwarding decision. In addition, the weights of the QoS metrics are self-configured. We have designed an algorithm to compute and update those weights throughout time so that nodes would be better classified according to the current state of the environment. In this way, each time the forwarding algorithm needs to classify nodes, a proper weight value for each metric will be updated so that the adaptative framework is able to self-configure. Also, with the aim to attain realistic results, we include the presence of obstacles in real maps [3] so that each time a node is going to send a packet, a previous check is done to ensure that no obstacles are found between the current and the next forwarding node; otherwise, the packet is dropped. Furthermore, our forwarding algorithm is building-aware so that the current forwarding node can avoid vehicles behind buildings to be chosen as next forwarding nodes. Simulation results show the benefits of our protocol in terms of average packet losses, average end-to-end delay, average jitter delay and PSNR.

Our research focuses on two different aspects: (1) The deployment of an efficient routing protocol to manage video-reporting messages in VANETs. This is a very important goal because it allows a fast warning of any incident, which potentially could alleviate possible consequences and even save lives. (2) The design of an algorithm able to give each metric a proper weight in a multimedia multimetric geographical routing protocol, which would help to classify nodes (*i.e.*, vehicles) as potential forwarding nodes in a better way. This algorithm seeks to further enhance the overall performance of the service.

The rest of the Chapter is structured as follows. Section 5.2 includes some relevant related work. In section 5.3 presents our multimedia multimetric geographical routing protocol, the metrics, the way metrics are evaluated and how we compute the final score for each candidate neighbour to be the next forwarding node. Section 5.4 analytically describes how to compute and update the values of the weights of the metrics. Simulation results are shown and analyzed in section 5.5. Finally, conclusions are given in section 5.6.

5.2 Related work

Routing in VANETs is the process of selecting the best vehicle or vehicles in the network through which data will be forwarded. The best forwarding nodes are not necessarily the closest ones to destination, although they usually are selected using the shortest path. Similar proposals of routing protocols for vehicular ad hoc networks close to our work can be classified in two categories: (a) geographical routing protocols for VANETs; and (b) routing protocols used to transmit video over VANETs. In the following we summarize some representative works related to our proposal in both categories.

(a) Regarding geographical routing protocols, many protocols were designed in the last years for VANETs. The work in [66] shows that the best routing protocols for VANETs are based on the information of the instantaneous locations of nodes. Geographic unicast protocols for VANETs can be classified into three categories [67]: (i) greedy, (ii) opportunistic, (iii) trajectory based. The most common approach in VANETs is the greedy strategy where a node forwards packets to its neighbour located closest to destination. Opportunistic strategies use the store-carry-and-forward technique to avoid dropping packets when no forwarding node is available. This strategy incurs high delays, which are not suitable for video-streaming of delay sensitive content. Using a trajectory-based strategy, a vehicle has more chances to be selected as a forwarding node if it is moving towards destination. On the other hand, GPSR [11] is a well-known greedy geographic unicast protocol designed for VANETs. Nodes are assumed to know their locations as well as the destination location. GPSR has two different modes to forward packets: greedy mode, which is used by default, and perimeter mode used when it is not possible to use the greedy mode. Several proposals have been presented in the literature to improve the basic GPSR. Movement prediction routing (MOPR) in [68] improves the routing process of GPSR by including the link stability concept. That approach is one of the first research works that uses the link stability idea to choose the best forwarding node for unicast communications. Authors in [69] propose GPSR-MA (greedy perimeter stateless routing with movement awareness), a modification of GPSR which exploits information about movement to improve the next forwarding node selection. They use information about position, moving direction and speed to select the next forwarding node showing improvement compared to GPSR. Authors in [70] present the I-GPSR (Improvement GPSR) that incorporates four metrics (distance to destination, vehicle density (VD), moving direction and vehicle speed) used to select the best forwarding node. In [71], authors propose MMMR that uses four metrics in the process of selecting next forwarding nodes (distance to destination, vehicle density, trajectory and available bandwidth). Map awareness is also achieved in MMMR by taking into account the possible presence of obstacles in a Manhattan scenario during the online selection process of the next forwarding node, whereas our proposal is building-aware in a real map scenario.

(b) Regarding routing protocols used to transmit video-streaming in VANETs, only a few studies have been proposed so far. Authors in [72] presented LIAITHON, a location-aware multipath video unicast scheme for urban VANETs. Depending on geographic advance, link stability and degree of closeness, the forwarding nodes are selected. LIAITHON discovers two relatively short paths with minimum route coupling effect using the location information. Simulations show that LIAITHON outperforms the single path solution and the node-disjoint multipath solution. Also, we highlight the work [73], where the authors present VIRTUS (VIdeo Reactive Tracking-based UnicaSt), a proposal which extends the duration of the

decision of nodes to forward packets from a single transmission moment to a time window. In addition, that decision depends on an equilibrium between link stability and geographic advancement, VIRTUS evaluates the suitability of a node to relay packets, including a density-aware relaying node selection in the video transmission process showing significant improvements. In [74], authors propose a multipath solution for VANETs with link disjoint and node-disjoint to provide a high quality video-streaming on VANETs. Due to the special characteristics of VANETs and the large amount of video data, extra interference and contention during the video-streaming are provoked by the redundancy of Forward Error Correction (FEC). To cope with this issue, authors use the TCP protocol to transmit the I-frames to ensure their transmissions and UDP protocol to transmit the P and B frames to reduce the delay of the transmissions. Furthermore, authors use the node disjoint and link disjoint algorithms to further minimize the delay by transmitting I-frames and inter-frames (P and B frames) through separate paths. Simulations show that the proposed multipath protocol provides a higher video quality with an acceptable delay in comparison with other protocols.

Our multimetric routing protocol takes the three aforementioned forwarding aspects (greedy, opportunistic and trajectory) into consideration to select the best next node to forward video-reporting messages over VANETs. In addition, we use realistic scenarios by considering obstacles present in real maps when a forwarding node is going to be selected. Our proposal includes five metrics to optimize the selection of the best forwarding node in our geographic-based routing protocol. These metrics are:

- **Distance to destination:** It is the distance between each candidate node and the destination node.
- **Vehicle density:** It is computed as the number of vehicles in the neighbours' list of each node I divided by $\pi \cdot TR_I^2$, being TR_I the transmission range of the candidate node I.
- **Trajectory:** It is computed as a comparison of the current distance of a candidate node to the destination node with a future distance between those same two nodes. This way we detect if the candidate node is getting closer to or going away from the destination node.
- **Available Bandwidth Estimation (ABE):** ABE [75] is used to estimate the available bandwidth in a link between two nodes. In our case we calculate ABE between the current node and each candidate node.
- **MAC layer losses:** Our routing protocol uses the packet losses computed at the MAC layer as a kind of local feedback information.

Then, we weight those five metrics into a single multimetric score using either equal or variable weights updated with an algorithm.

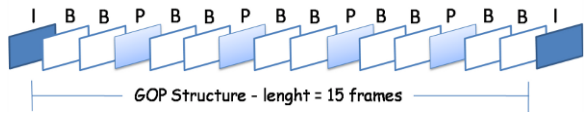

Figure 5.1: Typical MPEG-2 GoP structure with 15 frames per GoP.

To the best of our knowledge, the aim to use several metrics dynamically weighted to distribute video reporting messages over VANETs in realistic urban scenarios, is novel. We test our proposal in a realistic urban scenario, using the NS-2 simulator [56], including real maps from OpenStreetMaps [61], realistic mobility patterns with C4R [59] and a tool named REVsim [3] that we have developed to detect buildings efficiently. In Chapter 4 we have described the REVsim operation.

5.3 Multimedia Multimetric Map-Aware Routing Protocol (3MRP)

5.3.1 Basics of the general framework

Our novel geographical routing protocol for VANETs is based on the GPSR protocol to find the best next forwarding node in a hop-by-hop scheme from source to destination. Video is distributed using RTP (Real-time Transport Protocol) [18] over UDP as transport protocols. Our system uses a layered MPEG-2 VBR coding of the video flow, which is formed by sets of frames, 15 in our case, called GoP (Groups of Pictures), see Figure 5.1. A GoP has three types of frames: I, P and B, and has a unique frame-pattern in a video repeated in each GoP. I (Intra) frames encode spatial redundancy, they form the base layer, provide a basic video quality and carry the most important information for the decoding process at the receiving side. The whole GoP would be lost if the corresponding I frame were not available at decoding time. P (Predicted) and B (Bi-directional) frames carry differential information from preceding (P) or preceding and posterior (B) frames, respectively. Considering these characteristics, we assign different priorities to the video frames according to their importance within the video flow. Therefore, I frames should have the highest priority (AC3), P frames the medium priority (AC2) and B frames the lowest one (AC1), as shown in Table 5.1. This table shows the values for each access category (AC) of the minimum contention window (CW_{min}) and maximum (CW_{max}), and the AIFS. Basically, the lower those values, the sooner the AC tries to access the common medium so the higher is the priority.

Table 5.1: IEEE 802.11p Access categories.

AC in 802.11p	CW_{min}	CW_{max}	AIFS
0	15	1023	9
1	15	1023	6
2	7	15	3
3	3	7	2

5.3.2 Motivation of our routing protocol design

In a VANET, nodes are vehicles that move along roads, potentially at high speed, following transit rules, direction of streets, respecting traffic lights and also the presence of buildings and other vehicles. The vehicle density in VANETs constantly changes depending on environmental conditions such as the area, the time of the day and the day of the week. Thus, it is difficult to establish and maintain end-to-end communication paths between sources and destinations as it is traditionally done in MANETs. Our aim is to design a proper data forwarding mechanism to transmit video-reporting messages considering real scenarios and the special constraints of VANETs.

In this work, we propose a new routing protocol for VANETs in realistic urban scenarios, called 3MRP (Multimedia Multimetric Map-aware Routing Protocol). 3MRP seeks to improve the next forwarding node decision based on five metrics: distance to destination, vehicle density, vehicle trajectory, available bandwidth and MAC layer losses. We weight those five metrics to finally obtain a multimetric score associated to each neighbour node in LOS that is a candidate to be the next forwarding node. The weight distribution is self-configured and able to adapt to the changing environment conditions in real time.

In our proposal we can distinguish five processes: routing, signalling, evaluation of metrics and forwarding decision. We explain each one in the following.

5.3.3 3MRP routing

Our routing proposal 3MRP includes a forwarding decision similar to the one used in GPSR [11], although we use a multimetric score instead of just the distance to destination. Basically, it consists on choosing the neighbour with the highest multimetric score. Besides, it also includes new improvements so that the multimetric score adapts to the current environment. Furthermore, we substitute the inefficient perimeter mode of GPSR by the use of a local buffer.

First, we have included in our proposal the REVsim [3] tool described in Chapter 4. As said in Chapter 4, REVsim tackles the important issue of checking which neighbours cannot actually establish communication with the considered node due to any obstacle

and excludes them from the final list of real neighbours in LOS. This avoids sending packets to an unreachable node located behind a building. The neighbours' list will only include those nodes that are in LOS with the current node. When no forwarding node is found, the packet will be stored temporarily in a local buffer during a maximum of 2 seconds. A time-out value is set because higher delays will not be acceptable for video-streaming of real-time content.

Afterwards, the decision of the next forwarding node is done based on the combination of five metrics as it is detailed in section 5.3.5.

5.3.4 3MRP signalling

3MRP gathers information from the periodic interchange of hello messages (HM) that nodes use to announce their presence to their neighbours in transmission range. To obtain precise location information about each node, without introducing much extra overhead, new fields were added in those HM. The format of our new hello messages (NHM) is presented in Table 5.2, and they include these new fields, which are updated at the moment of sending the current hello message:

- **ID**. It is the identifier of each node.
- **Position** (x,y): This field represents the x and y axis positions that represent the geographic position of each node.
- **Velocity** (v_x,v_y): This field represents the speed v_x in x axis and the speed v_y in y axis. Each node updates its own speed from two consecutive position points taken at times t_j and t_{j+1}:

$$v_x = \frac{x_{j+1} - x_j}{t_{j+1} - t_j}, \qquad v_y = \frac{y_{j+1} - y_j}{t_{j+1} - t_j},\ j \geq 0 \tag{5.1}$$

  In our case, $t_{j+1} - t_j$ is equal to 1 second.
- **MAC layer losses (L_{MAC})**: Each node calculates the data losses suffered in the MAC layer and this value is sent in the hello message as a kind of local feedback information. This value is updated every 10 seconds of simulation to track the recent state of the neighbourhood.
- **Density (ρ)**: This field represents the number of neighbours within transmission range divided by $\pi \cdot TR^2$, being TR the transmission range of that node.

Table 5.2: Format of the new hello messages (NHM).

ID	x	y	v_x	v_y	L_{MAC}	ρ

When a node receives a hello message from a neighbour in transmission range, the node stores the moment of reception and updates all the values shown in Table 5.2 in its neighbours' list. This is done following Algorithm 3. If a hello message is received from a neighbour, the algorithm first checks if that node is in LOS before including or updating the information in the neighbours' list. If the node is not in LOS, it is discarded. To keep the neighbours' list updated and having only nodes that actually are in transmission range, nodes remain in a neighbours' list during twice the interval between consecutive hello messages, *i.e.*, during 2 sec. Similarly, when a node receives a hello message from a new neighbour (*i.e.*, a neighbour not registered in its list), it has first to check if that node is in LOS before adding it in the neighbours' list. To do this, a check is done using the output file *output.txt* from our Java program REVSim to see if this candidate neighbour could actually receive a packet if no obstacles are found between them. If this condition is not fulfilled, that neighbour will not be included in the neighbours' list.

Algorithm 3 . Updating the neighbours' list.

Require: A new hello message received with these parameters: ID, x, y, v_x, v_y, L_{MAC}, ρ.

```
# node is in LOS
if output value of REVSim == 1 then
  if Neighbour already is in the neighbours' list then
    Update neighbour information
  else
    if Neighbour is not in the neighbours' list then
      Add node in the neighbours' list
    end if
  end if
else
  # node is not in LOS
  Ignore hello message
end if
```

The sending period of hello messages could be smaller to obtain more accuracy in the composition of the neighbours' list, although a higher signaling traffic could produce an

increase in packet collisions. By default, the sending period of NHM is set to 1 second and the results are good.

If the output binary value $b_{i,j,k}$ from the tool REVsim to detect if obstacles are found between sender and receiver is 1 (*i.e.*, no obstacles are found between both nodes) and the neighbour is already found in the neighbours' list, then the algorithm updates the neighbour information depicted in Table 5.2 (Lines 1 to 3 in Algorithm 3). If the output binary value $b_{i,j,k}$ is 1 and the neighbour is not in the neighbours' list, then we add the node in the neighbours' list (Lines 5 to 6). If the output binary value $b_{i,j,k}$ is 0, we ignore this hello message because it means that an obstacle is found between sender and receiver (Lines 10 to 12).

Table 5.3: Additional information per node in the neighbours' list.

Neighbour Ngh	First NHM time	No. NHM	Last NHM time

The neighbours' list includes the data sent in hello messages (see Table 5.2) and the data shown in Table 5.3. For each neighbour *Ngh*, we store the moment when the last hello message arrived (*Last NHM time* in Table 5.3). This is done to estimate the future position of that neighbour node, as it is explained in the next section. Also, we store the moment when the first hello message arrived (*First NHM time*) and the total number of hello messages received (*No. NHM*). These values will be used to estimate the available bandwidth using a metric explained in the next section.

5.3.5 Design of routing metrics for 3MRP

In this section we detail the design of each one of the five metrics included in our multimedia multimetric map-aware routing protocol 3MRP, which is our proposal of geographic routing protocol based on hop-by-hop building-aware forwarding decisions. The use of these metrics improves the selection of the next forwarding node. The five metrics considered are: distance to destination, trajectory of the vehicles, nodes density, MAC losses and available bandwidth. According to the adhoc principle of using only local information (*i.e.*, infrastructureless operation) nodes will use those five metrics gathered from the hello messages (NHM) of the next hop candidates in their neighbourhood to take the decision of the best next forwarding node. The five metrics are described in the following.

Distance: Geographic routing protocols have the goal to forward packets hop-by-hop to their destination. In many routing protocols, the next forwarding hop is the closest neighbour to destination. Geographic protocols use the geographic information of every node to take forwarding decisions. We assume that all vehicles know their own position, the destination's position (x_D, y_D) as well as the positions of all their neighbours from periodic hello messages where nodes include their own position. Therefore, the position (x_{Ngh}, y_{Ngh}) of each neighbour Ngh can be obtained.

The Euclidian distance $d(Ngh, D)$ from each neighbour node Ngh to destination D can be computed using Equation (5.2), where d_{Ngh} is the distance of each neighbour Ngh to destination (D).

We have designed Equation (5.3) to compute the metric of the distance, $u_{dst,Ngh}$, for each neighbour node Ngh. In this case, the shorter the value of the distance $d(Ngh, D)$, the better. That is, we prefer a neighbour as close as possible to destination. However, all neighbours whose distance to destination (*i.e.*, $d(Ngh, D)$) is lower than the transmission range (TR), should have the maximum value of the metric because in this case all those neighbours could be the last hop towards destination D. Due to that, we have designed the metric of the distance $u_{dst,Ngh}$ as shown in Figure 5.3 and described in Equation (5.3). While $d(Ngh, D) < TR$, $u_{dst,Ngh} = 1$ and when $d(Ngh, D) \geq TR$, $u_{dst,Ngh}$ decreases linearly till a minimum value of $d(Ngh, D) = d(S, D)$ which means that neighbour Ngh and source S are the same node. We can observe from Figure 5.3 that $0 \leq u_{dst,Ngh} \leq 1$.

$$d(Ngh, D) = \|\vec{x}_{Ngh} - \vec{x}_D\| = \sqrt{(x_{Ngh} - x_D)^2 + (y_{Ngh} - y_D)^2} \tag{5.2}$$

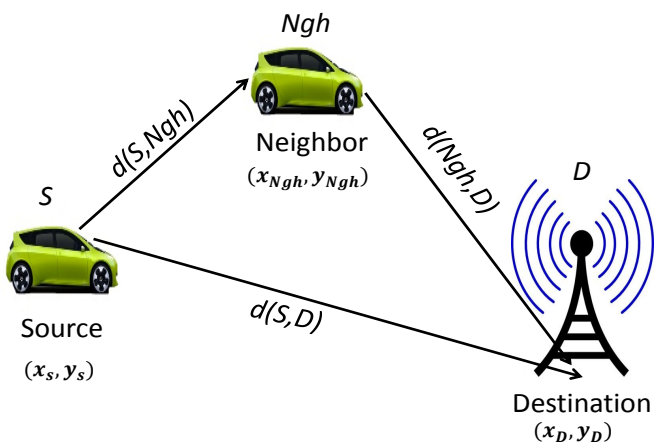

Figure 5.2: Distances $d(S, D)$ from source S to destination D, $d(S, Ngh)$ from source S to a neighbour Ngh and $d(Ngh, D)$ from a neighbour Ngh to destination D.

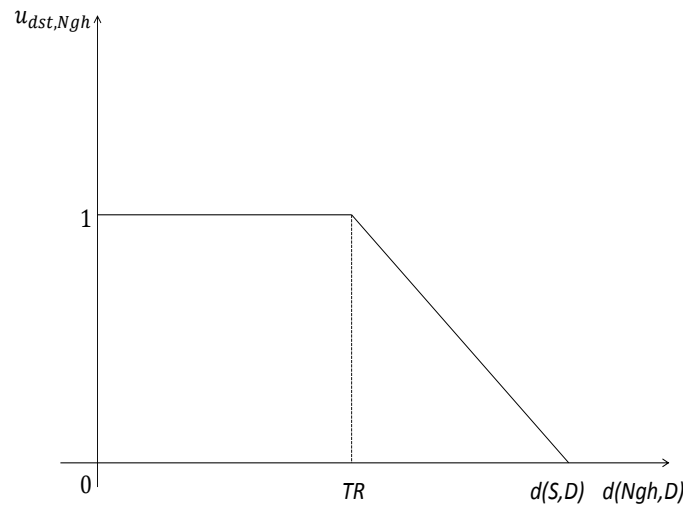

Figure 5.3: Distance metric $u_{dst,Ngh}$ for node Ngh.

$$u_{dst,Ngh} = \begin{cases} \frac{-d(Ngh,D)}{d(S,D)-TR} + \frac{d(S,D)}{d(S,D)-TR}, & \text{if } d(Ngh,D) \geq TR \\ 1, & \text{if } d(Ngh,D) < TR \end{cases} \tag{5.3}$$

Trajectory: The trajectory of vehicles in VANETs is a very important metric that might help to select a suitable next forwarding node that moves towards destination. We compute the trajectory of a node as a function of the current and the future distances of that node to destination using the v_x and v_y velocities. This helps to determine the trajectory of that vehicle and as a consequence to detect if the node is getting closer or going away from the destination node. The aim of this metric is to avoid that the source could take wrong forwarding decisions based only on the distance and send packets to vehicles that were actually going away from destination, which could make packet losses increase as a consequence. Due to that, taking the moving direction of vehicles into account to take forwarding decisions is an important benefit for VANETs.

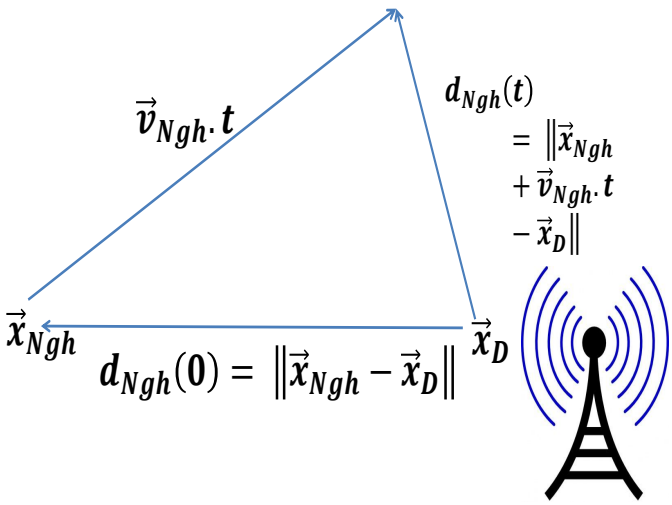

Figure 5.4: Trajectory of node Ngh towards the access point (AP) destination.

We obtain the trajectory metric $u_{trj,Ngh}$ of a candidate neighbour node Ngh using a future distance $d_{Ngh}(t)$ to destination of that node in the t moment and $d_{Ngh}(0) = d$ which is its current distance to destination. See Equation (5.4) and Figure 5.4 to see the meaning of the trajectory metric.

The distance $d_{Ngh}(t)$ is computed by estimating the future position of that candidate neighbour node Ngh using its speed according to Equation (5.5).

The speed of the node, $v_{\vec{Ngh}}$, helps us to give a higher score to nodes that sooner will be closer to destination (*i.e.*, the AP). The idea is that with a higher speed, nodes moving towards destination may arrive sooner to destination since the distance to destination decreases faster. We compute the $u_{trj,Ngh}$ metric using Equation (5.6).

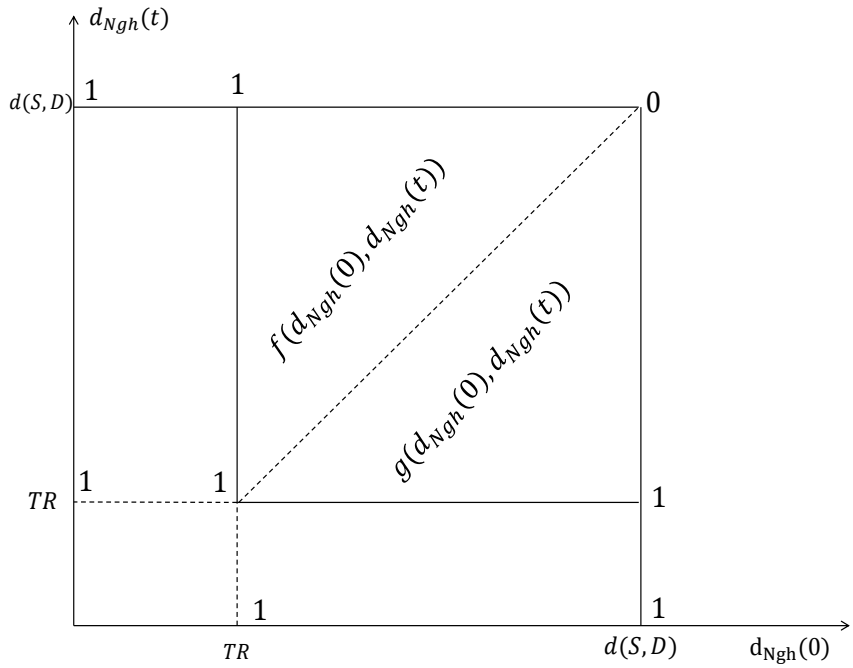

Figure 5.5: Projection of the function $u_{trj,Ngh}$ in ($d_{Ngh}(0)$,$d_{Ngh}(t)$) plane.

$$d_{Ngh}(0) = \| \vec{x}_{Ngh} - \vec{x}_D \| \tag{5.4}$$

$$d_{Ngh}(t) = \| \vec{x}_{Ngh} + \vec{v}_{Ngh} \cdot t - \vec{x}_D \| \tag{5.5}$$

$$u_{trj,Ngh} = \begin{cases} 1, & \text{if } d_{Ngh}(0) < TR \\ 1, & \text{if } d_{Ngh}(0) > TR \text{ and } d_{Ngh}(t) < TR \\ f(d_{Ngh}(0), d_{Ngh}(t)), & \text{if } d_{Ngh}(0), d_{Ngh}(t) > TR \\ & \text{and } d_{Ngh}(0) > d_{Ngh}(t) \\ g(d_{Ngh}(0), d_{Ngh}(t)), & \text{if } d_{Ngh}(0), d_{Ngh}(t) > TR \\ & \text{and } d_{Ngh}(0) < d_{Ngh}(t) \end{cases} \tag{5.6}$$

where

$$f(d_{Ngh}(0), d_{Ngh}(t)) = \frac{d_{Ngh}(t) - d(S,D)}{TR - d(S,D)} \tag{5.7}$$

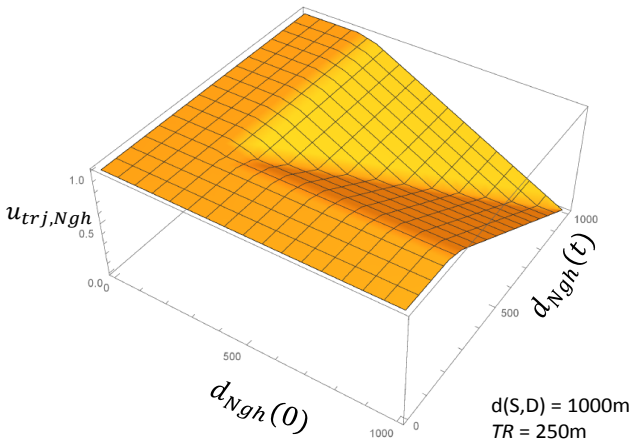

Figure 5.6: Representation of the trajectory metric $u_{trj,Ngh}$ for $TR = 250$m and $d(S, D) = 1000$m.

$$g(d_{Ngh}(0), d_{Ngh}(t)) = \frac{d_{Ngh}(0) - d(S, D)}{TR - d(S, D)} \tag{5.8}$$

$d_{Ngh}(t)$ is an estimation of the future position of the node Ngh in the moment t, as it is depicted in Figure 5.4. v_{Ngh} is the average speed of the evaluated neighbour Ngh with respect to destination and computed from two consecutive positions. $\vec{x}_{Ngh}$ and $\vec{x}_D$ are the neighbour and destination positions, respectively. Notice that $\| \cdot \|$ refers to the module function of a vector.

The trajectory metric increases when the vehicle moves towards destination, and decreases when the vehicle moves away from destination, as depicted in Equation (5.6). As the distance metric, the trajectory metric $u_{trj,Ngh}$ has a range between 0 and 1. Figure 5.5 is the projection of function $u_{trj,Ngh}$ in the ($d_{Ngh}(0)$,$d_{Ngh}(t)$) plane. We can observe that if $d_{Ngh}(0) < TR$, this means that the neighbour is within the transmission range of destination and as a consequence we should give $u_{trj,Ngh}$ its highest value (*i.e.*, 1) regardless of the value of $d_{Ngh}(t)$. In addition, if $d_{Ngh}(0) > TR$ and $d_{Ngh}(t) < TR$, this means that the future distance is within the transmission range of destination and as a consequence we should also give $u_{trj,Ngh}$ its highest value (*i.e.*, 1). Finally, if $d_{Ngh}(0)$ and $d_{Ngh}(t)$ are higher than TR, we must further analyze the subcases of $d_{Ngh}(0)$ being higher or lower than $d_{Ngh}(t)$. In the subcase of $d_{Ngh}(0) > d_{Ngh}(t)$, this means that the future distance to destination is smaller that the current distance (*i.e.*, neighbour is getting closer to destination D). This subcase is better than the subcase of $d_{Ngh}(0) < d_{Ngh}(t)$, which means that the future distance to destination is higher

that the current distance (*i.e.*, the neighbour is getting far from destination D). For these two subcases, we designed two functions f and g (see Figure 5.5) that satisfy the conditions mentioned before.

To understand more Figure 5.5, we have plotted in Figure 5.6 a 3D graph example for metric $u_{trj,Ngh}$ where $TR = 250$m and $d(S, D) = 1000$m.

Vehicles' density: It is computed as the number of vehicles in the neighbours' list of each node at the moment of sending the current hello message (N_v), divided by the area within the transmission range ($\pi \cdot TR^2$) of that vehicle. The neighbours' list of a node is composed by vehicles found in its transmission range. Each node computes its density of nodes ρ_{Ngh} using Equation (5.9) and includes it in the next hello message.

The algorithm gives a higher score when the neighbour node Ngh has a higher value of ρ_{Ngh}. Nodes with a denser area in the transmission range will have more possibilities to forward the packet to a next node. This is true until reaching a maximum nodes' density ρ_{max}, above which the very high number of vehicles in the surrounding area of the node increases the collisions' frequency. We set ρ_{max} to 200 vehicles/km^2. The reason is that, as mentioned before, with a vehicles' density above 200 vehicles/km^2, the VANET is in a very high density scenario and the chance of collisions increases exponentially as we have seen in our simulations.

We have designed a concave function for the density metric shown in Figure 5.7. This function has its maximum at $\rho_{Ngh} = \rho_{max}$ and above ρ_{max} it decreases till $2\rho_{max}$ where again it reaches zero and keeps on zero for all $\rho_{Ngh} > 2\rho_{max}$.

Equation (5.10) describes how we calculate the vehicles' density metric $u_{dns,Ngh}$ as shown in Figure 5.7. This way, we penalize those nodes whose number of neighbours in their transmission range is above a threshold (*i.e.*, $\rho_{Ngh} > \rho_{max}$). Following the same strategy as for the previous metrics, $0 \leq u_{dns,Ngh} \leq 1$.

$$\rho_{Ngh} = \frac{N_v}{\pi \cdot TR^2} \tag{5.9}$$

$$u_{dns,Ngh} = \begin{cases} \frac{-1}{\rho_{max}^2} \cdot \rho_{Ngh}^2 + \frac{2}{\rho_{max}} \cdot \rho_{Ngh}, & \text{if } \rho_{Ngh} \leq 2\rho_{max} \\ 0, & \text{if } \rho_{Ngh} > 2\rho_{max} \end{cases} \tag{5.10}$$

Available bandwidth: Video-reporting messages require a given amount of network resources (*e.g.*, bandwidth) to achieve a good performance. To provide a certain level of QoS, we use an estimator of the available bandwidth in VANETs based on an approach developed for IEEE 802.11 networks called available bandwidth estimator (ABE) [75]. We use ABE as a metric in our forwarding decision algorithm to help in the selection of the best next forwarding node.

In the following, we briefly summarize the ABE operation to estimate the available bandwidth in a link between two nodes. A complete explanation of the authors can be found in [76]. Basically, each node estimates its percentage of idle time by sensing the common wireless medium. This value is included in its hello messages. The available bandwidth estimation of a wireless link in ABE uses the idle times of the emitter (T_e) and the receiver (T_r) of a link of capacity C. ABE computes the collision probability of

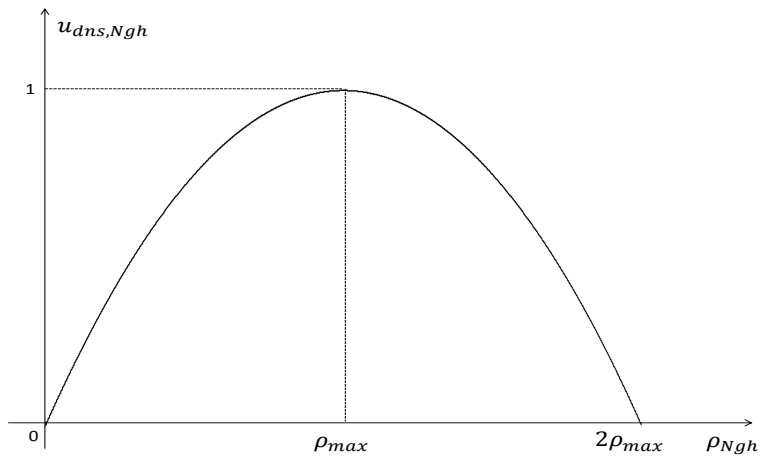

Figure 5.7: Designed function for the vehicles density' metric $u_{dns,Ngh}$.

the hello messages, named p_{hello}. The collision probability of packets of m bits, named p_m, is derived from the collision probability of the hello messages using Equation (5.11), where N is the number of nodes in the scenario and s is the average speed of the nodes.

$$p_{m,N,s} = f(m,N,s) \cdot p_{hello}(m,N,s) \tag{5.11}$$

The function $f(m,N,s)$ is used in Equation (5.11) to estimate the packet collision probability $p_{m,N,s}$. This $f(m,N,s)$ was obtained in [75] by computing the Lagrange interpolating polynomial, taking pairs of values of packet losses and losses of hello messages from many simulations of a VANET scenario. The authors of [75] obtained the final expression for $f(m,N,s)$, shown in Equation (5.12).

$$\begin{aligned} f(m,N,s) &= -7.475 \cdot 10^{-5} \cdot m - 8.983 \cdot 10^{-3} \cdot N - \\ &\quad 1.428 \cdot 10^{-3} \cdot s + 1,984 \end{aligned} \tag{5.12}$$

The additional overhead introduced by the binary exponential backoff mechanism was derived in [76], see Equation (5.13).

$$K = \frac{\text{DIFS} + \overline{\text{backoff}}}{T_m} \tag{5.13}$$

where T_m (in sec.) is the time separating the emission of two consecutive frames, DIFS (Distributed Coordination Function Interframe Space) [77] is a fixed interval so that nodes can have access to the medium if it is free for a time period longer than

DIFS. Finally, $\overline{\text{backoff}}$ is the number of backoff slots decremented on average for a single frame. Merging the different mechanisms that impact the available bandwidth, the sender estimates the available bandwidth ABE on each neighbour' wireless link using Equation (5.14) [75]. T_{Ngh} is T_r, being Ngh the receiver; and T_{Nan} is T_e, being (Nan) the node under analysis the emitter of the link.

$$\text{ABE}_{Ngh} = (1 - K) \cdot (1 - p_{m,N,s}) \cdot T_{Nan} \cdot T_{Ngh} \cdot C \tag{5.14}$$

Finally, we divide ABE_{Ngh} by the link capacity C, obtaining Equation (5.14) as the available bandwidth metric. Notice that $0 \leq u_{abe,Ngh} \leq 1$. A high value of $u_{abe,Ngh}$ means a high available bandwidth in the link formed with node Ngh.

$$u_{abe,Ngh} = \text{ABE}_{Ngh}/C \tag{5.15}$$

MAC layer losses: To compute the losses metric, we focus on the MAC layer instead of on the traditional routing layer since in VANETs we only manage local information instead of end-to-end information. This is an important principle in infrastructureless adhoc networks. We calculate the MAC layer losses and we use it in our routing protocol as a kind of local feedback information within the neighbourhood. Depending on this information, we can vary the decision of the best forwarding node. Furthermore, if we find that packet losses are very high, we can stop sending P and B frames and send only I frames, seeking to decrease the packet losses and improve the network performance.

$$u_{los,Ngh} = 1 - L_{MAC}(Ngh) \tag{5.16}$$

According to Equation (5.16), $L_{MAC}(Ngh)$ is the MAC layer losses in the link formed between nodes Ngh and Nan. A value of $u_{los,Ngh}$ closer to one means that a low number of packets were lost, while a value closer to zero means that a high number of packets were lost.

5.3.6 3MRP forwarding decision

3MRP takes hop-by-hop forwarding decisions based only on geographic information. When a node wants to send a packet it has first to choose the optimal next forwarding node from its list of actual neighbours.

When a sender node receives hello messages (HM) from its neighbours in transmission range, the node updates its neighbours' list with all those nodes in LOS that sent their HM with enough power to be considered as a neighbour. After that, the node evaluates and assigns a total multimetric qualification to each neighbour as a candidate for next forwarding node. As a first step, we assign the same weights $(w_1, w_2, w_3, w_4, w_5)$ to each metric $(u_{dst,Ngh}, u_{trj,Ngh}, u_{dns,Ngh}, u_{abe,Ngh}, u_{los,Ngh})$, respectively in the multimetric score $\bar{u}_{Ngh}$ of each neighbour Ngh.

$$\bar{u}_{Ngh} = \sum_{i=1}^{5} u_{i,Ngh} \cdot w_i = u_{dst,Ngh} \cdot w_1 + u_{trj,Ngh} \cdot w_2 + u_{dns,Ngh} \cdot w_3 + u_{abe,Ngh} \cdot w_4 + u_{los,Ngh} \cdot w_5 \quad (5.17)$$

We finally obtain a multimetric score for each candidate node using Equation (5.17). The final score varies between 0 and 5. The best next forwarding node is the neighbour with the highest multimetric value. We first give the same degree of importance to all the metrics, *i.e.*, $w_i = 1/5$, $1 \leq i \leq 5$. In the next section, we propose an algorithm to compute self-configured weights of the metrics to dynamically update the scores of the candidate neighbour nodes.

5.4 Algorithm to update the weights of the metrics to compute a multimetric score

5.4.1 Motivation

Several routing protocols for VANETs based on a hop-by-hop operation have been proposed in the literature, *e.g.* [11, 68, 69, 70, 71]. Some of them use several metrics to decide the next forwarding node. Usually, the weights of the metrics have the same value (*i.e.*, the metrics play the same importance in the calculation of the multimetric score). Nonetheless, we claim that a better scheme could give each metric a variable weight depending on the current network conditions. As a consequence, nodes could be classified in a more accurate way. We foresee that since our algorithm needs to classify nodes from best to worst each time a packet must be forwarded, the weights of the metrics in our multimedia multimetric routing protocol could better take different values than $\frac{1}{5}$, being 5 the number of metrics.

We propose an algorithm to update the weights dynamically (*i.e.*, re-calculate the multimetric score of neighbours) throughout time, so that those most decisive metrics are highlighted (their weights increase). This way, if a metric value in the nodes differs noticeably with respect to the average neighbours' value in that metric, we give more importance (*i.e.*, a higher weight) to that metric. That is, we define as a decisive metric when the neighbour nodes have different values in that metric. This points out that its value may help the forwarding algorithm to better classify neighbour nodes. Conversely, a more constant metric value (*i.e.*, all the neighbour nodes have roughly the same value) indicates that this metric is not so decisive to arrange the neighbour nodes, thus our algorithm gives a lower value to its weight. We call our algorithm to update the multimetric score of neighbours as Dynamic Self-configured Weights (DSW) algorithm.

5.4.2 DSW algorithm description

Each time a node needs to forward a packet, that node has to classify the nodes included in its neighbours' list (which are in LOS) from the best to the worst by using the multimetric score of Equation (5.17). In Equation (5.17), the weights $w_1, w_2, ..., w_5$ are now computed by our algorithm so that they are dynamically updated depending on the current state of the neighbourhood. The idea is to highlight those decisive metrics that can better help the current node under analysis (Nan) to choose the best next forwarding node among the nodes in its neighbours' list.

As we mentioned before, we have five metrics: $(u_1, u_2, u_3, u_4, u_5) = (u_{dst,Ngh}, u_{trj,Ngh}, u_{dns,Ngh}, u_{abe,Ngh}, u_{los,Ngh})$ computed with Equations (5.3), (5.6), (5.10), (5.15) and (5.16), respectively.

Let us denote R_m as the variation value for each metric m between time t_1 and time t_2 where $t_2 > t_1$, defined as:

$$R = \begin{cases} R_1 = \dfrac{[u_1(t_2) - A_1(t_2)] - [u_1(t_1) - A_1(t_1)]}{2} \\ R_2 = \dfrac{[u_2(t_2) - A_2(t_2)] - [u_2(t_1) - A_2(t_1)]}{2} \\ \vdots \\ R_5 = \dfrac{[u_5(t_2) - A_5(t_2)] - [u_5(t_1) - A_5(t_1)]}{2} \end{cases} \tag{5.18}$$

where $0 \leq u_m(t_1)$,$u_m(t_2) \leq 1$ and $0 \leq A_m(t_1)$,$A_m(t_2) \leq 1$; $m \in [1, 5]$. $u_m(t_1)$ and $u_m(t_2)$ are the current scores of each metric m for times t_1 and t_2 respectively. $A_m(t_1)$ and $A_m(t_2)$ are the average score values of each metric m computed for all the neighbours of the forwarding node. Now, if $R_m \leq 0$; this means that metric m is getting worst in the period of (t_2-t_1). As a consequence, R_m should be equal to zero.

This way, we will have a vector $R = [R_1, R_2, ..., R_5]$. Suppose that the maximum value found in vector R is $R_{max} = R_x$ where x $\in [1, 5]$. Now, we normalize vector R to be between 0 and 1 (*i.e.*, $0 \leq R \leq 1$) and this new vector is named S.

$$S = \begin{cases} S_1 = \dfrac{R_1}{R_x} \\ S_2 = \dfrac{R_2}{R_x} \\ \vdots \\ S_x = \dfrac{R_x}{R_x} = 1 \\ \vdots \\ S_5 = \dfrac{R_5}{R_x} \end{cases} \tag{5.19}$$

To be sure that the sum of weights of all the metrics is equal to one, we calculate the parameter ξ value using Equation (5.20)

$$\xi = \frac{1}{\sum_{i=1}^{5} S_i} \tag{5.20}$$

Next, the new normalized vector of weights W is:

$$W = \begin{cases} W_1 = S_1 \cdot \xi \\ W_2 = S_2 \cdot \xi \\ \vdots \\ W_x = S_x \cdot \xi = \xi \\ \vdots \\ W_5 = S_5 \cdot \xi \end{cases} \tag{5.21}$$

Thus, instead of using equal weights (w_1, w_2, w_3, w_4, w_5) in Equation (5.17), with $w_i = 1/5$, $1 \leq i \leq 5$, we use dynamic weights (W_1, W_2, W_3, W_4, W_5) computed as depicted in Equation (5.21).

Finally, we must mention that in case that all the metrics for a specific node are getting worst, no preferences could be given to any metric and as a consequence we give all of them equal weights $W_i = \frac{1}{5}$. The probability for this special case to happen is very low.

5.5 Simulation results

We implemented our proposal in the open source network simulator NS-2 [56] where we conducted simulations to evaluate the benefits of our approach. In the simulations, we used a real city area obtained from the example district of Barcelona, Spain (see Figure 6.6). In order to simulate a realistic scenario, the CityMob for Roadmaps (C4R) [59] simulator was used to obtain the mobility model of the vehicles. C4R is a mobility generator that uses the Simulation of Urban MObility (SUMO) engine [60]. Besides, C4R imports maps directly from OpenStreetMap [61] and generates NS-2 compatible files to specify the mobility model for the vehicles through the city along the whole simulation. Video flows are transmitted from a vehicle that suffers an accident to an access point (AP), set at the Hospital Clinic of Barcelona. The AP represents an emergency unit where the vehicle sends its video-reporting message upon the event of the traffic accident. A crashed vehicle sends its video-reporting message to the closest AP in the city. The simulation settings of the scenario are shown in Table 6.2. All the Figures show confidence intervals (CI) of 90 percent obtained from 20 simulations per point, each simulation with an independent mobility scenario.

We analyse the performance of our multimetric algorithm 3MRP compared to GPSR [11]. The simulation area is 1700 m x 580 m. We consider two densities of vehicles, 50 vehicles/km^2 (scenario 1) and 100 vehicles/km^2 (scenario 2) which are

randomly positioned. The average speed of the vehicles is 50 km/h while the maximum speed is 120 km/h. The multimetric score used in the forwarding scheme of our proposed routing protocol, has equal weights (3MRP) or dynamic weights (3MRP+DSW). There is one fixed destination, an access point (AP), through which vehicles connect to the network to report traffic information, in this case a video-reporting message about a traffic accident.

Table 5.4: Simulation settings of the VANET scenario.

Map Zone	**Example District of Barcelona**
Area	1700×580 m^2
Density of vehicles	50 vehicle/km^2 (scenario 1),
	100 vehicle/km^2 (scenario 2)
Number of nodes	50 and 100 vehicles
Transmission range	250 m
Mobility generator	SUMO [60]/C4R [59]
MAC specification	IEEE 802.11p
Nominal bandwidth	12 Mbps
Simulation time	300 s
Video encoding	MPEG-2 VBR
Video bit rate	150 Kbps
Video sources	1
Video sequence sent	Traffic accidents [58]
Routing protocol	GPSR, 3MRP, 3MRP + DSW
Transport protocol	RTP/UDP
Maximum packet size	1500 Bytes
Weighting metric values	1/5 or dynamic
Queue sizes	50 packets

Figure 5.9 shows the average percentage of packet losses using our routing protocol (3MRP) with equal weights and using our dynamic self-configured weights (3MRP+DSW) scheme. We compare both proposals to GPSR and we present results for low and medium vehicles density. We can clearly notice how 3MRP+DSW obtains the best results in both scenarios reducing losses around 10%. This is due to the optimal

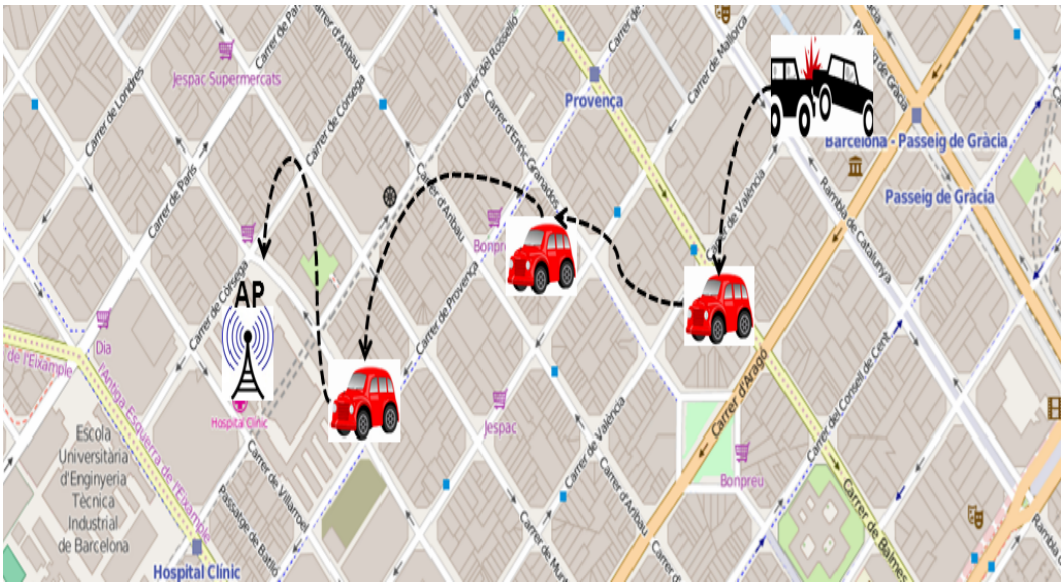

Figure 5.8: Simulation scenario of Barcelona. It includes one emergency unit in the Hospital Clinic of Barcelona, named access point (AP) in the map.

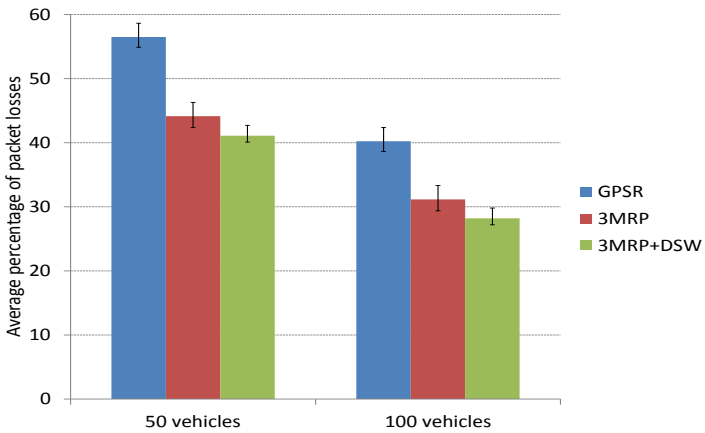

Figure 5.9: Average percentage of packet losses.

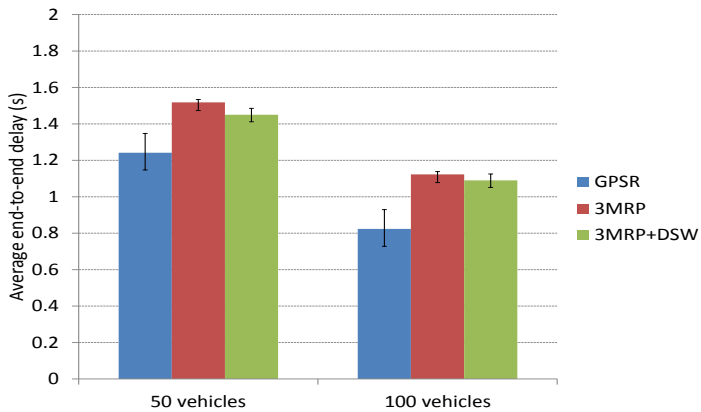

Figure 5.10: Average end-to-end packet delay (sec).

selection of the next forwarding node based on the five proposed metrics with dynamic self-configured weights.

Figure 5.10 shows the results of the average packet delay. The delay is calculated based on those packets that successfully arrived at destination. Since GPSR takes the forwarding decision considering only distance, it obtains the lowest packet delay in both scenarios. However, GPSR shows the highest losses (see Figure 5.9). This is because with GPSR, a lower number of packets arrived at destination and much of the lost packets traveled through a considerable number of hops before being dropped. Conversely, our proposal 3MRP is able to reduce packet losses although the delay slightly increases in about 0.3 seconds. Nonetheless, 3MRP+DSW even reduces more the packet losses with a lower delay than the previous 3MRP.

Figure 5.11 depicts the peak signal-to-noise ratio (PSNR) obtained for GPSR, 3MRP and 3MRP+DSW. Both versions of 3MRP clearly outperform GPSR in more than 4 dB. We can see that the case including the five metrics and the dynamic metric weigh distribution (3MRP+DSW) improves the PSNR in 2 dB compared to the case of using equal weights in 3MRP. This is because 3MRP+DSW selects the best forwarding node based on special characteristics for VANETs and also it uses a dynamic metric weigh distribution that classifies nodes in a better way giving each metric its importance depending on the current environment conditions.

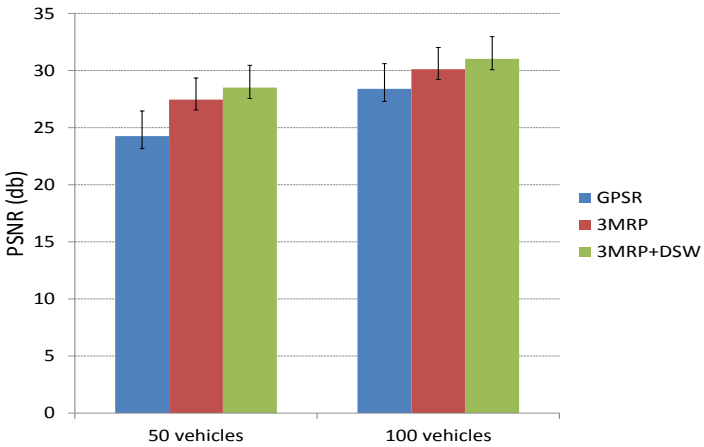

Figure 5.11: Peak Signal to Noise Ratio (PSNR).

5.5.0.1 Gain for I, P and B video frames

To better see separately the benefits of our proposal obtained for I, P and B video frames, we define the following parameters:

$$\%GainI = \left(\frac{IL_{GPSR} - IL_{3MRP+DSW}}{IL_{GPSR}} \right) \cdot 100 \tag{5.22}$$

$$\%GainP = \left(\frac{PL_{GPSR} - PL_{3MRP+DSW}}{PL_{GPSR}} \right) \cdot 100 \tag{5.23}$$

$$\%GainB = \left(\frac{BL_{GPSR} - BL_{3MRP+DSW}}{BL_{GPSR}} \right) \cdot 100 \tag{5.24}$$

where:

- IL_{GPSR}: percentage of packet losses for I frames when GPSR is used.
- $IL_{3MRP+DSW}$: percentage of packet losses for I frames when 3MRP+DSW is used.
- PL_{GPSR}: percentage of packet losses for P frames when GPSR is used.
- $PL_{3MRP+DSW}$: percentage of packet losses for P frames when 3MRP+DSW is used.
- BL_{GPSR}: percentage of packet losses for B frames when GPSR is used.

- $BL_{3MRP+DSW}$: percentage of packet losses for B frames when 3MRP+DSW is used.
- $GainI$: Gain obtained for I frames using 3MRP+DSW with respect to GPSR.
- $GainP$: Gain obtained for P frames using 3MRP+DSW with respect to GPSR.
- $GainB$: Gain obtained for B frames using 3MRP+DSW with respect to GPSR.

Figure 5.12 shows the average of all the simulation results for $\%GainI$, $\%GainP$ and $\%GainB$. We can see that using 3MRP+DSW, the gain is 7% (9%) for I packets, 21% (24%) for P packets and 22% (26%) for B packets, for 50 vehicles scenario (100 vehicles scenario) with respect to GPSR. As we can observe, $\%GainB > \%GainP > \%GainI$ in all the cases. The improvement is higher for the high density scenario, since there are more vehicles to choose the best candidates to forward packets according to our multimetric algorithm. Besides, the gain is much noticeable for P and B frames than for I frames. We impute this fact to the higher size of I frames, which makes it more difficult to enhance the performance so notably as with smaller P and B frames.

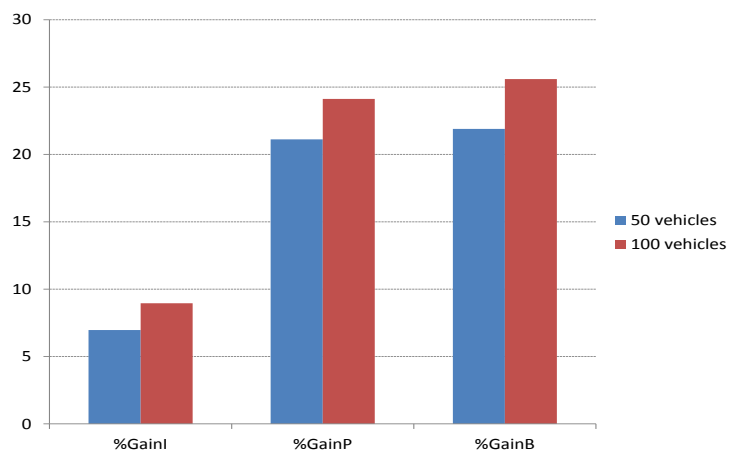

Figure 5.12: Average percentage gain for I, P and B frames.

5.6 Conclusion

In this Chapter, we have presented a new routing protocol named (3MRP) for VANETs to send video-reporting messages in urban scenarios. Our framework could be used in smart cities where prevention and management of accidents is an important goal. We

understand that with a video message, the level of seriousness of the accident could be much better evaluated by the authorities (*e.g.*, hospitals, paramedics, ambulances) allowing a fast warning of the incident to emergency units, which potentially could save lives. Besides, the transport unit in charge of the traffic information services would quickly be warned by the vehicles immediately after the event of any incident (*e.g.*, traffic jam or traffic accident). Furthermore, vehicles would instantaneously warn other vehicles about any accident in the roads. That would improve the quality of life in the smart cities. That would require the design of a proper dissemination protocol, which we will start in a future work. All theses actions would improve the quality of life in the smart cities and even avoid accidents and save lives.

3RMP includes five metrics (distance, trajectory, density, available bandwidth and MAC layer losses) to take local forwarding decisions. Moreover, the proposal is building-aware, which avoids to select those nodes in transmission range located behind a building. This feature allows the network simulator to send packets only to nodes that are not behind buildings, thus mimicking what happens in reality which makes our simulations more realistic. The reason is that in real life buildings would block the signal and packets would be dropped if the receiver was behind a building. For that purpose, we have developed a program named REVSim [3] in Chapter 4 that gives the state (*i.e.*, in LOS or not) of any neighbour with respect to the current forwarding node in order to see if that neighbour can be a candidate as next forwarding node. Otherwise, this neighbour node will be deleted from the neighbour list, since it is behind a building.

In addition, a local buffer is used to temporarily store those packets when the routing protocol fails in finding a proper next forwarding node. A timer is activated and if the timer expires over 3 seconds, the packet is dropped since the video frame would reach destination too late for the decoding process.

The multimetric forwarding algorithm computes a global score value used to select the best next forwarding node among all the neighbours in LOS within the transmission range. In addition, we have developed an algorithm able to update the weights of the metrics dynamically (*i.e.*, updating the multimetric score of neighbours) throughout time, so that most decisive metrics are highlighted. This helps the overall protocol to give each metric its importance at each moment and as a consequence we attain better results compared to giving fixed weights to all the metrics. We evaluated our proposal compared to GPSR in two scenarios with low and medium vehicles' density. In terms of packet losses and throughput, 3MRP+DSW improves both 3MRP and GPSR, due to the new way of selecting the next forwarding node and the dynamic scheme to give each metric its corresponding weight. We conclude that 3MRP+DSW performs better in both scenarios with low and medium vehicles' density. Our proposal makes the network more efficient as well as achieves a higher degree of satisfaction of the users by receiving much more frames with a good average end-to-end delay. This definitively will improve the quality of the video perceived by the end user as the PSNR value shows.

Chapter 6

A Game-theoretical Multimedia Multimetric Map-Aware Routing Protocol (G-3MRP)

In this Chapter we propose a geographical routing protocol for VANETs to provide video-reporting messages in urban scenarios based on a novel game-theoretical scheme [2]. The REVsim [3] tool that was explained in Chapter 4 is included in our proposal in order to detect the presence of buildings. Finally, simulations show the benefits of our proposal, taking into account the mobility of the nodes and the presence of interfering obstacles.

6.1 Introduction

Recently, game theory is considered one of the most interesting theoretical framework to analyze and optimize resource allocation problems in digital communication scenarios [78]. For example, a shared wireless environment can be defined as a game where each node (each player) competes with the others for the access to the channel [79].

Nonetheless, some recent works in the literature show that the game theory analysis can also be employed for other purposes, such as wireless channels modeling [80] and distributed optimization [81]. In addition, the effectiveness of the video transmission depends on how packets are routed and transmitted as it is shown in some experimental results [82, 83, 84, 85]. For this purpose, we think that game theory (GT) may provide some help in the way that packets of video-reporting messages can be sent over VANETs enhancing the overall performance. Our research in this Chapter focuses on the deployment of an efficient geographical routing protocol based on a game-theoretical approach to forward video-reporting messages over VANETs. This contribution seeks to further enhance the overall performance of the network. As a starting point, we use our geographical routing protocol 3MRP presented in Chapter 5.

6.2 Related Work

During the last years, game theory was taken into account in several approaches to optimize video transmission across heterogeneous channels [86, 87] or across ad hoc networks [49, 23]. Here in this section, we report some of the most recent works that employ game theory, which has been recently an active topic in communications. Regarding these works, several distributed resource allocation strategies between multiple competing users were implemented using game theory. For example, authors in [88] proposed a distributed algorithm to optimize data rate of a multihomed video which is transmitted via several streams. Every time the sender needs to provide multiple QoS levels, different bandwidth allocations also need to be negotiated: In [89], the authors introduced a cross-layer optimization framework so that the optimal resource allocation can be done to each path of the multipath routed video source over wireless networks. This allocation scheme maximizes the total weighted QoE of multiple video streams that are transmitted over a wireless environment. A scalable video codec architecture at the video source coding level gives us the opportunity to specify different quality levels. Regarding this case, an important role was played by game theory in minimizing the playout delays [90] or shaping the bit rate [91]. Normally, the approaches based on game theory are focused on noncooperative games to model contention or conflicts in resource allocation. We can also find some collaborative strategies that aim at maximizing the final performance via a synergetic cooperation between nodes, *e.g.* [92] and [93]. Furthermore, authors in [94] propose a cross-layer distributed classification algorithm based on game theory that runs independently on each uploading node of a distributed content delivery network. Packets are scheduled into multiple QoS classes via a non cooperative game that aims at minimizing the channel distortion which affects each stream as well as the final reconstructed sequence.

6.3 A Game-Theoretical Routing Protocol for VANETs

In this Chapter, we apply game theory in our multimetric routing protocol with the dynamic self-configured weights (3MRP+DSM) that we have presented in Chapter 5 to further improve the overall performance of VANETs. We assume that each source node has a set of I, P and B video frames of a video flow to be transmitted. Also, we assume that each source has three forwarding nodes classified as (*i.e.*, excellent (E), good (G) and bad (B) nodes through which those frames could be sent. Nodes *play* a *routing game* to distribute the video flows seeking their own best performance. The *players* of the game are the VANET nodes and the *action* of the game is to select the proper forwarding node to forward their video-streams. In the following section, we will introduce the game-theoretical proposal included in the our geographical routing scheme 3MRP+DSW.

6.3.1 The Bases of Our Proposal

Figure 6.1 shows the proposed architecture. We assume N connections (S_1-D_1, S_2-D_2, ..., S_N-D_N) and three selecting forwarding nodes. It is likewise possible to apply the same proposal to any VANET independently of the number of connections and nodes.

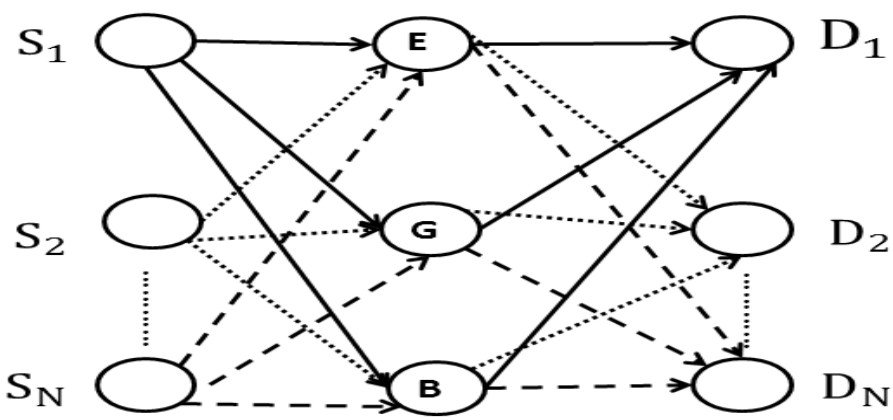

Figure 6.1: Proposed framework to send the video frames. E represents the *excellent node*, G the *good node* and B the *bad node*.

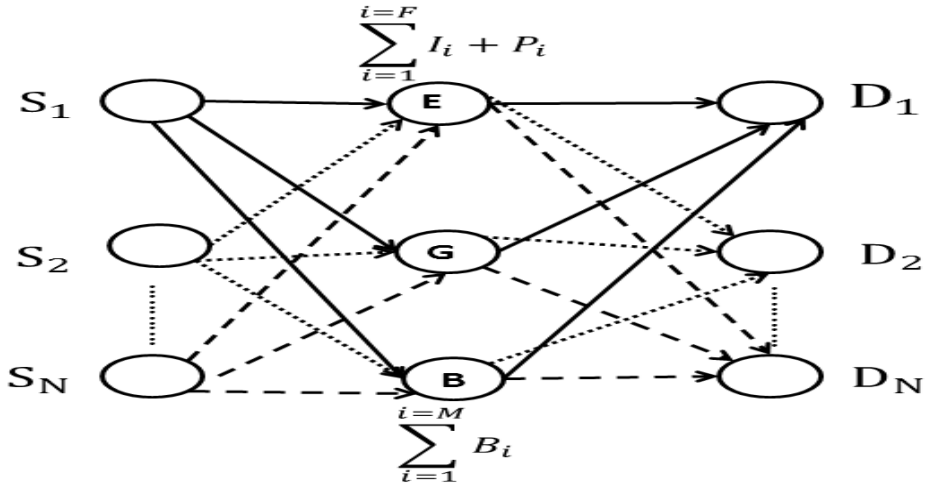

Figure 6.2: All the F(I+P) frames are sent through the excellent forwarding node (E).

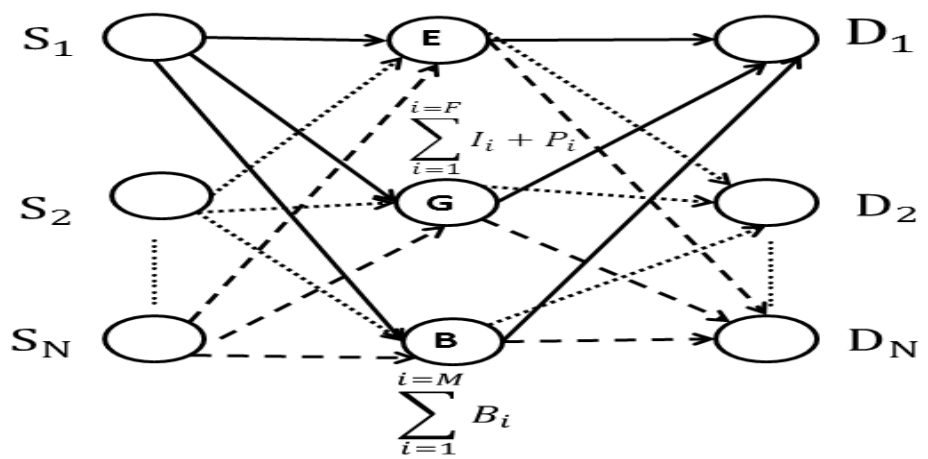

Figure 6.3: All the F(I+P) frames are sent through the good-quality forwarding node (G).

By default, nodes always would try to send the most important video frames through the best available node obtained by the 3MRP+DSW. This means that I frames, which are the biggest ones and carry the most important video information, would

be sent through the excellent forwarding node (E); P frames would be sent through the good-quality node (G); whereas the least important frames (*i.e.*, B frames) would be sent through the bad one (B). Nevertheless, if each node sent the most important frames through the excellent forwarding node (E), this node could get congested. As a consequence, that excellent forwarding node could suffer more losses than the others, which would lead to classify it as a worse node. This behavior could produce an oscillatory performance that might affect the video experience of users if it happened frequently.

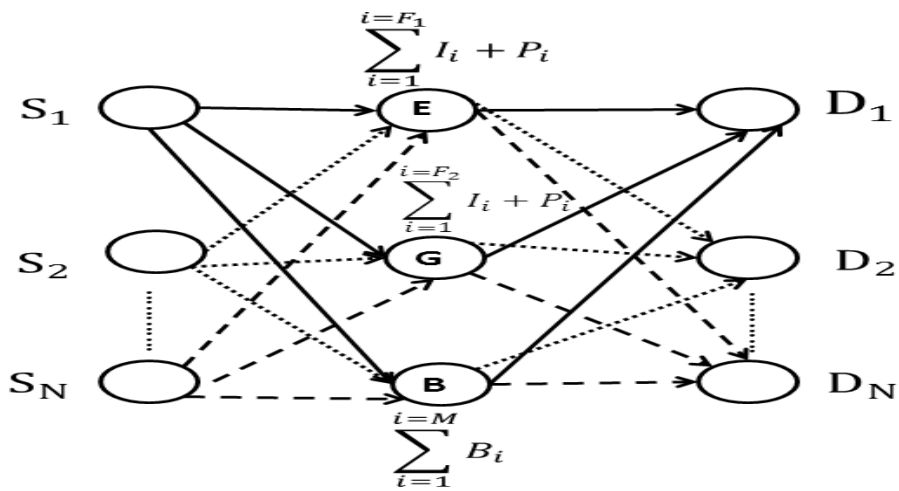

Figure 6.4: I+P frames will be sent through the excellent forwarding node with a certain probability p and through the good-quality forwarding node with a probability *1-p*. F_1 and F_2 represent the number of (I+P) frames sent through the excellent forwarding node and through the good-quality forwarding node, respectively, being $F = F_1 + F_2$.

To cope with this issue, users could *play a game* such that the best two nodes (excellent, good) could be selected by each player to transmit the most important video frames (*i.e.*, I+P frames). That is, each user could prefer to send sometimes the most important frames through the good-quality node. Just for simplicity, B frames are considered always to be sent through the third node, which is the bad one. Also, I and P frames belonging to the same video stream are going to be sent through the same node to make more evident the inconveniences of sharing the same node, since there are more P frames than I frames per flow. We follow this same design option as we did for MANETs in Chapter 3.

In our game, in each iteration, users select nodes for their respective video flows. As it is shown in Figures 6.2, 6.3 and 6.4, we have three possible situations. Without playing

the game, all users would always send the important frames through the excellent forwarding node (Figure 6.2). Alternatively, they could play our game-theoretical routing game. Notice that case (Figure 6.3) is worse than (Figure 6.2) for all users since they are sending their frames together through the good-quality node instead of through the excellent node (this should not happen often). In the third case (Figure 6.4), I+P frames will be sent through the excellent available forwarding node by each user with a certain probability p and through the good-quality node available with a probability $1 - p$.

Notice that players (users) must decide their choices (*i.e.*, their corresponding p value) simultaneously and without communicating with each other. If we have a number of I+P frames equal to F to be sent, depending on the p value, a number of I+P frames equal to F_1 will be sent through the excellent forwarding node (E) and a number of I+P frames equal to F_2 will be sent through the good-quality one (G), being $F = F_1 + F_2$. M represents the number of B frames to be sent, always through the bad node.

In the next section we will compute the optimal probability p (called p^*) of sending I+P frames through the best path that produces the best outcome for each player.

6.4 Game-Theoretical Routing Scheme for Video-Streaming in VANETs

Here we refer to the reader to section 3.5.1 where the general basis of our game-theoretical approach were stayed,

6.4.1 The benefit of using a particular node to transmit the I+P video frames

Before defining the player's utility of the game, we will define a parameter that evaluates the benefit of using a particular node. As we have mentioned before, we assume that we always have at least two available nodes (excellent and medium-quality nodes) to send packets. Each node will have its own benefit.

Let us assign ϕ_E as the benefit for the excellent forwarding node and ϕ_G as the benefit for the medium-quality node, where ϕ_E and $\phi_G \in \mathbb{R}^*$. Later, we will relate ϕ_E and ϕ_G with the global score obtained from 3MRP. Strategy α_i is defined as follows:

$$\alpha_i = \begin{cases} \text{Transmit using the excellent forwarding node (E).} \\ \text{Transmit using the good-quality forwarding node (G).} \end{cases} \tag{6.1}$$

Probability p is the probability of sending (I+P) frames through the excellent forwarding node and probability $(1 - p)$ is the probability of sending those frames through the medium-quality forwarding node.

6.4.2 Design of the Utility Function

The utility function U_i designed for our game-theoretical routing protocol aims at achieving a goal which is to minimize the percentage of (I+P) frames lost, since this parameter is the most significant in video-streaming services. The proposed utility function for player i is the following:

$$U_i = \underbrace{\left(\frac{n_{rE,i} - n_{sE,i}}{n_{sE,i}}\right) \cdot \phi_{E,i} \cdot p_i^2}_{\text{Excellent forwarding node}} + \underbrace{\left(\frac{n_{rG,i} - n_{sG,i}}{n_{sG,i}}\right) \cdot \phi_{G,i} \cdot (1 - p_i)^2}_{\text{Good forwarding node}} \tag{6.2}$$

All variables presented in Equation (6.2) are defined in Table 6.1.

Table 6.1: Definitions of the variables presented in Equation (6.2).

Variable	**Definition**
$i = 1, 2, 3..., N$	i is a generic player, being N the number of players
p_i	Player's i probability of sending the (I+P) frames through his/her excellent node
$\phi_{E,i}$	Player's i benefit if selecting the excellent node
$\phi_{G,i}$	player's i benefit if selecting the good-quality node
$n_{s,i}$	Number of (I+P) frames sent by player i through the excellent and the good-quality node.
$n_{sE,i}$	Number of (I+P) frames sent by player i through the excellent node
$n_{rE,i}$	Number of (I+P) frames received from player i through the excellent node
$n_{sG,i}$	Number of (I+P) frames sent by player i through the good-quality node
$n_{rG,i}$	Number of (I+P) frames received from player i through the good-quality node

Now, let us relate $n_{sE,i}$ and $n_{sG,i}$ with $n_{s,i}$:

$$n_{sE,i} = p_i \cdot n_{s,i} \tag{6.3}$$

$$n_{sG,i} = (1 - p_i) \cdot n_{s,i} \tag{6.4}$$

where $n_{s,i} = n_{sE,i} + n_{sG,i}$.

Substituting Equations (6.3) and (6.4) in Equation (6.2) we get the following expression for the utility function U_i:

$$U_i = \underbrace{\left(\frac{n_{rE,i} - p_i \cdot n_{s,i}}{p_i \cdot n_{s,i}}\right) \cdot \phi_{E,i} \cdot p_i^2}_{\text{Excellent forwarding node}} + \underbrace{\left(\frac{n_{rG,i} - (1 - p_i) \cdot n_{s,i}}{(1 - p_i) \cdot n_{s,i}}\right) \cdot \phi_{G,i} \cdot (1 - p_i)^2}_{\text{Good forwarding node}} \tag{6.5}$$

Notice that each player makes his/her own nodes classification, *i.e.*, each player might have different excellent and good-quality nodes.

In Equation (6.2), we have designed our utility function U_i to be proportional to the negative of the I+P frames losses. This way, the utility increases as the losses decrease, for both the excellent and the good-quality nodes. Besides, U_i is a concave function so that we ensure to have a p value that produces the maximum utility. In Equation (6.2), $\left(\frac{n_{rE,i}-n_{sE,i}}{n_{sE,i}}\right)$ is the negative of the I+P frame losses through the excellent forwarding node and $\left(\frac{n_{rG,i}-n_{sG,i}}{n_{sG,i}}\right)$ is the negative of the I+P frame losses through the good-quality node.

Besides, U_i is proportional to the benefit of the excellent and good forwarding nodes ϕ_E and ϕ_G, respectively. We can see a numerical example of the utility function in section (6.6.2.2).

Depending upon the values of the utilities, pure strategies may not exist, but in that case there are always mixed strategies [54, 55]. The mixed strategy α_i^* is a (NE) if the utilities $U_i(i = 1, ..., N)$, satisfy Equation (3.11). If there exists a mixed Nash equilibrium, player i will have a best response. To obtain it, U_i must be maximized:

$$\frac{\partial U_i}{\partial p_i} = 0 \tag{6.6}$$

For the sake of a simpler writing we will omit the i index to refer the user in the previous variables shown in Table 6.1. Thus, we will use n_{sE} instead of $n_{sE,i}$, and so on.

Then, applying Equation (6.6) in Equation (6.5) we obtain:

$$\frac{\partial U_i}{\partial p_i} = -2 \cdot p_i \cdot (\phi_E + \phi_G) + \phi_E \cdot \frac{n_{rE}}{n_s} - \phi_G \cdot \frac{n_{rG}}{n_s} + 2 \cdot \phi_G \tag{6.7}$$

To simplify the previous Equation, we assume that n_{sE}, n_{sG} and n_s are higher than zero. This assumption has sense since at least one frame should have been sent as well. We define the following variables:

$$\hat{n}_E = \frac{n_{rE}}{n_s},\ \hat{n}_G = \frac{n_{rG}}{n_s} \tag{6.8}$$

Next, we substitute Equation (6.8) in Equation (6.7) and we get:

$$\frac{\partial U_i}{\partial p_i} = -2 \cdot p_i \cdot (\phi_E + \phi_G) + \phi_E \cdot \hat{n}_E - \phi_G \cdot \hat{n}_G + 2 \cdot \phi_G \tag{6.9}$$

Then, by combining both Equations (6.6) and (6.9), we attain the solution for the best probability of sending (I+P) frames through the excellent forwarding node, that gives a NE in the utility function U_i. This is called as the best response of the game. Thus, using p_i^* to compute the probability of sending I+P frames through the excellent

forwarding node, is a strategy which produces the most favorable outcome for player i, taking the other players' strategies as given.

$$p_i^* = \frac{\phi_E \cdot \hat{n}_b + \phi_G \cdot (2 - \hat{n}_G)}{2\,(\phi_b + \phi_m)} \tag{6.10}$$

This way, each player i will continuously update his/her best response p_i^* using Equation (6.10). To do so, the user easily obtains this feedback information from the hello messages of 3MRP+DWS: the number of I+P frames received so far through the excellent and the good-quality nodes (n_{rE} and n_{rG}, respectively) and the number of I+P frames sent so far (n_s). In the next section, we explain how the user computes the benefits for the excellent and the good-quality forwarding nodes.

6.4.3 Nodes' Benefits Computation

We have designed the value of the benefit of a node to be proportional to the global score obtained from our routing protocol 3MRP+DSW. As the global score takes into account five metrics (*i.e.*, distance, trajectory, vehicles' density, available bandwidth estimation and MAC layer losses) it can be considered as a global measure of the QoS.

Accordingly, we define the following Equations to compute the benefits of the excellent and good-quality nodes, ϕ_E and ϕ_G, respectively:

$$\phi_E = k_E \cdot S_E \;\; and \;\; \phi_G = k_G \cdot S_G \tag{6.11}$$

where k_E and k_G are constants, $[k_E\ ,\ k_G] \in \mathbb{R}^*$.

Next, using Equation (6.11) in Equation (6.10) we have this expression for the best response probability, p_i^*:

$$p_i^* = \frac{k_E \cdot S_E \cdot \hat{n}_E + (k_G \cdot S_G) \cdot (2 - \hat{n}_G)}{2 \cdot (k_E \cdot S_E + k_G \cdot S_G)} \tag{6.12}$$

Let $\frac{k_E}{k_G} = k_{E/G}$. As k_G is different from zero, we can divide the whole Equation (6.12) by k_G. After substituting, we obtain the Nash Equilibrium strategy for player i:

$$p_i^*(k_{E/G}) = \frac{k_{E/G} \cdot S_E \cdot \hat{n}_E + S_G \cdot (2 - \hat{n}_G)}{2 \cdot \left(k_{E/G} \cdot S_E + S_G\right)} \tag{6.13}$$

We have designed in Equation (6.5) U_i to be a concave function, so that there is one p^* value where U_i is on its maximum value. Due to that, $\frac{\partial^2 U_i}{\partial^2 p_i}$ must be less than zero. This way, deriving Equation (6.9) we obtain:

$$\frac{\partial^2 U_i}{\partial^2 p_i} = -2 \cdot (\phi_E + \phi_G) \tag{6.14}$$

As we need that $\frac{\partial^2 U_i}{\partial^2 p_i} < 0$,

$$\phi_E + \phi_G > 0 \ ; \ \forall \ [\phi_E, \ \phi_G] \in \ \mathbb{R}^* \tag{6.15}$$

Concluding, if player i adopts the strategy to send his/her (I+P) frames through the excellent forwarding node with a certain probability that equals p_i^* (see Equation (6.13)), his/her own benefit and the whole benefit of the network will be the highest.

All values needed to compute p_i^*, except $k_{E/G}$, can be obtained during normal network operation from the local information given by the hello messages. This way, users will update the probability p_i^* with the current QoS parameters carried in the last received hello message packet. Thus, $k_{E/G}$ is the single pending parameter to be obtained in Equation (6.13). In the next section, we will give a method to calculate analytically this parameter.

6.5 A Method to Calculate $k_{E/G}$

S_E and S_G are the global score values measured in the excellent (E) and the good-quality forwarding node (G), respectively. They can take any value between 0 and 5 as shown in Chapter 5.

Now, our goal is to calculate $k_{E/G}$ so we can compute the value of p_i^* using Equation (6.13). Three conditions will limit the computing of $k_{E/G}$: $0 \leq p_i \leq 1$ and U_i being a concave function. Below, we will study separately those three conditions.

6.5.1 Condition 1: $p_i \geq 0$

Combining Equation (6.10) with $p_i \geq 0$, we get that:

$$\frac{k_{E/G} \cdot S_E \cdot \hat{n}_E + S_G \cdot (2 - \hat{n}_G)}{2 \cdot \left(k_{E/G} \cdot S_E + S_G\right)} \geq 0 \tag{6.16}$$

Remember that Equation (6.15), which is the denominator of Equation (6.16) must also be fulfilled.

Thus, we need:

$$k_{E/G} \cdot S_E \cdot \hat{n}_E + S_G \cdot (2 - \hat{n}_G) \geq 0 \tag{6.17}$$

Now, we multiply the whole inequation (6.17) by $\frac{1}{S_E \cdot \hat{n}_E}$ ($\forall \ S_E \ , \ \hat{n}_E \ \in \ \mathbb{R}^+$):

$$k_{E/G} \geq \frac{S_G \cdot (\hat{n}_G - 2)}{S_E \cdot \hat{n}_E} \tag{6.18}$$

6.5.2 Condition 2: $p_i \leq 1$

Combining Equation (6.10) with $p_i \leq 1$ leads to:

$$\frac{k_{E/G} \cdot S_E \cdot \hat{n}_E + S_G \cdot (2 - \hat{n}_G)}{2 \cdot \left(k_{E/G} \cdot S_E + S_G\right)} \leq 1 \tag{6.19}$$

Looking at Equation (6.15), we can write:

$$k_{E/G} \cdot S_E \cdot \hat{n}_E + S_G \cdot (2 - \hat{n}_G) \leq 2 \cdot \left(k_{E/G} \cdot S_E + S_G\right) \tag{6.20}$$

and solving Equation (6.20), we reach to:

$$k_{E/G} \cdot S_E \cdot (2 - \hat{n}_E) \geq -S_G \cdot \hat{n}_G \tag{6.21}$$

Now, before we continue we will find out which is the sign of the expression $(2 - \hat{n}_E)$. $\hat{n}_E$ was defined in Equation (6.8) as the relation between the number of I+P frames received in the excellent forwarding node (n_{rE}) and the total number of I+P frames sent (n_s).

$$\hat{n}_E = \frac{n_{rE}}{n_s} \leq 1 \tag{6.22}$$

Therefore,

$$\hat{2} - n_E \geq -1 \geq 0 \tag{6.23}$$

Finally, the second inequation to be fulfilled by $k_{b/m}$ is:

$$k_{E/G} \geq \frac{S_G \cdot \hat{n}_G}{S_E \cdot (\hat{n}_E - 2)} \tag{6.24}$$

6.5.3 Condition 3: Concave Function U_i

For U_i to be a concave function, Equation (6.15) must be fulfilled such that:

$$\phi_E + \phi_G = k_E \cdot S_E + k_G \cdot S_G > 0 \tag{6.25}$$

If we multiply the whole inequation by $\frac{1}{k_G}$ ($\forall\, k_m \in \mathbb{R}^+$) and rename $\frac{k_E}{k_G}$ by $k_{E/G}$, we get:

$$k_{E/G} \cdot S_E > -S_G \tag{6.26}$$

Finally, we obtain Equation (6.27) as the third condition to be fulfilled by $k_{b/m}$:

$$k_{E/G} > \frac{-S_G}{S_E} \tag{6.27}$$

6.5.4 The Three Inequations to Be Fulfilled by $k_{E/G}$

We first rewrite the three inequations to be satisfied by $k_{E/G}$: Equations (6.18), (6.24) and (6.27). Besides, we will rename the thresholds of the three inequations as α_0, α_1 and α_2, respectively.

$$\begin{aligned} k_{E/G} &> \frac{-S_G}{S_E} = \alpha_0 \\ k_{E/G} &\geq \frac{S_G \cdot (\hat{n}_G - 2)}{S_E \cdot \hat{n}_E} = \alpha_1 \\ k_{E/G} &\geq \frac{S_G \cdot \hat{n}_G}{S_E \cdot (\hat{n}_E - 2)} = \alpha_2 \end{aligned} \tag{6.28}$$

We need to find a value for $k_{E/G}$ that satisfies the three inequations. First of all, the range of solutions for $k_{E/G}$ is $]K_{E/G}, +\infty)$, where $K_{E/G}$ will be the maximum value among α_0, α_1 and α_2. The probability $p_i^*(k_{E/G})$ of sending (I+P) frames through the excellent forwarding node is depicted in Figure 6.5. The limit of $p_i^*(k_{E/G})$ when $k_{E/G} \to \infty$ (horizontal asymptote) can be obtained from Equation (6.13) and it has the following value:

$$\lim_{k_{E/G} \to \infty} p_i^*(k_{E/G}) = \frac{\hat{n}_E}{2} \tag{6.29}$$

The vertical asymptote occurs at $k_{E/G}$-value that makes the denominator zero (*i.e.*, $k_{E/G} = \alpha_0$). We should find a value for $k_{E/G}$ in the range $]K_{E/G}, +\infty)$ with which $p_i^*(k_{E/G})$ changes softly throughout time. This way, the transition in the selection between the excellent and the good-quality nodes will be smooth producing a more stable system. For that, we calculate the first derivative $\frac{\partial p_i^*(k_{E/G})}{\partial k_{E/G}}$, which represents the slope value for each $k_{E/G} > K_{E/G}$ (*i.e.*, zone of interest).

$$\begin{aligned} \frac{\partial p_i^*(k_{E/G})}{\partial k_{E/G}} = {} & \frac{\hat{n}_E \cdot S_E \cdot \left(2 \cdot k_{E/G} \cdot S_E + 2 \cdot S_G\right)}{4 \cdot \left(k_{E/G} \cdot S_E + S_G\right)^2} - \\ & \frac{2 \cdot S_E \cdot \left(\cdot k_{E/G} \cdot S_E \cdot \hat{n}_E + \cdot S_G \cdot (2 - \hat{n}_G)\right)}{4 \cdot \left(k_{E/G} \cdot S_E + S_G\right)^2} \end{aligned} \tag{6.30}$$

After simplifying the Equation, we obtain:

$$\frac{\partial p_i^*}{\partial k_{E/G}} = \frac{S_E \cdot S_G \cdot (\hat{n}_E + \hat{n}_G - 2)}{2 \cdot \left(k_{E/G} \cdot S_E + S_G\right)^2} \tag{6.31}$$

Now, we isolate $k_{E/G}$ from Equation (6.31) in terms of $\frac{\partial p_i^*(k_{E/G})}{\partial k_{E/G}}$ and we get the following expression:

$$k_{E/G} = \frac{\pm\sqrt{\frac{S_G \cdot S_E \cdot (\hat{n}_E + \hat{n}_G - 2)}{2 \cdot \frac{\partial p_i^*(k_{E/G})}{\partial k_{E/G}}}} - S_G}{S_E} \tag{6.32}$$

Here, we can see that $(\hat{n}_E + \hat{n}_G - 2) \leq 0$, since $\hat{n}_E = \frac{n_{rE}}{n_s} \leq 1$, and $\hat{n}_G = \frac{n_{rG}}{n_s} \leq 1$. We refer the reader to Equation (6.22) to see the easy justification for both expressions.

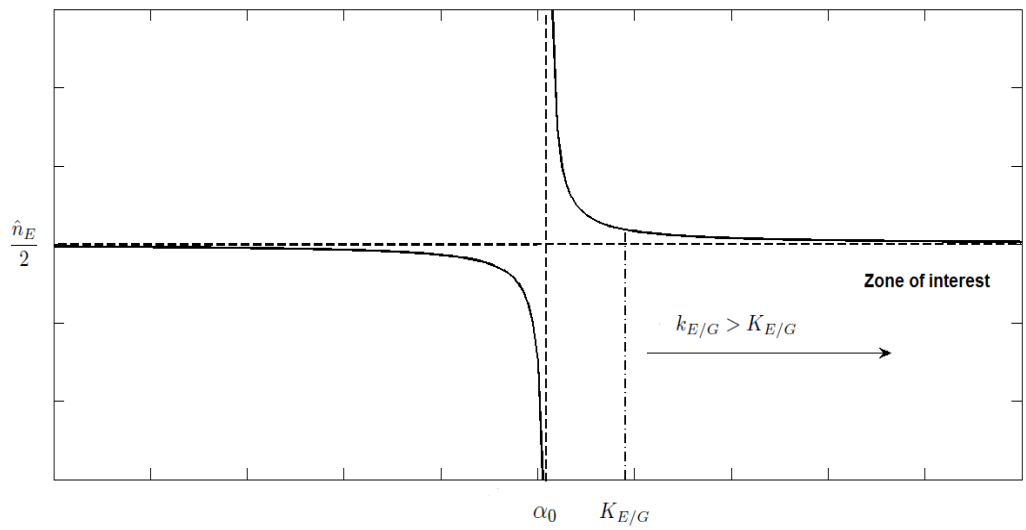

Figure 6.5: Best response probability p_i^* as a function of $k_{E/G}$, see Equation (6.13).

Consequently, we need that $\frac{\partial p_i^*}{\partial k_{E/G}} \leq 0$ to compute a proper $k_{E/G}$ value.

The parameters of Equation (6.32) that can be calculated during operation time are: the number of I+P frames received in the excellent forwarding node (n_{rE}) and the number of I+P frames sent through the excellent forwarding node (n_{sE}) to compute $\hat{n}_E = \frac{n_{rE}}{n_s}$; the number of I+P frames received in the medium-quality forwarding node (n_{rG}) and the number of I+P frames sent through the medium-quality forwarding node (n_{sG}) to compute $\hat{n}_G = \frac{n_{rG}}{n_s}$ obtained from the hello message packets; and the global score of the excellent and the medium-quality forwarding nodes, computed from the 3MRP routing protocol.

The only variable in Equation (6.32) that is not defined yet is $\frac{\partial p_i^*(k_{E/G})}{\partial k_{E/G}}$. To design a proper value for $\frac{\partial p_i^*(k_{E/G})}{\partial k_{E/G}}$, we carried out a high amount of simulations under different network conditions and with different values of $\frac{\partial p_i^*(k_{E/G})}{\partial k_{E/G}}$ and we noticed that with a

value of $\frac{\partial p_i^*(k_{E/G})}{\partial k_{E/G}} = -0.655$, the variation of p_i^* throughout time was soft without sharp changes. From Equation (6.32), we see that we have two possible values for $k_{E/G}$, one of them is higher than $K_{E/G}$ and the other one is lower than $K_{E/G}$, so we take the one which belongs to the range $]K_{E/G}, +\infty)$.

To conclude with, Algorithm 4 summarizes the methodology to compute the best response probability p_i^* for player i to send his/her I+P frames through the excellent forwarding node.

Algorithm 4 Calculation of p_i^*, the best response probability for player i that maximizes his/her utility function U_i.

Require: Obtain updated QoS values from periodically received hello messages packets.

1: Obtain the values of (S_E, S_G, $\hat{n}_E$, $\hat{n}_G$)

2: Compute the $k_{E/G}$ parameter designed that fulfills the requirements.

$$k_{E/G} = \frac{\pm\sqrt{\frac{S_G \cdot S_E \cdot (\hat{n}_E + \hat{n}_G - 2)}{2 \cdot \frac{\partial p_i^*(k_{E/G})}{\partial k_{E/G}}}} - S_G}{S_E}$$

3: Calculate the probability p_i^* to send I+P frames through the best path, that maximizes the utility function U_i

$$p_i^*(k_{E/G}) = \frac{k_{E/G} \cdot S_E \cdot \hat{n}_E + S_G \cdot (2 - \hat{n}_G)}{2 \cdot \left(k_{E/G} \cdot S_E + S_G\right)}$$

6.6 Simulation Results

In this section, we first depict a case study in a smart city that involves an emergency situation in VANETs to transmit a video-reporting message to the closest emergency unit and also to the emergencies services (*e.g.*, 112 or 911) so that they can alert other citizens around. Simulations are done using the NS2 [56] simulator.

6.6.1 A Case Study in a Smart City

In this Chapter, we focus on a realistic smart city VANET scenario, where emergency prevention and response are key issues. In this scenario under consideration, we assume

that in a given moment an accident happened. In the VANET scenario, we assume that a smart driver witnesses the situation, makes a short video-reporting message (the driver will just push a button that will make a small exterior car-mounted camera shoot the video) about the accident and sends it through the VANET to the nearest emergency unit (e.g., police, ambulances, hospitals). Authorities will respond upon receiving the video and will take proper actions. As explained before, with a video-reporting message the emergency can be evaluated much better than with a simple text. It would be easier to ensure an accurate interpretation of the situation and the accident could be treated with the adequate level of seriousness. The smart driver sends a multimedia message which includes different information regarding the incident, e.g., the GPS location, a voice message and a short video of the incident. A suitable kind of smart-112 (911 in U.S.A) application in the citizen's vehicle sends the multimedia message to the smart-112 emergency center, who manages the proper actions for that incident. For instance, ambulances and paramedical will be sent there, traffic lights will turn to red around the accident, a green wave of traffic lights will help the ambulances get there sooner, the nearest hospital is warned, the doctors wait for the injuries, *etc.* A video of the incident facilitates a preliminary evaluation of the wounded people as well as helps to better determine the requirements needed to manage the dangerous situation. Our purpose in this Chapter is to design a game-theoretical geographical routing protocol suitable to transmit those video-reporting messages over VANETs in this kind of smart city scenario. In the next section, a detailed performance evaluation of our proposal in a VANET scenario is done.

6.6.2 Performance Evaluation in a VANET Scenario

In this subsection we introduce a performance evaluation of our proposal in a VANET scenario, where we proved the 3MRP+DSW protocol including also the multi-user game-theoretical approach described in section 6.4. Video flows are transmitted from two vehicles to two access points AP1 and AP2 (see Figure 6.6), respectively. AP1 is the Ana Torres Institute (a surgery clinic) and AP2 is the Hospital Clinic of Barcelona, which represent two emergency units where vehicles will send their multimedia reporting messages upon the event of a traffic accident. Each vehicle will send its multimedia reporting message to the closest AP. We carried out ten simulations per point using the NS2 [56]. Figures 6.7, 6.8 and 6.9 show the results with confidence intervals (CI) of 90 percent using a different scenario in each repetition. We considered two densities of vehicles, 50 vehicles/km^2 (scenario 1) and 100 vehicles/km^2 (scenario 2) which were randomly positioned. In the simulations, we used a real city area obtained from the example district of Barcelona, Spain (see Figure 6.6). In order to simulate a realistic scenario, the CityMob for Roadmaps (C4R) [59] simulator was used to obtain the mobility model. C4R is a mobility generator that uses the Simulation of Urban MObility (SUMO) engine [60]. Besides, C4R imports maps directly from OpenStreetMap [61] and generates NS2 compatible files to specify the mobility model for the vehicles through the

city along the whole simulation. Furthermore, we included in our proposal the REVsim [3] tool described in Chapter 4 to detect obstacles and in this way our proposal can be easily building-aware. The simulation settings of the VANET scenario are shown in Table 6.2.

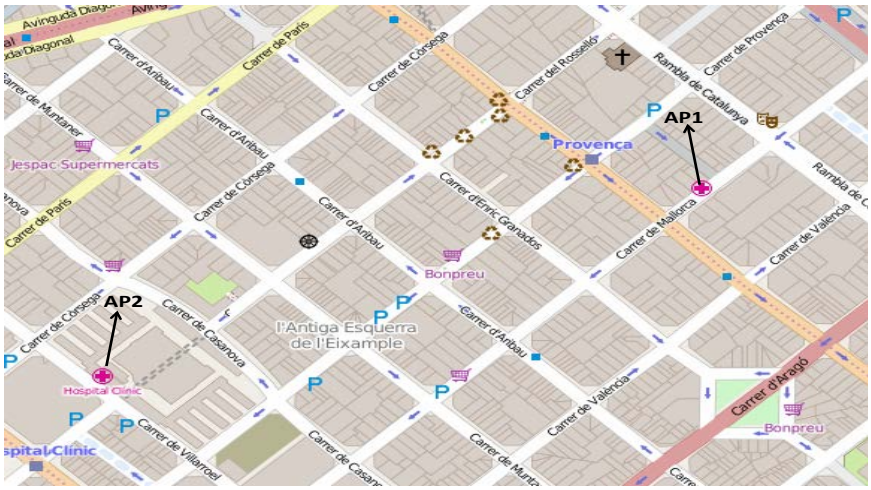

Figure 6.6: Simulation scenario of Barcelona, Spain ($N = 2$ users). It includes two emergency units: AP1 (Ana Torres surgery clinic) and AP2 (Hospital Clinic of Barcelona).

Figure 6.7 shows the average percentage of packet losses for $N = 2$ users when using the game-theoretical scheme against the case of non using it (*Non game* option). We can see how including the game-theoretical routing scheme, the average video packet losses are reduced from 53% to 45% in a 50 vehicles scenario and from 37% to 28% in a 100 vehicles scenario. This decrement of the average packet losses is due to the optimal selection of nodes based on a probability value (*i.e.*, p^*) that balances the load among the two nodes at stake (*i.e.*, the excellent and the medium-quality nodes) depending on the current quality of the nodes. Figure 6.8 depicts the average end-to-end packet delay. We can see that the case including the *Game* scheme improves the delay compared to the *Non Game* case for both 50 and 100 vehicles scenario.

Figure 6.9 depicts the peak signal-to-noise ratio (PSNR) obtained for 2 players. Also, we can see that the case including the Game scheme improves the PSNR compared to the Non Game case in both scenarios.

Results of this performance evaluation show clear benefits after including our game-theoretical approach in our multimetric geographical routing protocol 3MRP+DSW over VANETs.

Table 6.2: Simulation settings of the VANET scenario.

Map Zone	**Example District of Barcelona**
Area	1700 × 580 m^2
Density of vehicles	50 vehicle/km^2 (scenario 1) and 100 vehicle/km^2 (scenario 2)
Number of nodes	50 and 100 vehicles
Video sources	2
Transmission range	250 m
Mobility generator	SUMO [60]/C4R [59]
MAC specification	IEEE 802.11p
Nominal bandwidth	11 Mbps
Simulation time	300 s
Video encoding	MPEG-2 VBR
Video bit rate	150 Kbps
Video sequence sent	Traffic accidents [58]
Routing protocol	3MRP + DSW, 3MRP + DSW+ GT
Transport protocol	RTP/UDP
Maximum packet size	1500 Bytes
Weighting values	dynamic
Queue sizes	50 packets

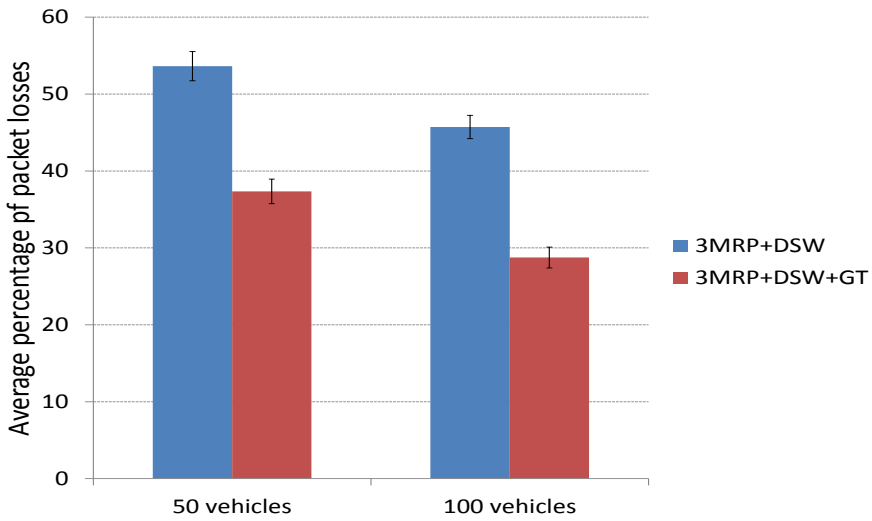

Figure 6.7: Average percentage of packet losses for $N = 2$ users.

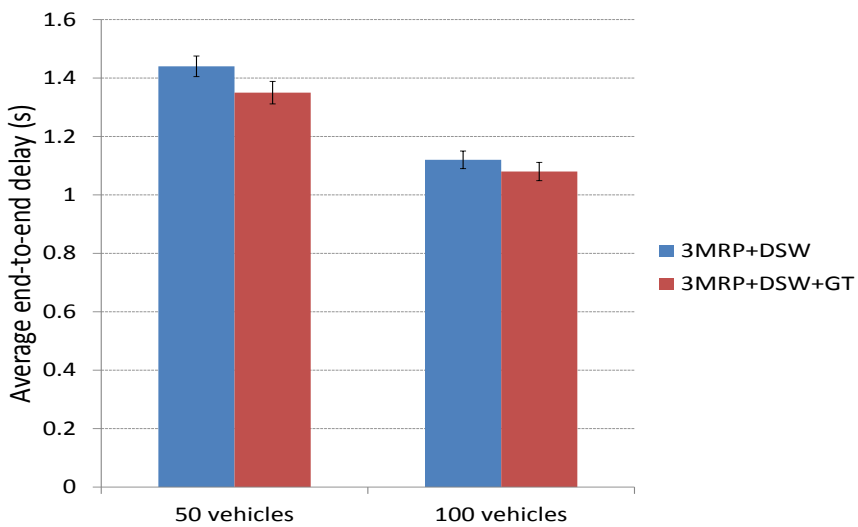

Figure 6.8: Average end-to-end packet delay for $N = 2$ users.

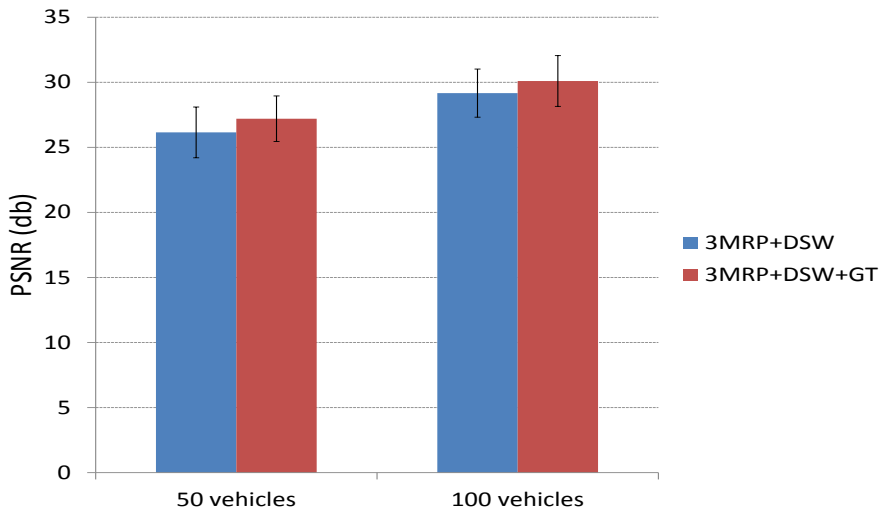

Figure 6.9: Peak Signal to Noise Ratio (PSNR) for $N = 2$ users.

6.6.2.1 Utility Function Values

In this section, we will compute the gain of our game-theoretical routing scheme. Let us define U_{G_i} as the utility function for player i when the game-theoretical scheme is used and U_{NG_i} as the utility function when it is not used. Both utility function values will be computed using Equation (6.5). G_i is the gain obtained for player i by using the game-theoretical scheme with respect to not using it, $0 \leq G_i \leq 1$.

$$G_i = \frac{U_{G_i} - U_{NG_i}}{U_{G_i}} = \frac{U_{p=p_i^*} - U_{p=1}}{U_{p=p_i^*}} \tag{6.33}$$

Using Equation (6.5) in Equation (6.33) we obtain:

$$G_i = \frac{U_{G_i} - U_{NG_i}}{U_{G_i}} = 1 - \frac{\left(\frac{n_{rE,i} - n_{s,i} \cdot 1}{n_{s,i} \cdot 1}\right) \cdot \phi_{E,i} \cdot 1}{\left(\frac{n_{rE,i} - n_{s,i} \cdot p_i^*}{n_{s,i} \cdot p_i^*}\right) \cdot \phi_{E,i} \cdot (p_i^*)^2 + \left(\frac{n_{rG,i} - n_{s,i} \cdot (1-p_i^*)}{n_{s,i} \cdot (1-p_i^*)}\right) \cdot \phi_{G,i} \cdot (1-p_i^*)^2} \tag{6.34}$$

6.6.2.2 A Numerical Example

In this section, we show a numerical example to calculate the gain obtained with our proposal for $N = 2$ users using Equation (6.34), *i.e.*, G_1 and G_2. To do that, we use the values obtained during simulation. They are shown in Table 6.3.

Table 6.3: Simulation output values for $N = 2$ users.

$\hat{n}_{E,1}$, $\hat{n}_{E,2}$	(0.8, 0.75)
$\hat{n}_{G,1}$, $\hat{n}_{G,2}$	(0.55, 0.5)
$S_{E,1}$, $S_{E,2}$	(4.5, 4.2)
$S_{G,1}$, $S_{G,2}$	(3.8, 3.6)

We calculate the variable $k_{E/G,1}$ and $k_{E/G,2}$ for players 1 and 2 using Equation (6.32) and the simulation output values shown in Table 6.3. Results are shown in Table 6.4.

Table 6.4: Best response probabilities p_i^* for $N = 2$ users.

$k_{E/G,1}$, $k_{E/G,2}$	(-0.197, -0.157)
p_1^*, p_2^*	(0.82, 0.84)

After that, we simplify $\left(\frac{n_{rE,i}-n_{sE,i}}{n_{sE,i}}\right)$ and $\left(\frac{n_{rG,i}-n_{sG,i}}{n_{sG,i}}\right)$ as seen in Equations (6.35) and (6.36) in order to be easily calculated later using Table 6.3.

$$\left(\frac{n_{rE,i} - n_{sE,i}}{n_{sE,i}}\right) = \frac{n_{rE,i} - n_{s,i} \cdot p_i^*}{n_{s,i} \cdot p_i^*} = \frac{\hat{n}_{E,i}}{p_i^*} - 1 \tag{6.35}$$

$$\left(\frac{n_{rG,i} - n_{sG,i}}{n_{sG,i}}\right) = \frac{n_{rG,i} - n_{s,i} \cdot (1 - p_i^*)}{n_{s,i} \cdot (1 - p_i^*)} = \frac{\hat{n}_{G,i}}{(1 - p_i^*)} - 1 \tag{6.36}$$

Next, we calculate ϕ_b and ϕ_m for each player using Equation (6.11) so they can be substituted in Equation (6.5).

$$\phi_{E,1} = k_{E,1} \cdot S_{E,1} = k_{E/G,1} \cdot k_{G,1} \cdot S_{E,1} = -0.886 \cdot k_{G,1} \tag{6.37}$$

$$\phi_{E,2} = k_{E,2} \cdot S_{E,2} = k_{E/G,2} \cdot k_{G,2} \cdot S_{E,2} = -0.659 \cdot k_{G,2} \tag{6.38}$$

$$\phi_{G,1} = k_{G,1} \cdot S_{G,1} = 3.8 \cdot k_{G,1} \tag{6.39}$$

$$\phi_{G,2} = k_{G,2} \cdot S_{G,2} = 3.6 \cdot k_{G,2} \tag{6.40}$$

Finally, substituting Equations (6.35) to Equation (6.40) in Equation (6.34), we obtain that $G_1 \approx 0.95$ and $G_2 \approx 0.8$.

These values mean that for player 1 the gain is 95% more using the game-theoretical model instead of not using it. In the same way, for player 2 the gain is 80%.

6.7 Conclusions and Future Work

In this Chapter, we have designed a new routing protocol for VANETs to transmit video-reporting messages in a smart city. The geographical routing protocol is based on a game-theoretical scheme for N users. Our framework could be used in smart cities where prevention and fast management of accidents is an important goal. We understand that with a video message, the level of seriousness of the accident could be much better evaluated by the authorities allowing a fast warning of the incident to emergency units, which potentially could save lives.

The users of the framework could be any vehicle that could participate in the VANET by transmitting a video-reporting message to the competent authorities. In this way, other vehicles would easily be warned about any situation in the city, which would improve the quality of life in the smart cities.

In our framework, the probability p of sending the most important video frames (*i.e.*, I+P frames) through the most excellent available forwarding node varies depending on some network characteristics. This way, instead of sending the I+P video frames always through the excellent forwarding node, users play a strategic routing game where these frames will be sent through one of the two available best nodes according to a certain probability p^*.

Simulation results in the VANET scenario show the benefits of our proposal that outperforms the results compared to the case of non using our game-theoretical routing. In terms of packets losses, delay and PSNR, results notably improve due to the new way of selecting the next forwarding node based on p^*. Our proposal makes the network more efficient as well as achieves a higher degree of satisfaction of the users by receiving much more (I+P) frames with a lower average end-to-end delay. This definitively will improve the quality of the video perceived by the end user.

Chapter 7

Conclusions and Future Work

7.1 Conclusions

Throughout the research work of this thesis, our main focus has been the design and the implementation of a useful framework to transmit video-reporting messages over both MANETs and VANETs in urban environments. This thesis aims to provide a basis for smart city services that require video-streaming, for instance to transmit video-reporting messages in case of an accident in order to fast alert the emergencies services (*e.g.*, 112 or 911).

We have tackled the issue of the design of a realistic scenario for VANETs to be able to test our proposals using simulations as close to real life as possible. For that purpose, we have developed a tool named REVSim [3] that helps us to attain realistic simulation results by taking into account the presence of buildings in real maps. Basically, REVsim avoids forwarding a packet to those neighbours behind a building. The tool gives the state (*i.e.*, to be in line of sight or not) of any neighbour with respect to the current forwarding node to see if that neighbour under check can be a candidate as next forwarding node. If not, this means that this neighbour is behind a building and as a consequence it will be deleted from the neighbour list. Furthermore, instead of a time-consuming checking during simulation, we provide a fast way to look up the corresponding information from our output file provided by REVsim with the real map, so simulation time is almost not affected by our building-aware scheme.

In the coming years significant improvements are expected in the VANETs field as manufactures start to introduce them in brand new vehicles. We have analysed the main issues related to VANETs in urban environments about the service of video-reporting messages. As a consequence, several characteristics of the behaviour of the vehicles were taken into consideration to enhance the communications such as the high speed

of the nodes and the quickly change of neighbours. After that, we found the pertinent convenience to develop a multi-metric routing protocol for VANETs to transmit video-reporting messages in urban scenarios that includes several improvements to reduce the packet losses and increase the PSNR. Such improvements are: including five metrics (distance, trajectory, vehicles' density, available bandwidth and MAC layer losses) to select the best forwarding node to transmit packets. In vehicular networks, forwarding decisions are taken hop-by-hop due to the few seconds that a communication link lasts between two nodes. Due to that, we chose the geographical protocol GPSR (Greedy Perimeter Stateless Routing) [11] as a starting point to develop our approaches. We have focused our efforts in the design of suitable forwarding decision to help in having a high number of packets delivered to destination.

As a result of our research work, we have developed several proposals. We list the main contributions of this PhD thesis as follows:

- Firstly, we have designed a new routing protocol for MANETs to transmit video-reporting messages in a smart city based on a game-theoretical scheme for N users. This framework could be used in smart cities where one of the important goals is to prevent accidents and to warn quickly the emergency units after the occurrence of an incident. In our framework, instead of sending the I+P video frames always through the best available path, users play a strategic routing game where those video frames will be sent through one of the two best available paths according to a certain probability p^*. Simulation results in MANETs scenarios show the benefits of our proposal when compared to the case of non using our game-theoretical routing and also compared to other traditional routing protocols. Results notably improve in terms of packets losses, delay and jitter due to the new way of selecting the forwarding path based on p^*. Our proposal also outperforms the quality of the video perceived by the end user. Besides, improvements are also shown in preliminary simulation results of a VANET scenario for $N = 2$ source vehicles, in terms of percentage of packet losses, average packet delay and average delay jitter.

- Secondly, it is very important to take into account the presence of obstacles (mainly buildings in cities) in real map scenarios for VANET simulations to obtain trusted results. The reason is that in real life buildings would block the signal and packets would be dropped if a next forwarding node was behind a building. For that purpose, we have developed a program named REVSim [3] that gives the state of any neighbour (*i.e.*, in line of sight or not) with respect to the current forwarding node in order to see if a neighbour can be a candidate as next forwarding node. If the candidate node is not in line of sight, this neighbour node is considered behind a building and will be deleted from the actual neighbour list.

- Thirdly, we have presented a new routing protocol named 3MRP (*Multimedia Multimetric Map-Aware Routing Protocol*) [1] for VANETs to transmit video-reporting messages in urban scenarios. This framework could be used in smart cities where prevention and management of accidents is an important goal. A video-reporting message allows a better evaluation of the situation. Due to that, lives could be saved by allowing a fast warning of the emergency units. Furthermore, our proposal is building-aware, avoiding to select those nodes in transmission range but located behind a building. In this way, our simulations are more realistic since our network simulator sends packets only to those nodes that are not behind buildings. For that task, we have used our program named REVSim [3] explained in Chapter 4. In addition, when the routing protocol fails to find a proper next forwarding node, a local buffer is used to temporarily store those packets and a timer is activated. If the timer expires above a timeout, the packet is dropped since the video frame would reach destination too late for the decoding process. Five metrics (distance, trajectory, density, available bandwidth and MAC layer losses) are considered in 3RMP. Furthermore, we have developed an algorithm able to give each metric a proper weight depending on a suitable relative current value and on the previous average value of that metric in all the neighbour nodes. This helps the overall protocol to give each metric its importance at each moment and as a consequence a better performance is obtained, compared to the case of giving fixed weights to all the metrics. We have evaluated our proposal compared to GPSR in two different scenarios with low and medium vehicles' density. Regarding results, 3MRP+DSW improves both 3MRP and GPSR in terms of packets losses and throughput, due to the new way of selecting the next forwarding node as well as the new way to give each metric a dynamic weight. We also show that the quality of the video perceived by the end user improves in terms of PSNR.

- Finally, we have designed a new routing protocol for VANETs to send video-reporting messages in a smart city based on a game-theoretical scheme for N users. Our program REVSim [3] is also used to avoid selecting those nodes in transmission range that are located behind a building. In our framework, instead of sending I+P video frames always through the best forwarding node, nodes play a strategic routing game where those frames will be sent through one of the two best available nodes according to a certain probability p^*. The benefits of our proposal are shown with simulation results in the VANET scenario and the results improve the case of non using our game-theoretical routing. Notable advances are achieved in terms of packets losses and delay, due to the new way of sending the I+P video frames through the best forwarding node based on p^*. Definitively, a better quality of the video is perceived by the end user in terms of PSNR.

7.2 Research papers published as a result of the thesis work

This thesis has been developed within the framework of several Spanish R&D projects, in particular, TEC2010-20572-C02-02 "Continuity of Service, Security and QoS for Transportation Systems" (CONSEQUENCE), TEC2013-47665-C4-1-R "EMergency Response In Smart COmmunities. Privacy and QoS" (EMRISCO) and TEC2014-54335-C4-1-R "INcident monitoRing In Smart COmmunities. QoS and Privacy" (INRISCO). Also, this research was supported by the FI-AGAUR grant, from the Government of Catalonia. Most of the research results presented in this dissertation have been published in journals and conferences. In this section, we list the publications that have been generated from the research work done in this thesis. Papers can be downloaded or accessed from:

https://sites.google.com/site/ahmadmezher1982/

JCR Publications

- [2] **A. M. Mezher**, M. Aguilar Igartua, L. J. de la Cruz Llopis, E. Sanvicente Gargallo, "A Game Theoretical Map-aware Routing Protocol to Provide Video-Reporting messages over VANETs in Smart Cities", IEEE Transactions on Vehicular Technology. (IF 2014 = 1.978, Q1). *In preparation.*
- [1] **A. M. Mezher**, M. Aguilar Igartua, "Multimedia Multimetric Map-aware Routing Protocol to Provide Video-Reporting messages over VANETs in Smart Cities", IEEE Transactions on Vehicular Technology. (IF 2014 = 1.978, Q1). *Submitted.*
- [23] **A. M. Mezher**, M. Aguilar, L. J. de la Cruz Llopis,, E. Pallarès, C. Tripp, L. Urquiza, J. Forné, E. Sanvicente, "A Multi-User Game-Theoretical Multipath Routing Protocol to Send Video-Warning Messages over Mobile Ad Hoc Networks", Sensors, Special Issue on Sensors and Smart Cities, ISSN: 1424-8220, 2015. (IF 2014 =2.245, Q1). DOI: *http://dx.doi.org/10.3390/s150409039.*

International Conferences

- [95] C. Tripp-Barba, M. Aguilar Igartua, L. Urquiza Aguiar, **A. M. Mezher**, A. Zaldívar, I. Guérin-Lassous, "Available Bandwidth Estimation in GPSR for VANETs", 3rd ACM International Symposium on Design and Analysis of Intelligent Vehicular Networks and Applications (DIVANet'13), November 2013, Barcelona, Spain.

- [96] C. Tripp Barba, **A. M. Mezher**, M. Aguilar Igartua, I. Guérin-Lassous, C. Sarr, "Available bandwidth-aware routing in Urban Vehicular Ad-hoc Networks", 76th IEEE Vehicular Technology Conference (VTC-Fall'12), September 2012, pp. 1-5, ISBN: 978-1-4673-1881-5, Quebec City, Canada.
- [97] C. Tripp Barba, M. A. Mateos, P. Regañas, **A. M. Mezher**, M. Aguilar Igartua, "Smart city for VANETs using warning messages, traffic statistics and intelligent traffic lights", IEEE Intelligent Vehicles Symposium (IV'12), June 2012, pp. 902-907, ISBN: 978-1-4673-2117-4, Alcalá de Henares, Madrid.
- [3] **A. M. Mezher**, J. Jurado, L. Urquiza Aguiar, C. Iza Parades C. Tripp Barba, M. Aguilar Igartua, "Realistic environment for VANET simulations to detect the presence of obstacles in Vehicular Ad Hoc Networks", 11th ACM Symposium on Performance Evaluation of Wireless Ad Hoc, Sensor, & Ubiquitous Networks (PEWASUN'14), September 2014, pp. 77-84, ISBN: 978-1-4503-3025-1, Montreal, Quebec City, Canada.

Spanish Conferences

- [24] **A. M. Mezher**, C. Tripp-Barba, L. Urquiza Aguiar, M. Aguilar Igartua, I. Martín Faus, L. J. de la Cruz, E. Sanvicente, "Optimized path selection in a game-theoretic routing protocol for video-Streaming services over MANETs", XI Jornadas de Ingeniería Telemática (JITEL'13), October 2013, Granada, Spain.
- [98] C. Iza Parades, **A. M. Mezher**, M. Aguilar Igartua, "Performance evaluation of dissemination protocols for emergency messages in Vehicular Ad-Hoc networks", XII Jornadas de Ingeniería Telemática (JITEL'15), October 2015, Palma de Mallorca, Spain.
- [99] **A. M. Mezher**, C. Iza Parades, L. Urquiza Aguiar, A. Torres Moreira, M. Aguilar Igartua, "Design of smart services and routing protocols for VANETs in smart cities", XII Jornadas de Ingeniería Telemática (JITEL'15), October 2015, Palma de Mallorca, Spain.
- [100] **A. M. Mezher**, C. Iza Parades, C. Tripp-Barba, M. Aguilar Igartua, "A dynamic multimetric weights distribution in a multipath routing Protocol using video-streaming services over MANETs", XII Jornadas de Ingeniería Telemática (JITEL'15), October 2015, Palma de Mallorca, Spain.

Other collaborations

- [101] C. Tripp-Barba, L. Urquiza Aguiar, M. Aguilar Igartua, D. Rebollo-Monedero, **A. M. Mezher**, L. J. de la Cruz Llopis, "A Multimetric, Map-Aware

Routing Protocol for VANETs in Urban Areas", Sensors, ISSN: 1424-8220, 2014. (IF 2013 =2.048, Q1). DOI: *http://dx.doi.org/10.3390/s140202199.*

- [102] L. Urquiza Aguiar, C. Tripp-Barba,D. Rebollo-Monedero, M. Aguilar Igartua, **A. M. Mezher**, J. Forné, "Coherent, Automatic Address Resolution for Vehicular Ad Hoc Networks", International Journal of Ad Hoc and Ubiquitous Computing, ISSN: 1424-8220, 2014. (IF 2013 =0.900, Q3). *In press http://www.inderscience.com/info/ingeneral/forthcoming.php?jcode=ijahuc.*

- [103] L. Urquiza Aguiar, A. Vázques Rodas, C. Tripp Barba, **A. M. Mezher**, M. Aguilar Igartua, L. J. de la Cruz Llopis, "Efficient deployment of gateways in multi-hop Ad-hoc Wireless Networks", 11th ACM Symposium on Performance Evaluation of Wireless Ad Hoc, Sensor, & Ubiquitous Networks (PEWASUN'14), September 2014, pp. 93-100, ISBN: 978-1-4503-3025-1, Montreal, Quebec City, Canada.

7.3 Future work

During the development of this thesis, several issues have arisen which we think that deserve further research in the future. Some potential research directions and improvements are summarized below:

- Development of a new way to design the output file of the building-aware tool REVsim, so that the NS2 simulator can access to it even faster than the current design.

- Development of an approach to improve vehicular positioning based on the cooperation of vehicles. Typically, the GPS nominal accuracy is about 15 meter, which is not sufficient for active safety and advanced driver assistance systems (ADAS). This will help all vehicles to correct their positioning and as a consequence have a better estimation about their neighbours' positions. It is worthy to mention that there are several proposals in the literature that treat this issue and we would like to make our contribution in this aspect.

- A data dissemination model could be designed to tackle the issue of smart dissemination of video-reporting messages to reduce accidents and increase road safety, by warning drivers near the accidents.

- Development of an anonymity communications scheme for vehicular ad hoc networks. Some smart services require privacy of the sender, so this requirement is of paramount importance for the users.

- Test all our proposals employing Scalable Video Coding (H.264/SVC) instead of the basic MPEG-2 video format that we have used here. H.264/SVC is composed

of a base layer (lowest representation) and one or more enhancements layers that increase video quality when they are added to the base layer. We can employ a cross layer design where the sender can adapt the bit rate of the video by adding or removing SVC layers depending on the value of the available bandwidth computed in this thesis.

Appendix A

A.1 A.1 Video tests to score the MOS

In this appendix, we describe the test that we made to attain Figure 3.6. We followed the ITU-T recommendation P.800 (1996) to make our test.

In this test, ten people, 7 men and 3 women, aged 25–50 from the department of Telematics Engineering of the Universitat Politècnica de Catalunya (UPC) participated. We asked them to give their mean opinion score (MOS) value to a video received through a MANET urban scenario (see Table 3.3) when the fraction of packet losses (FPL) increased. The video sequence used in the tests was the "Traffic accidents" [58] sequence. Users took into consideration that they were in a MANET scenario, were nodes move, links break often and the network topology is dynamic. The average of the results are shown in Table 3.2 and Figure 3.6.

A.2 A.2 Relation between MOS and FPL

To compute p_i^* with Equations (3.26) and (3.50) and to attain Figures 3.17 and 3.18, we designed a expression to relate the MOS with the FPL. To do that, we used all the values obtained from the video test depicted in the Appendix A, see Figure 3.6, and we applied a lineal regression method to derive an Equation to approximate the graph shown in Figure 3.6.

$$MOS \simeq c \cdot FPL + d \tag{A.1}$$

where $c = -8.1081$ and $d = +5.2703$.

To draw Figure 3.17, we made constant all the parameters of Equation (3.26) except FPL_m. These constant values were taken from simulations. To evaluate the behaviour of p_i^* when FPL_m increases, we used Equation (A.1) to be substituted in Equation (3.26). Similarly, to draw Figure 3.18, we made constant all parameters of Equation

(3.26) except FPL_b. Now, to evaluate the behaviour of p_i^* when FPL_b increases, we used Equation (A.1) to be substituted in Equation (3.26).

For all these methods, the perceptual video quality ratings obtained from the evaluators are averaged to obtain the Mean Opinion Score (MOS).

Bibliography

[1] A. Mezher and M. A. Igartua, "Multimedia multimetric map-aware routing protocol to provide video-reporting messages over VANETs in smart cities," *Vehicular Technology, IEEE Transactions on*, 2016, *submitted*.

[2] A. Mezher, M. A. Igartua, L. J. de la Cruz Llopis, and E. S. Gargallo, "A game theoretical map-aware routing protocol to provide video-reporting messages over VANETs in smart cities," *Vehicular Technology, IEEE Transactions on*, 2016, *In preparation*.

[3] A. Mezher, J. Oltra, L. Urquiza-Aguiar, C. Iza-Parades, C. Tripp-Barba, and M. A. Igartua, "Realistic environment for vanet simulations to detect the presence of obstacles in vehicular ad hoc networks," in *11th ACM Symposium on Performance Evaluation of Wireless Ad Hoc, Sensor, & Ubiquitous Networks PE-WASUN '14*, vol. 47, no. 11, November 2014, pp. 77–84.

[4] "Cisco systems cisco visual networking index: Forecast and methodology," Technical report, Cisco Systems (2014-2019), Tech. Rep., 2014.

[5] C. E. Perkins, *Ad Hoc Networking*, 1st ed. Addison-Wesley Professional, 2008.

[6] G. Dimitrakopoulos and P. Demestichas, "Intelligent Transportation Systems," *IEEE Vehicular Technology Magazine*, vol. 5, no. 1, pp. 77–84, March 2010.

[7] S. Y. Wang and C. L. Chou, "NCTUns tool for wireless vehicular communication network researches," *Simulation Modelling Practice and Theory*, vol. 17, no. 7, pp. 1211–1226, August 2009.

[8] S. Al-Sultan, M. M. Al-Doori, A. H. Al-Bayatti, and H. Zedan, "A comprehensive survey on vehicular ad hoc network," *Journal of Network and Computer Applications*, vol. 37, pp. 380 – 392, 2014. [Online]. Available: http://www.sciencedirect.com/science/article/pii/S108480451300074X

[9] A. Boukerche, H. A. B. F. Oliveira, E. F. Nakamura, and A. A. F. Loureiro, "Vehicular ad hoc networks: A new challenge for localization-based systems," *Computer Communications*, vol. 31, no. 12, pp. 2838–2849, July 2008.

[10] M. Aguilar and V. Carrascal, "Self-configured multipath routing using path lifetime for video-streaming services over ad hoc networks," *Computer Communications*, vol. 33, pp. 1879–1891, 2010.

[11] B. Karp and H. T. Kung, "GPSR: greedy perimeter stateless routing for wireless networks," in *6th International Conference on Mobile Computing and Networking*, ser. MobiCom, 2000, pp. 243–254.

[12] "RFC 4728, the dynamic source routing protocol (DSR) for mobile ad hoc networks for IPV4," 2007. [Online]. Available: http://www.ietf.org/rfc/rfc4728.txt

[13] P. Tudor, "MPEG-2 video compression," *Electronics Communication Engineering Journal*, vol. 7, no. 6, pp. 257–264, Dec 1995.

[14] "Standard 802.11," 2014. [Online]. Available: http://standards.ieee.org/getieee802/download/802-2014.pdf

[15] "Standard 802.11e," 2005. [Online]. Available: https://standards.ieee.org/findstds/standard/802.11e-2005.html

[16] S. Association. (2010, July) "IEEE Standard 802.11p". [Online]. Available: http://standards.ieee.org/getieee802/download/802.11p-2010.pdf

[17] "Moving picture experts group." [Online]. Available: http://www.chiariglione.org/mpeg/

[18] "RFC 3550, RTP: A transport protocol for real-time applications," 2003. [Online]. Available: http://www.ietf.org/rfc/rfc4728.txt

[19] "RFC 3393, packet delay variation (PDV)," 2003. [Online]. Available: http://tools.ietf.org/html/rfc3393

[20] "Methodology for the subjective assessment of the quality of television pictures," 2002. [Online]. Available: http://www.itu.int/dms_pubrec/itu-r/rec/bt/R-REC-BT.500-11-200206-S!!PDF-E.pdf(accessedon11February2016)

[21] "Subjective video quality assessment methods for multimedia applications," 1999. [Online]. Available: http://www.itu.int/rec/T-REC-P.910-200804-I(accessedon11February2016)

[22] Z. Wang, L. Lu, and A. Bovik, "Video quality assessment using structural distortion measurement," in *Image Processing. 2002. Proceedings. 2002 International Conference on*, vol. 3, 2002, pp. III–65–III–68 vol.3.

[23] A. M. Mezher, M. A. Igartua, L. J. de la Cruz Llopis, E. P. Segarra, C. Tripp-Barba, L. Urquiza-Aguiar, J. Forné, and E. S. Gargallo, "A multi-user game-theoretical multipath routing protocol to send video-warning messages over mobile ad hoc networks," *Sensors*, vol. 15, no. 4, p. 9039, 2015. [Online]. Available: http://www.mdpi.com/1424-8220/15/4/9039

[24] A. M. Mezher, C. Tripp-Barba, L. Urquiza Aguiar, M. Aguilar Igartua, and I. Martín, "Optimization of the path selection in a Game-theoretic routing protocol for video-streaming services over Mobile Ad hoc Networks," in *XI Jornadas de Ingeniería Telemática (JITEL)*, October 2013, *submitted*.

[25] A. Boukerche, *Algorithms and Protocols for Wireless, Mobile Ad Hoc Networks*. Wiley-IEEE Press, 2008.

[26] L. Lao and J. Cui, "Reducing multicast traffic load for cellular networks using ad hoc networks," in *2nd Int'l Conference on Quality of Service in Heterogeneous Wired/Wireless Networks (QShine'05)*, August 2005, pp. 1–10.

[27] L. Chen and W. Heinzelman, "QoS-aware routing based on bandwidth estimation for mobile ad hoc networks," *IEEE J. Sel. Areas Commun.*, vol. 23, pp. 561–572, 2005.

[28] G. Quddus, R. Khan, R. Iqbal, and W. Ahmed, "Finding a stable route through aodv by using route fragility coefficient as metric," in *IEEE International Conference on Networking and Services*, July 2006, pp. 107–112.

[29] M. Al-Gabri, C. Li, Z. Yang, N. Hasan, and X. Zhang, "Improved the energy of ad hoc on-demand distance vector routing protocol," *IERI Procedia*, vol. 2, pp. 355–361, 2012.

[30] M. Rao and N. Singh, "An improved routing protocol (AODV nthbr) for efficient routing in MANETs," *Adv. Comput. Netw. Inform.*, vol. 2, pp. 215–223, 2014.

[31] A. Pirzada, A. Datta, and C. McDonald, "Incorporating trust and reputation in the dsr protocol for dependable routing," *Comput. Commun.*, vol. 29, pp. 2806–2821, 2006.

[32] M. Sjaugi, M. Othman, and M. Rasid, ""A new route maintenance strategy for dynamic source routing protocol "," in *International Conference on Information Networking*, January 2008, pp. 1–4.

[33] S. Shubhajeet and S. Das, "Ant colony optimization based enhanced dynamic source routing algorithm for mobile ad-hoc network," *Inf. Sci.*, vol. 295, pp. 67–90, 2015.

[34] C. E. Perkins and E. M. Royer, "Ad-hoc on-demand distance vector routing," in *Proceedings of the Second IEEE Workshop on Mobile Computer Systems and Applications*. Washington, DC, USA: IEEE Computer Society, 1999, pp. 90–. [Online]. Available: http://dl.acm.org/citation.cfm?id=520551.837511

[35] A. Tran and H. Raghavendra, "Routing with congestion awareness and adaptivity in mobile ad hoc networks," in *IEEE Wireless Communications and Networking Conference*, March 2005, pp. 1988–1994.

[36] C. Mbarushimana and A. Shahrabi, "Congestion avoidance routing protocol for qos-aware manets," in *International Wireless Communications and Mobile Computing Conference*, August 2008, pp. 129–134.

[37] M. Al-Tarazi, "Load Balancing Using Multiple Paths in Mobile Ad Hoc networks," Ph.D. dissertation, Jordan University of Science and Technology, 2009.

[38] C. Ahn, S. Chung, T. Kim, and S. Kang, "A node-disjoint multipath routing protocol based on aodv in mobile ad hoc networks," in *IEEE 26th International Conference on Advanced Information Networking and Applications*, March 2012, pp. 399–405.

[39] Y. Tashtoush, O. Darwish, and M. Hayajaneh, "Fibonacci sequence based multipath load balancing apprach for mobile ad hoc networks," *Ad Hoc Netw.*, vol. 16, pp. 237–246, 2014.

[40] S. Mao, Y. T. Hou, X. Cheng, H. D. Sherali, and S. F. Midkiff, "Multipath routing for multiple description video in wireless ad hoc networks," in *IEEE INFOCOM*, March 2005, pp. 740–750.

[41] E. S. X. Zhu and G. Brend, "Congestion-distortion optimized video transmission over ad hoc networks," *Signal Processing: Image Communication*, vol. 20, pp. 773–783, 2005.

[42] A. Boushaba, A. Benabbou, R. Benabbou, A. Zahi, and M. Oumsis, "Intelligent multipath optimized link state routing protocol for QoS and QoE enhancement of video transmission in MANETs," in *Networked Systems*, ser. Lecture Notes in Computer Science, G. Noubir and M. Raynal, Eds. Springer International Publishing, 2014, vol. 8593, pp. 230–245. [Online]. Available: http://dx.doi.org/10.1007/978-3-319-09581-3_16

[43] C. Lal, V. Laxmi, M. Gaur, and S.-B. Ko, "Bandwidth-aware routing and admission control for efficient video streaming over MANETs," *Wireless Networks*, vol. 21, no. 1, pp. 95–114, 2015. [Online]. Available: http://dx.doi.org/10.1007/s11276-014-0774-2

[44] H. Shen and Z. Li, "Game-theoretic analysis of cooperation incentive strategies in mobile ad hoc networks," *IEEE Transactions on Mobile Computing*, vol. 11, no. 8, pp. 1287–1303, 2012.

[45] F. Wu, T. Chen, S. Zhong, C. Qiao, and G. Chen, "A game-theoretic approach to stimulate cooperation for probabilistic routing in opportunistic networks," *Wireless Communications, IEEE Transactions on*, vol. 12, no. 4, pp. 1573–1583, April 2013.

[46] M. Naserian and K. Tepe, "Dynamic probabilistic forwarding in wireless ad hoc networks based on game theory," in *Vehicular Technology Conference (VTC Spring), 2014 IEEE 79th*, May 2014, pp. 1–5.

[47] P. Coucheney, B. Gaujal, and C. Touati, "Self-optimizing routing in manets with multi-class flows," in *Personal Indoor and Mobile Radio Communications (PIMRC), 2010 IEEE 21st International Symposium on*, Sept 2010, pp. 2751–2756.

[48] J. Liu, X. Jiang, H. Nishiyama, R. Miura, N. Kato, and N. Kadowaki, "Optimal forwarding games in mobile ad hoc networks with two-hop f-cast relay," *Selected Areas in Communications, IEEE Journal on*, vol. 30, no. 11, pp. 2169–2179, December 2012.

[49] M. Aguilar, L. de la Cruz, V. Carrascal, and E. Sanvicente, "A game-theoretical multipath routing for video-streaming services over mobile ad hoc networks," *Comput. Netw.*, vol. 55, pp. 2985–3000, 2011.

[50] "IEEE 802.11e standard with quality of service enhancenments," 2005. [Online]. Available: http://standards.ieee.org/getieee802/download/802.11e-2005.pdf

[51] V. Loscri, F. De Rango, and S. Marano, "Performance evaluation of on-demand multipath distance vector routing protocol over two mac layers in mobile ad hoc networks," in *Wireless Communication Systems, 2004, 1st International Symposium on*, Sept 2004, pp. 413–417.

[52] M. Naserian and K. Tepe, "Game theoretic approach in routing protocol for wireless ad hoc networks," *Ad Hoc Networks*, vol. 7, no. 3, pp. 569 – 578, 2009. [Online]. Available: http://www.sciencedirect.com/science/article/pii/S1570870508000966

[53] J. Nash, "Non-cooperative games," *Annals of Mathematics*, vol. 54, no. 2, pp. 286–295, 1951. [Online]. Available: http://www.jstor.org/stable/1969529

[54] P. Dutta, *Strategies and Games: Theory and Practice*. MIT Press, 2001.

[55] M. Osborne and A. Rubinstein, *A Course in Game Theory*. MIT Press, 1994.

[56] "The network simulator, ns-2," http://nsnam.isi.edu/nsnam/. [Online]. Available: http://nsnam.isi.edu/nsnam/

[57] "Bonnmotion, a mobility scenario generation and analysis tool," 2005. [Online]. Available: http://web.informatik.uni-bonn.de/IV/Mitarbeiter/dewaal/BonnMotion/

[58] "Traffic accidents." [Online]. Available: http://www.youtube.com/watch?v=jmZ4iRRTrzs

[59] M. Fougue, P. Garrido, F. Martinez, J. Cano, C. Calafate, and P. Manzoni, "A realistic simulation framework for vehicular networks," in *5th International ICST Conference on Simulation Tools and Techniques Simutools'12*, March 2012, pp. 37–46.

[60] D. Krajzewicz, J. Erdmann, M. Behrisch, and L. Bieker, "Recent development and applications of sumo—simulation of urban mobility," *nt. J. Adv. Syst. Meas.*, vol. 5, pp. 128–138, 2012.

[61] "Open street maps." [Online]. Available: http://www.openstreetmap.org/

[62] M. Fiore, J. Härri, F. Filali, and C. Bonnet, "Vehicular Mobility Simulation for VANETs," in *Proc. 40th Annual Simulation Symposium (ANSS)*, March 2007, pp. 301–309.

[63] "U.s. census bureau - tiger/line files." [Online]. Available: http://www.census.gov/geo/www/tiger/shp.html

[64] L. Bajaj, M. Takai, R. Ahuja, K. Tang, R. Bagrodia, and M. Gerla, "GloMoSim: A scalable network simulation environment," Network Research Lab at UCLA, Tech. Rep., 1999.

[65] "QualNet," September 2012. [Online]. Available: http://www.qualnet.com/content/component/content/article/13-products/82-qualnet

[66] K. Lee, U. Lee, and M. Gerla, "Survey of Routing Protocols in Vehicular Ad Hoc Networks," 2009, pp. 149–170.

[67] H. Y. A. Wahid and D. Kim, "Unicast geographic routing protocols for inter-vehicle communications: A survey," in *Proc. 5th ACM workshop on Performance monitoring and measurement of heterogeneous wireless and wired networks*, Octuber 2010, pp. 17–24.

[68] H. Menouar, M. Lenardi, and F. Filali, "Movement prediction-based routing (MOPR) concept for position-based routing in vehicular networks," in *IEEE Vehicular Technology Conference (VTC) Fall*, 2007.

[69] F. Granelli, D. K. G. Boato, and G. Vernazza, "Enhanced GPSR Routing in Multi-Hop Vehicular Communications through Movement Awarness," in *IEEE Communications Letters*, vol. 11, no. 10, 2007, pp. 781–783.

[70] D. Xiao, L. Peng, C. O. Asogwa, and L. Huang, "An Improved GPSR Routing Protocol," in *International Journal of Advancements in Computing Technology*, vol. 3, no. 5, June 2011, pp. 132–139.

[71] C. Tripp-Barba, L. Urquiza-Aguiar, M. A. Igartua, D. Rebollo-Monedero, L. J. de la Cruz Llopis, A. M. Mezher, and J. A. Aguilar-Calderón, "A multimetric, map-aware routing protocol for VANETs in urban areas," *Sensors*, vol. 14, no. 2, p. 2199, 2014. [Online]. Available: http://www.mdpi.com/1424-8220/14/2/2199

[72] R. Wang, C. Rezende, H. S. Ramos, R. W. Pazzi, A. Boukerche, and A. A. F. Loureiro, "Liaithon: A location-aware multipath video streaming scheme for urban vehicular networks," in *Computers and Communications (ISCC), 2012 IEEE Symposium on*, July 2012, pp. 000 436–000 441.

[73] C. Rezende, A. Boukerche, H. S. Ramos, and A. A. F. Loureiro, "A reactive and scalable unicast solution for video streaming over VANETs," *IEEE Transactions on Computers*, vol. 64, no. 3, pp. 614–626, March 2015.

[74] H. Xie, A. Boukerche, and A. A. F. Loureiro, "A multipath video streaming solution for vehicular networks with link disjoint and node-disjoint," *IEEE Transactions on Parallel and Distributed Systems*, vol. 26, no. 12, pp. 3223–3235, Dec 2015.

[75] C. Tripp-Barba, L. Urquiza-Aguiar, M. A. Igartua, A. M. Mezher, A. Zaldivar-Colado, and I. Guérin-Lassous, "Available bandwidth estimation in GPSR for VANETs," in *3rd ACM Symposium on Design and Analysis of Intelligent Vehicular Networks and Applications*, November 2013, pp. 1–8.

[76] C. Sarr, C. Chaudet, G. Chelius, and I. Lassous, "Bandwidth estimation for IEEE 802.11-based ad hoc networks," *Mobile Computing, IEEE Transactions on*, vol. 7, no. 10, pp. 1228–1241, Oct 2008.

[77] "IEEE 802.11 standard: Part 11: Wireless lan medium access control (mac) and physical layer (phy) specifications." [Online]. Available: http://standards.ieee.org/getieee802/download/

[78] E. Jorswieck, E. Larsson, M. Luise, and H. Poor, "Game theory in signal processing and communications," *Signal Processing Magazine, IEEE*, vol. 26, no. 5, pp. 17–132, September 2009.

[79] F. Meshkati, H. Poor, and S. Schwartz, "Energy-efficient resource allocation in wireless networks," *Signal Processing Magazine, IEEE*, vol. 24, no. 3, pp. 58–68, May 2007.

[80] A. Leshem and E. Zehavi, "Game theory and the frequency selective interference channel," *Signal Processing Magazine, IEEE*, vol. 26, no. 5, pp. 28–40, September 2009.

[81] D. Schmidt, C. Shi, R. Berry, M. Honig, and W. Utschick, "Distributed resource allocation schemes," *Signal Processing Magazine, IEEE*, vol. 26, no. 5, pp. 53–63, September 2009.

[82] J. Rückert, O. Abboud, T. Zinner, R. Steinmetz, and D. Hausheer, "Quality adaptation in p2p video streaming based on objective qoe metrics," in *NETWORKING 2012*, ser. Lecture Notes in Computer Science, R. Bestak, L. Kencl, L. Li, J. Widmer, and H. Yin, Eds. Springer Berlin Heidelberg, 2012, vol. 7290, pp. 1–14. [Online]. Available: http://dx.doi.org/10.1007/978-3-642-30054-7_1

[83] S. Milani, G. Calvagno, R. Bernardini, and R. Rinaldo, "A low-complexity packet classification algorithm for multiple description video streaming over ieee802.11e networks," in *Image Processing, 2008. ICIP 2008. 15th IEEE International Conference on*, Oct 2008, pp. 3072–3075.

[84] Z. Liu, Y. Shen, S. Panwar, K. Ross, and Y. Wang, "P2P video live streaming with MDC: Providing incentives for redistribution," in *Multimedia and Expo, 2007 IEEE International Conference on*, July 2007, pp. 48–51.

[85] S. Milani and G. Calvagno, "A game theory based classification for distributed downloading of multiple description coded video," in *Image Processing (ICIP), 2009 16th IEEE International Conference on*, Nov 2009, pp. 3077–3080.

[86] E. Jorswieck, E. Larsson, M. Luise, and H. Poor, "Game theory in signal processing and communications," *Signal Processing Magazine, IEEE*, vol. 26, no. 5, pp. 17–132, September 2009.

[87] J. Han, D. Farin, and P. de With, "A mixed-reality system for broadcasting sports video to mobile devices," *MultiMedia, IEEE*, vol. 18, no. 2, pp. 72–84, Feb 2011.

[88] X. Zhu, P. Agrawal, J. Singh, T. Alpcan, and B. Girod, "Distributed rate allocation policies for multihomed video streaming over heterogeneous access networks," *Multimedia, IEEE Transactions on*, vol. 11, no. 4, pp. 752–764, June 2009.

[89] P. Goudarzi and M. R. N. Ranjbar, "Bandwidth allocation for video transmission with differentiated quality of experience over wireless networks," *Computers & Electrical Engineering*, vol. 37, no. 1, pp. 75 – 90, 2011. [Online]. Available: http://www.sciencedirect.com/science/article/pii/S0045790610000947

[90] S. Asioli, N. Ramzan, and E. Izquierdo, "A game theoretic approach to minimum-delay scalable video transmission over P2P," *Signal Processing: Image Communication*, vol. 27, no. 5, pp. 513 – 521, 2012. [Online]. Available: http://www.sciencedirect.com/science/article/pii/S0923596512000410

[91] S. Parakh and A. K. Jagannatham, "Game theory based dynamic bitrate adaptation for h.264 scalable video transmission in 4G wireless systems," in *Int. Conf. Signal Process. Commun. (SPCOM)*, July 2012, pp. 1–5.

[92] S. Meng, L. Liu, and J. Yin, "Scalable and reliable iptv service through collaborative request dispatching," in *Web Services (ICWS), 2010 IEEE International Conference on*, July 2010, pp. 179–186.

[93] S. Milani, S. Busato, and G. Calvagno, "Multiple description peer-to-peer video streaming using coalitional games," in *Signal Processing Conference, 2011 19th European*, Aug 2011, pp. 1105–1109.

[94] S. Milani and G. Calvagno, "Distributed multiple description video transmission via noncooperative games with opportunistic players," *Circuits and Systems for Video Technology, IEEE Transactions on*, vol. 25, no. 1, pp. 125–138, Jan 2015.

[95] C. Tripp-Barba, M. Aguilar Igartua, L. Urquiza Aguiar, A. M. Mezher, A. Zaldívar-Colado, and I. Guérin-Lassous, "Available bandwidth estimation in gpsr for vanets," in *Proceedings of the Third ACM International Symposium on Design and Analysis of Intelligent Vehicular Networks and Applications*, ser. DIVANet '13. New York, NY, USA: ACM, 2013, pp. 1–8. [Online]. Available: http://doi.acm.org/10.1145/2512921.2516961

[96] C. Tripp Barba, A. M. Mezher, I. Guérin-Lassous, C. Sarr, and M. Aguilar Igartua, "Available Bandwidth-aware Routing in Urban Vehicular Ad-hoc Networks," in *Proc. 76th IEEE Vehicular Technology Conference (VTC-Fall)*, September 2012, pp. 1–5.

[97] C. Tripp Barba, M. A. Mateos, P. Regañas, A. M. Mezher, and M. Aguilar Igartua, "Smart city for VANETs using warning messages, traffic statistics and intelligent traffic lights," in *Proc. IEEE Intelligent Vehicles Symposium (IV)*, June 2012, pp. 902–907.

[98] C. I. Paredes, A. M. Mezher, and M. A. Igartua, "Performance evaluation of dissemination protocols for emergency messages in Vehicular Ad-Hoc networks," in *XII Jornadas de Ingeniería Telemática (JITEL 2015)*, Palma de Mallorca, Spain, October 2015.

[99] A. M. Mezher, C. I. Paredes, L. Urquiza-Aguiar, A. T. Moreira, and M. A. Igartua, "Design of smart services and routing protocols for VANETs in smart cities," in *XII Jornadas de Ingeniería Telemática (JITEL 2015)*, Palma de Mallorca, Spain, October 2015.

[100] A. M. Mezher, C. I. Paredes, C. T. Barba, and M. A. Igartua, "A Dynamic Multimetric Weights Distribution in a Multipath Routing Protocol using Video-Streaming Services over MANETs," in *XII Jornadas de Ingeniería Telemática (JITEL 2015)*, Palma de Mallorca, Spain, October 2015.

[101] C. Tripp-Barba, L. Urquiza-Aguiar, M. A. Igartua, D. Rebollo-Monedero, L. J. de la Cruz Llopis, A. M. Mezher, and J. A. Aguilar-Calderón, "A multimetric, map-aware routing protocol for vanets in urban areas," *Sensors*, vol. 14, no. 2, p. 2199, 2014. [Online]. Available: http://www.mdpi.com/1424-8220/14/2/2199

[102] L. Urquiza-Aguiar, C. Tripp-Barba, D. Rebollo-Monedero, A. M. Mezher, M. Aguilar-Igartua, and J. Forné, "Coherent, Automatic Address Resolution for Vehicular Ad Hoc Networks," *International Journal of Ad Hoc and Ubiquitous Computing*, vol. (in press), pp. 1–18, 2015.

[103] L. Urquiza-Aguiar, A. V. Rodas, C. Tripp-Barba, A. Mezher, M. A. Igartua, and L. J. de la Cruz Llopis, "Efficient deployment of gateways in multi-hop ad-hoc wireless networks," in *11th ACM Symposium on Performance Evaluation of Wireless Ad Hoc, Sensor, & Ubiquitous Networks PE-WASUN '14*, vol. 47, no. 11, november 2014, pp. 93–100.